Pierre-Yves Lagrée

"Hydrodynamic and erosion models for flows over erodible beds 1/2"

Chalès 01/07/14

Institut Jean Le Rond ∂'Alembert

UNIVERSITE PIERRE & MARIE CURIE LA SCIENCE A PARIS

Lomé Togo

exemple in the lab Hele Shaw

D. Doppler T. Loiseleux

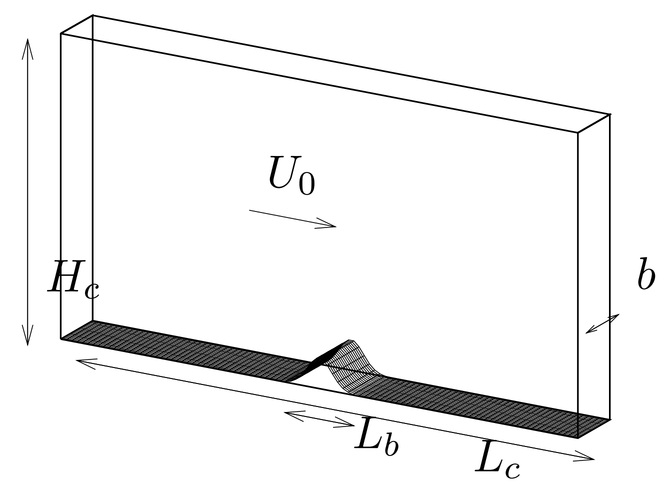

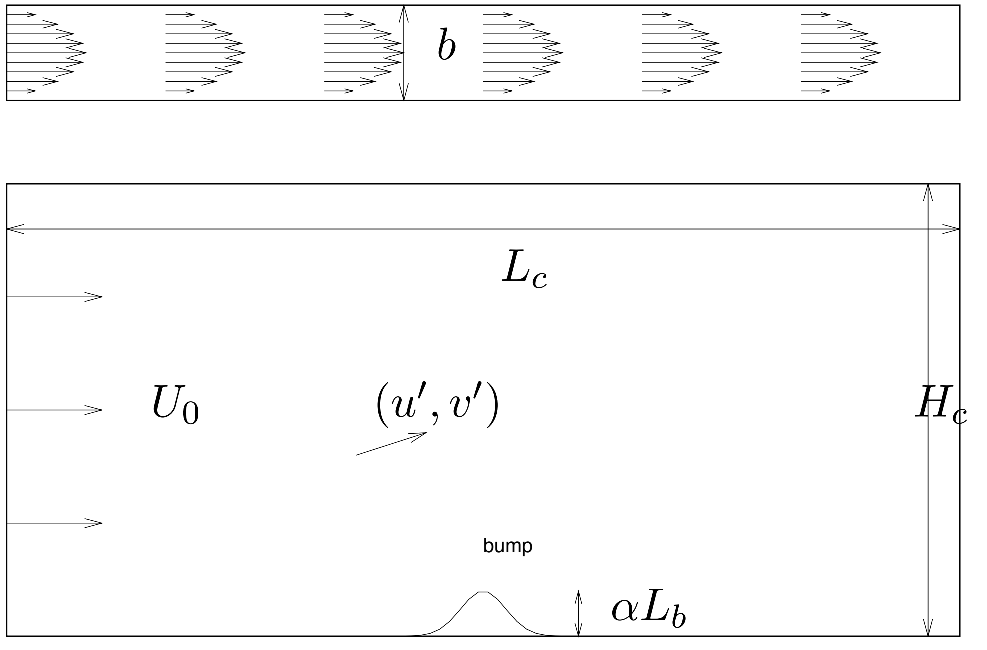

exemple in the lab Hele Shaw

D. Doppler T. Loiseleux

- continuum models
- bed load suspension

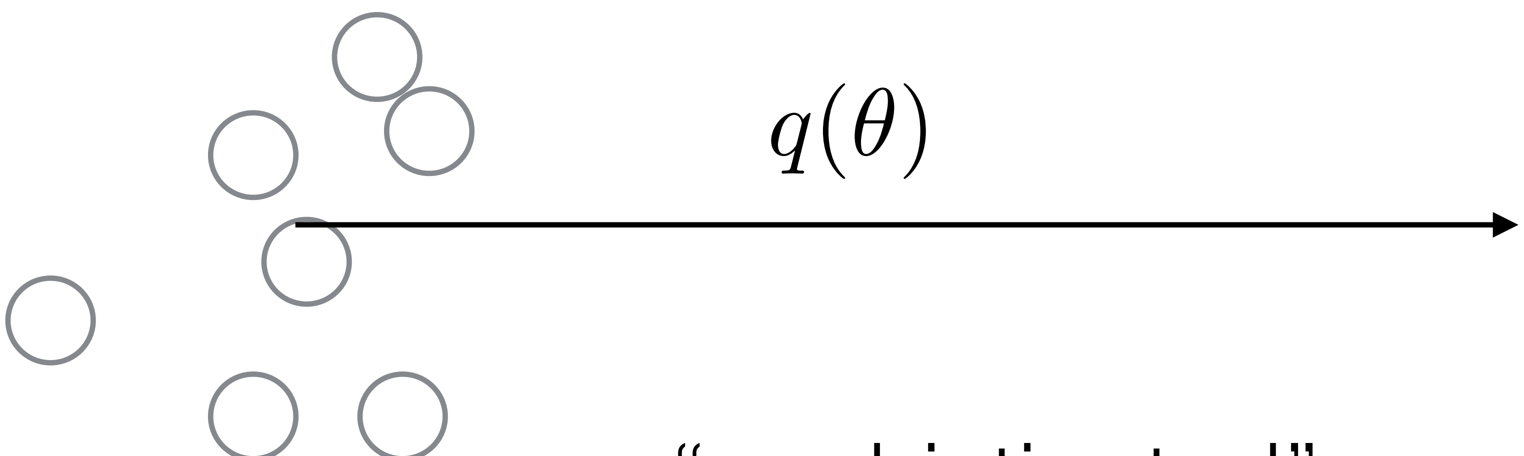

“sophisticated” models
Jackson 00
Charru & Mouilleron Arnoud 02
Ouiremi, Aussillous & Guazzelli 09
Chauchat Medale 10

Lagrangian dilute

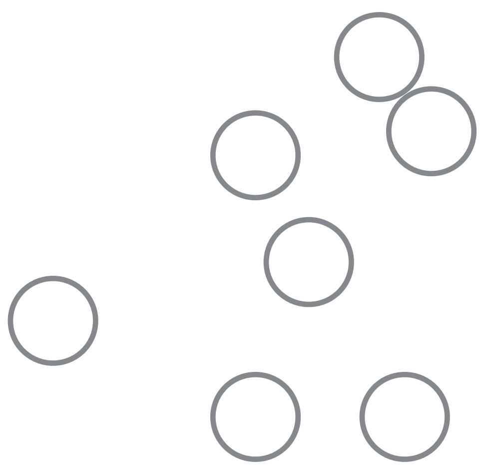

feel each other

collisional

grains water bifluids

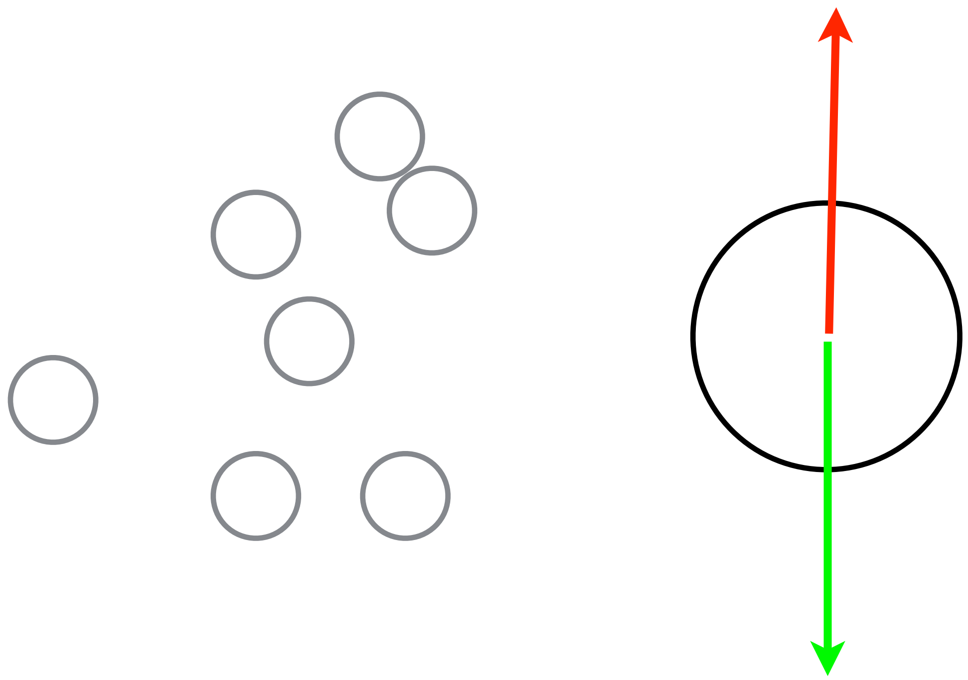

free fall equilibrium

$$\color{green}{\frac{4}{3}\pi(\Delta\rho)R^3 g} = \color{red}{6\pi\eta R V_s}$$

terminal velocity

$$V_s = \frac{d^2}{18\eta}(\Delta\rho)g$$

Stokes velocity

Reynolds of the particule

$$Re = \frac{d^2}{\nu}\frac{\partial u}{\partial y}$$

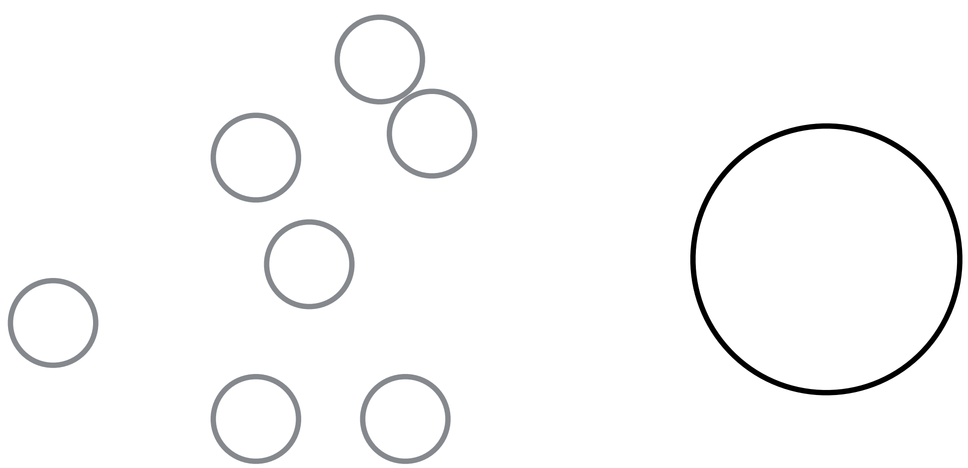

terminal velocity

$$V_s = \frac{d^2}{18\eta}(\Delta\rho)g$$

Reynolds associated= Galileo

$$Ga = \frac{(\Delta\rho)gd^3}{\eta^2}$$

Erosion Model

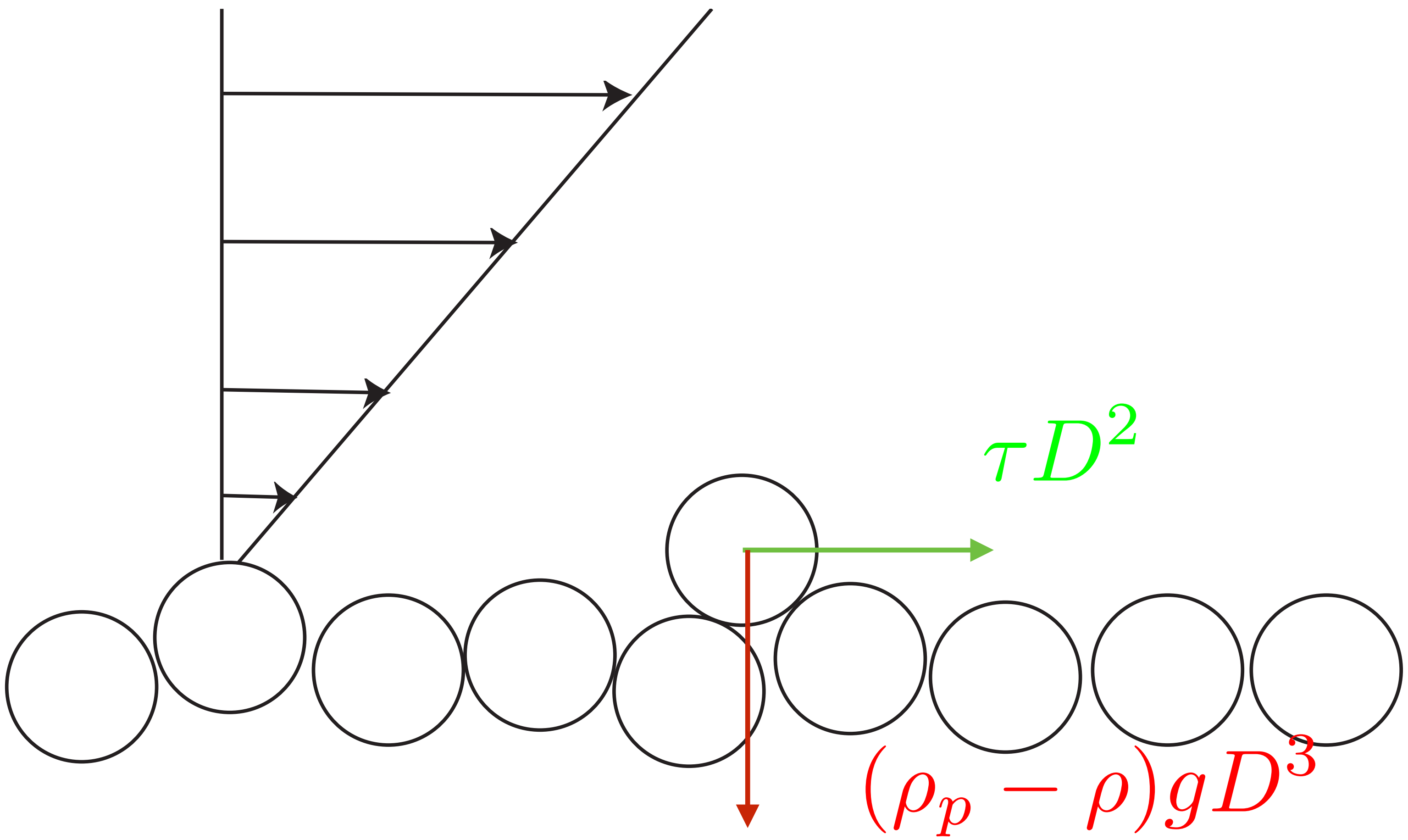

Stress larger than a threshold $\tau > \tau_s$

Shields number $\dfrac{\tau}{(\rho_p - \rho) g D}$

Albert F. Shields (1908–1974) no publication: phD Technischen Hochschule Berlin, 1936

Erosion Model

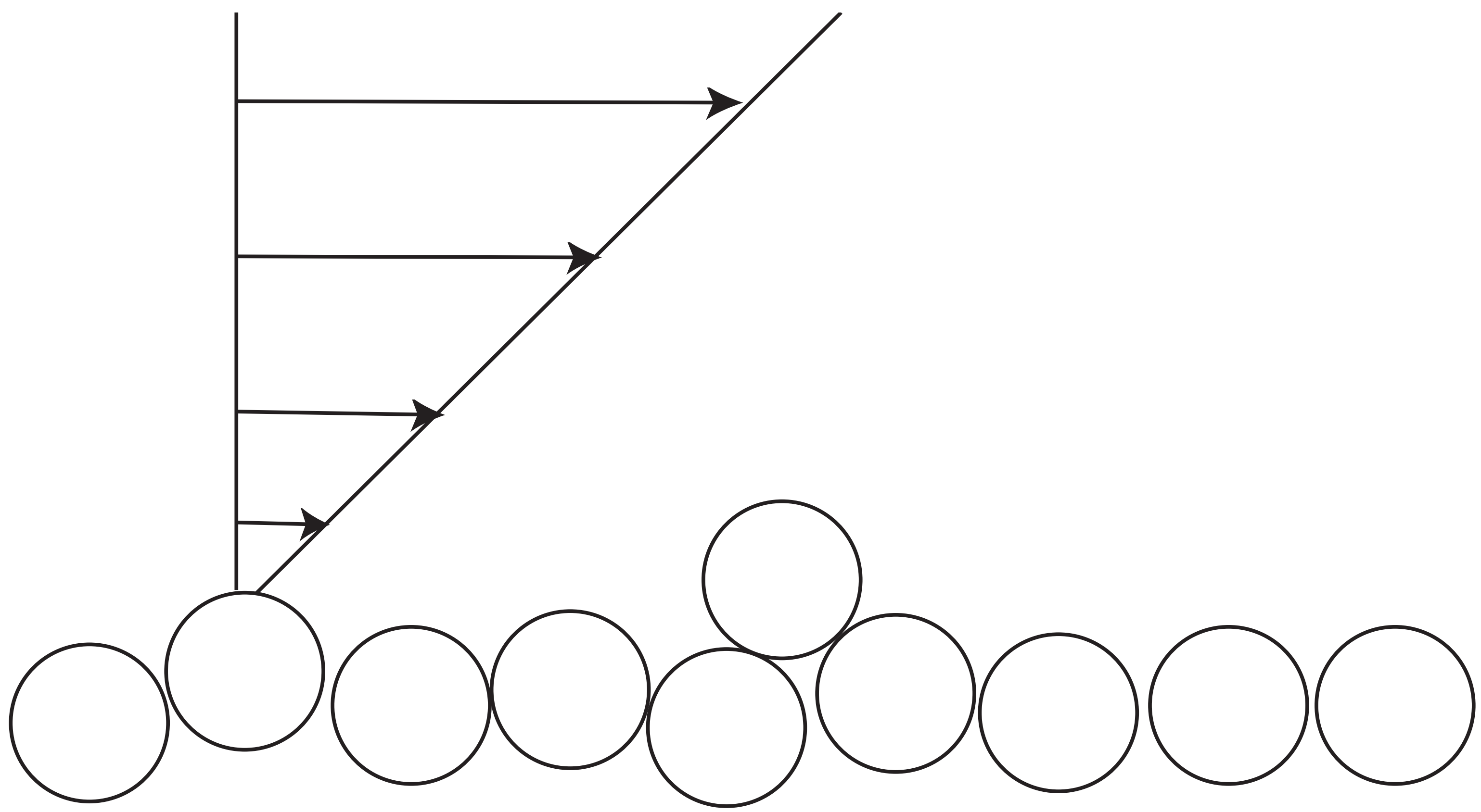

Stress larger than a threshold $\tau > \tau_s$

Shields number $$\frac{\tau}{(\rho_p - \rho)gD}$$

Erosion Model

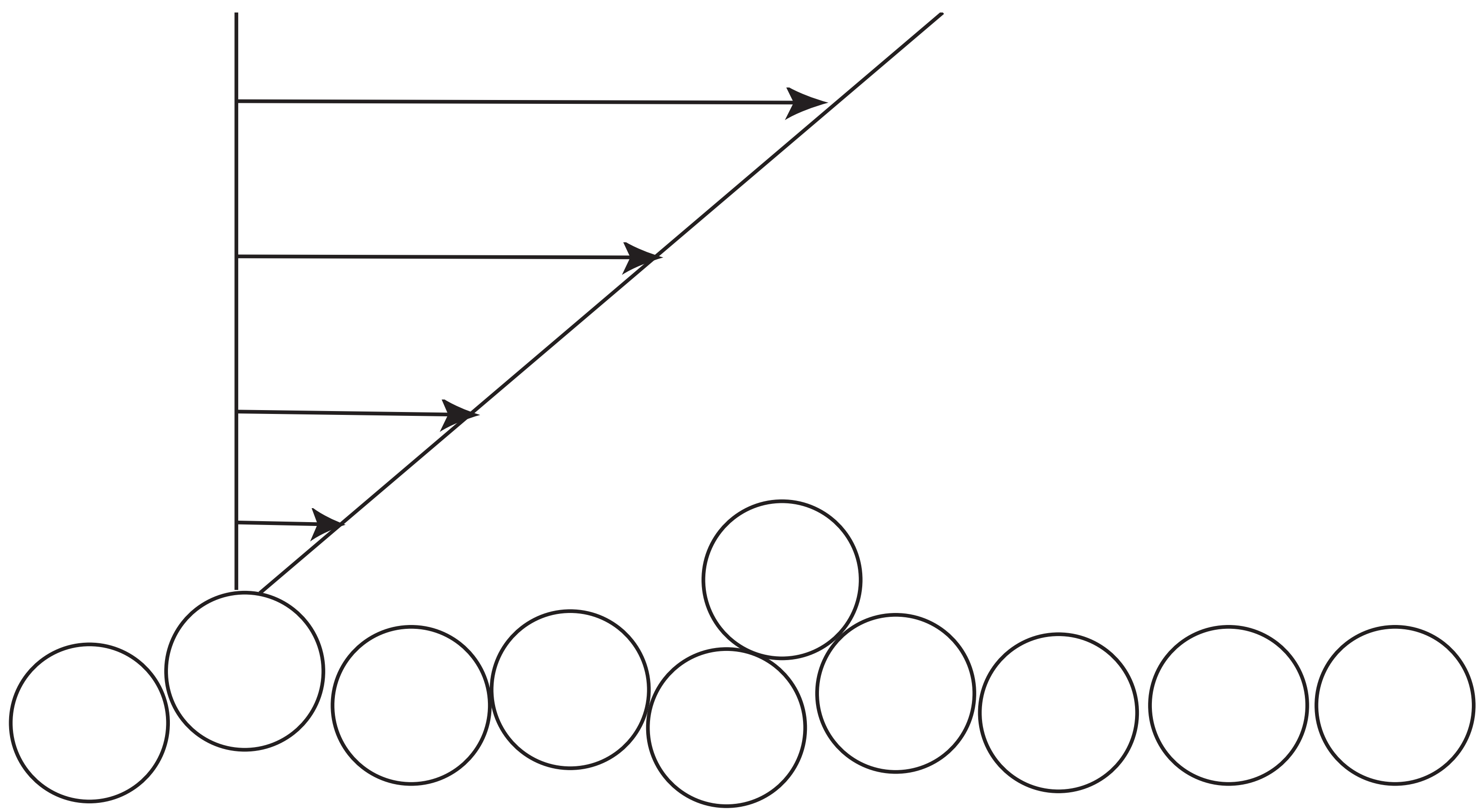

Stress larger than a threshold $\tau > \tau_s$

Shields number $$\frac{\tau}{(\rho_p - \rho) g D}$$

Erosion Model

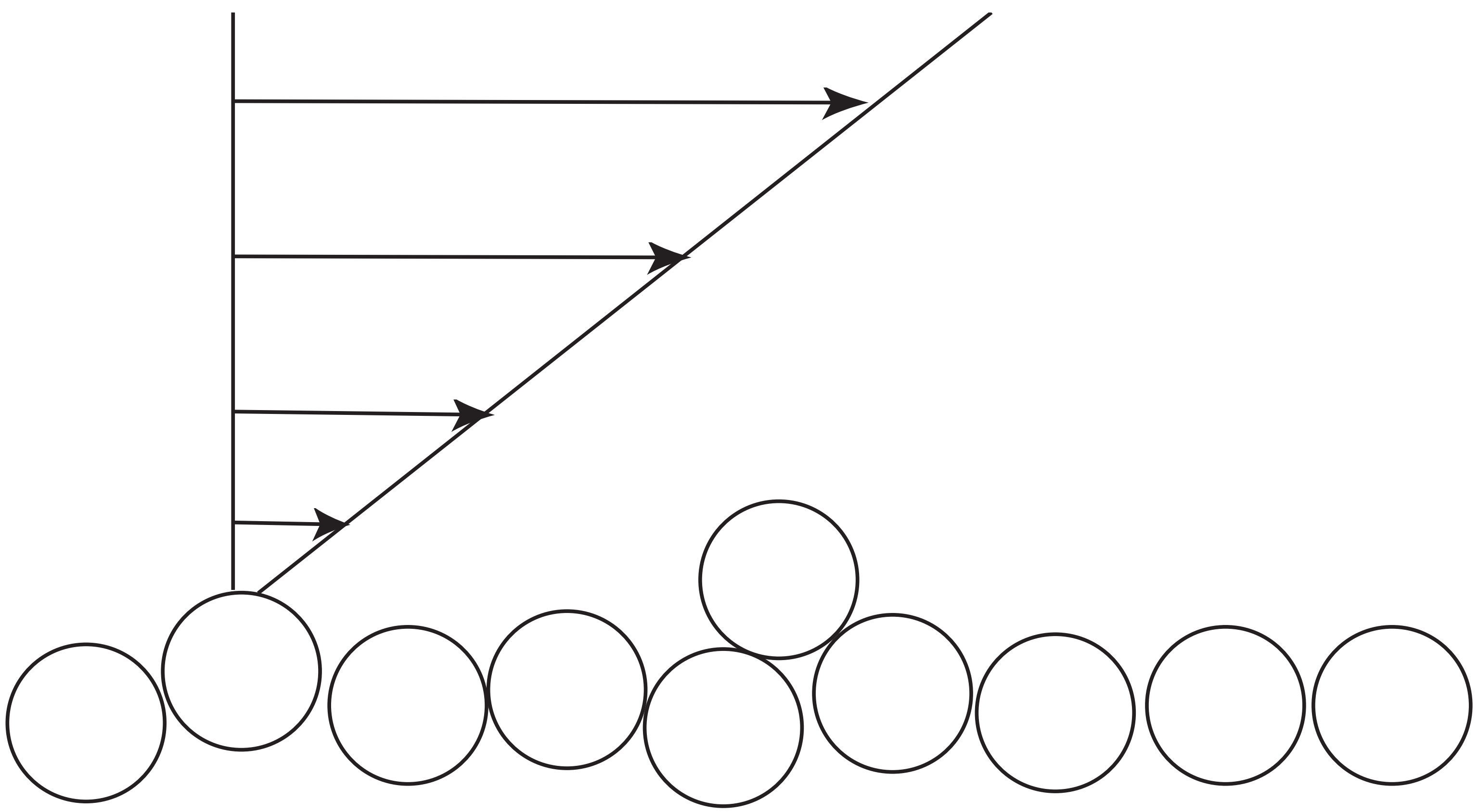

Stress larger than a threshold $\tau > \tau_s$

Shields number $\dfrac{\tau}{(\rho_p - \rho) g D}$

Erosion Model

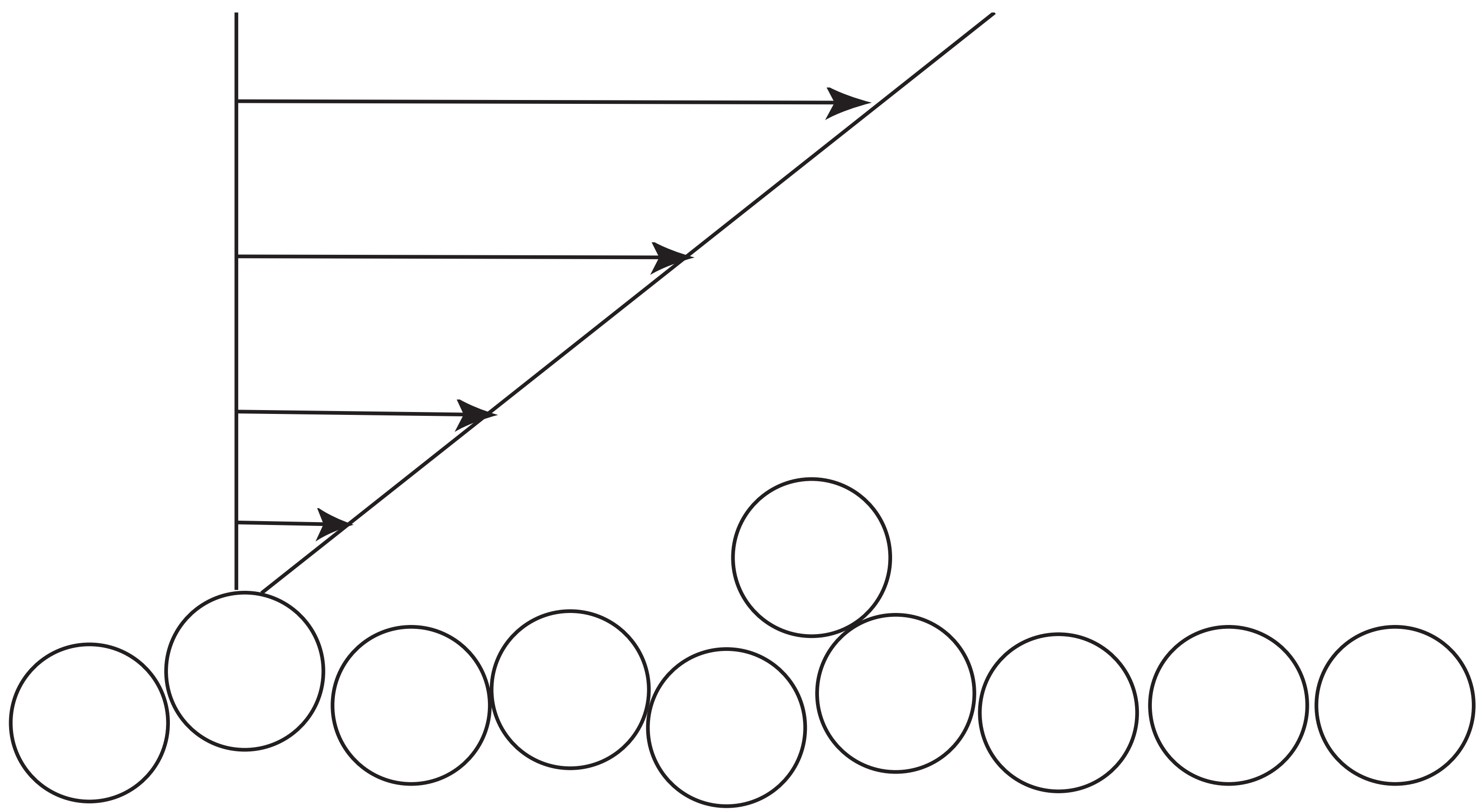

Stress larger than a threshold $\quad \tau > \tau_s$

Shields number $\quad \dfrac{\tau}{(\rho_p - \rho) g D}$

Erosion Model

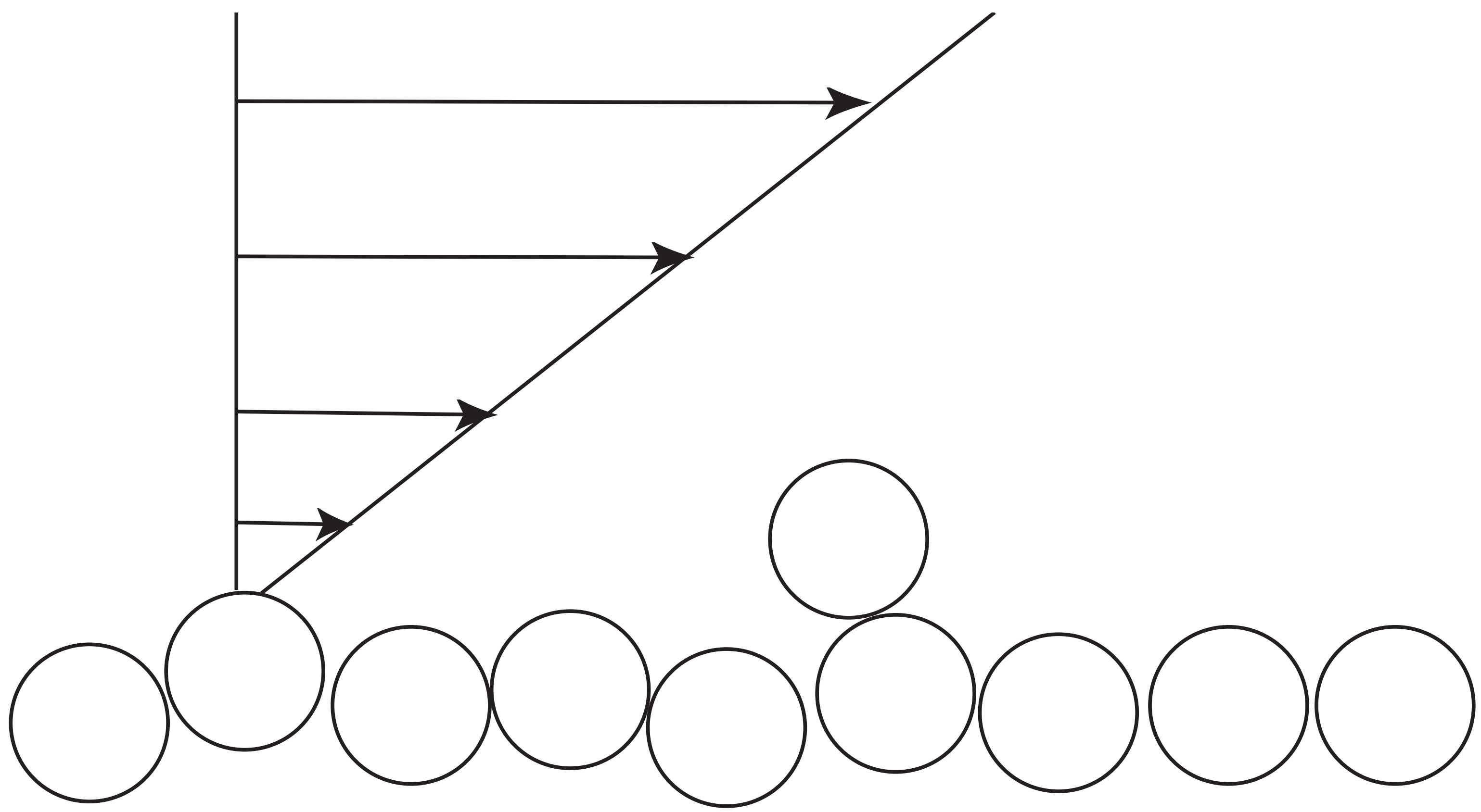

Stress larger than a threshold $\tau > \tau_s$

Shields number $\dfrac{\tau}{(\rho_p - \rho) g D}$

Erosion Model

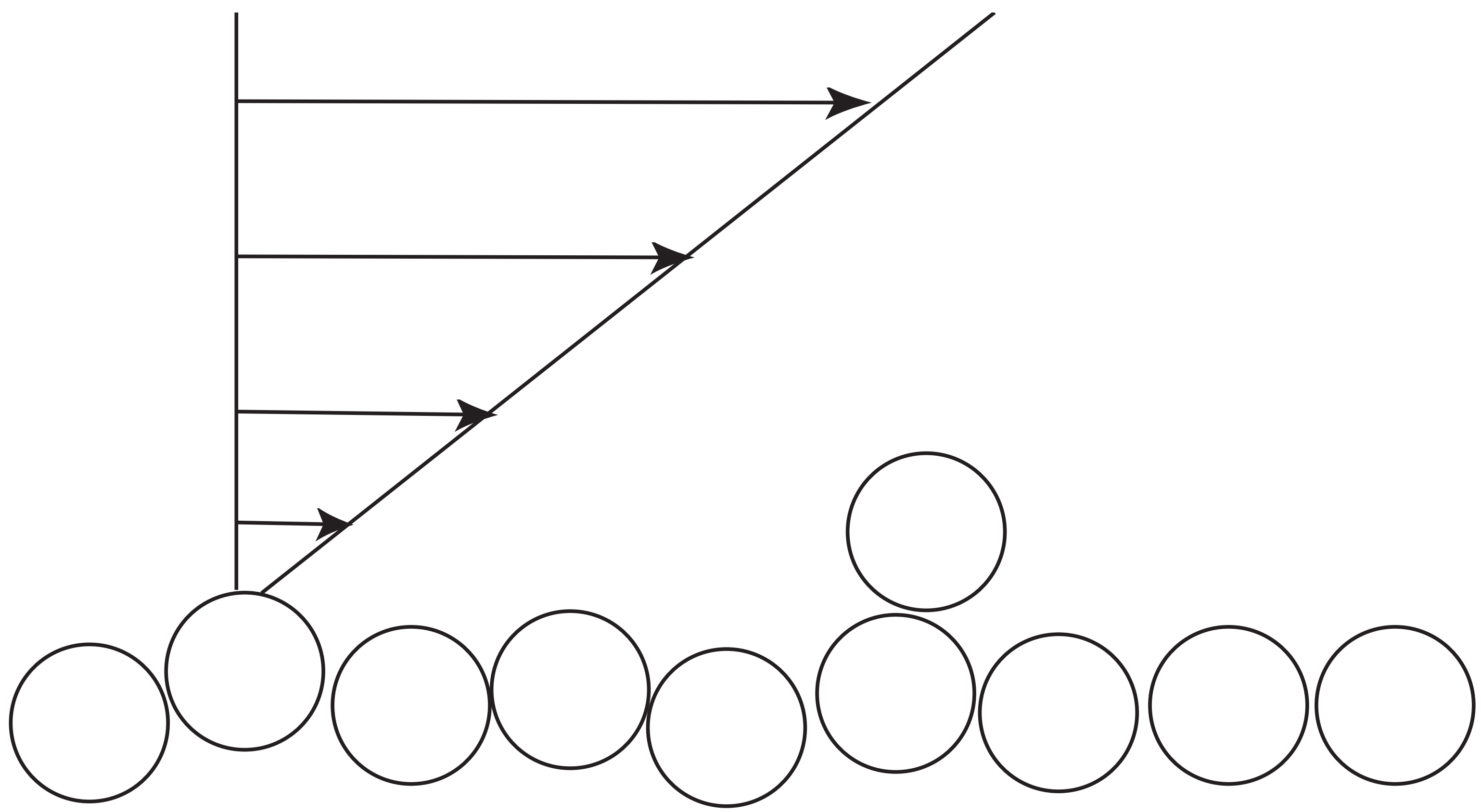

Stress larger than a threshold $\tau > \tau_s$

Shields number $$\frac{\tau}{(\rho_p - \rho) g D}$$

Erosion Model

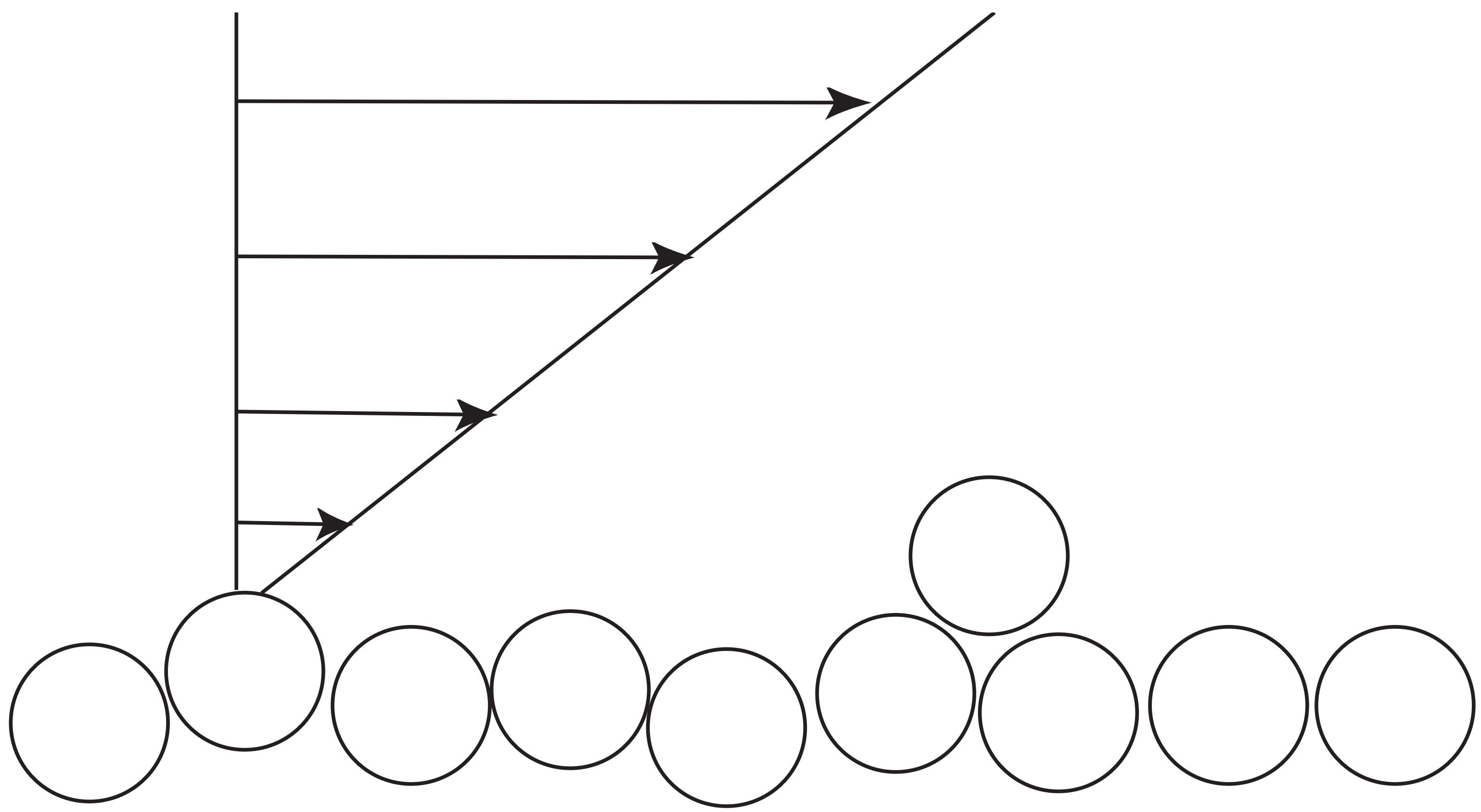

Stress larger than a threshold $\quad \tau > \tau_s$

Shields number $\quad \dfrac{\tau}{(\rho_p - \rho) g D}$

Erosion Model

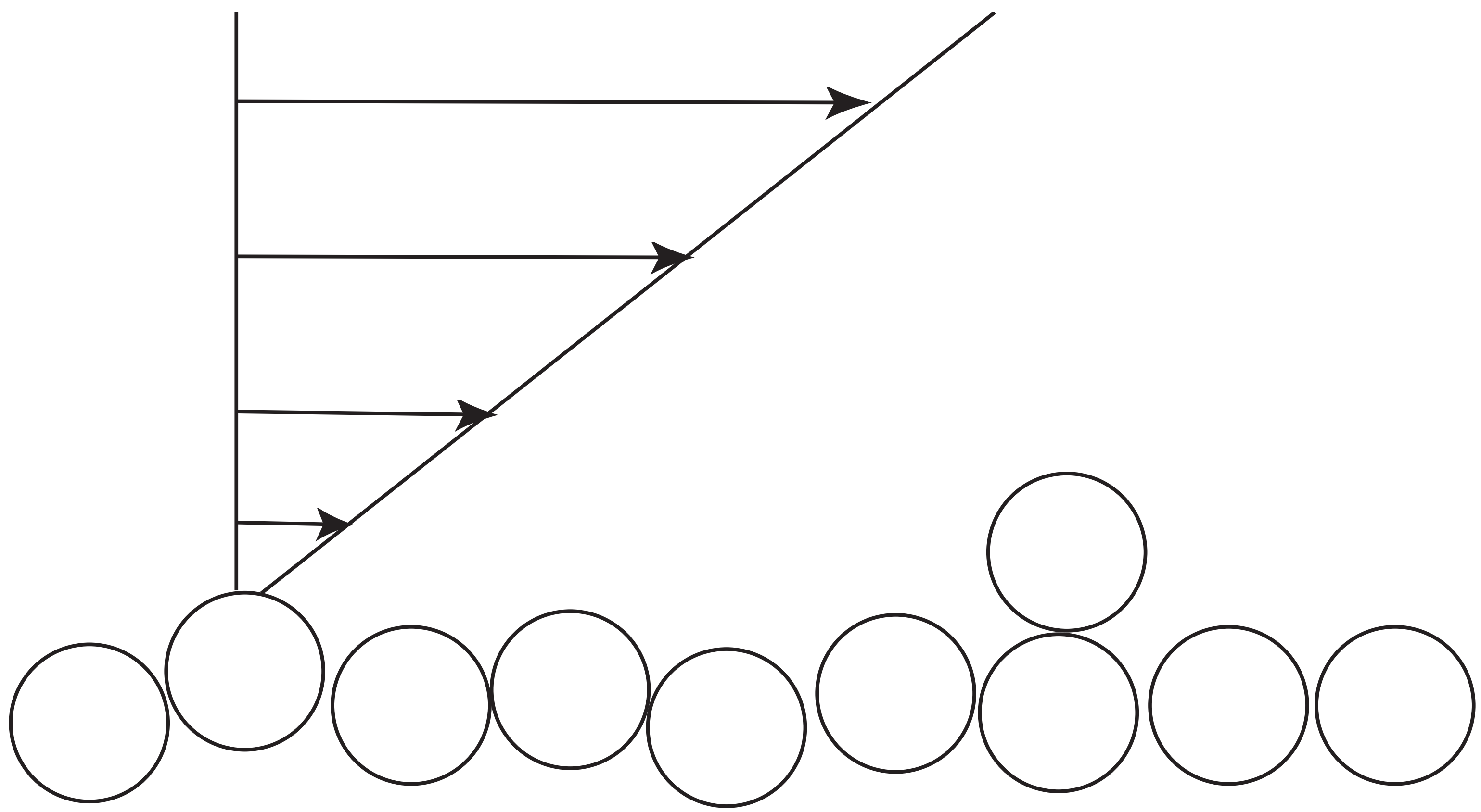

Stress larger than a threshold $\tau > \tau_s$

Shields number $$\frac{\tau}{(\rho_p - \rho) g D}$$

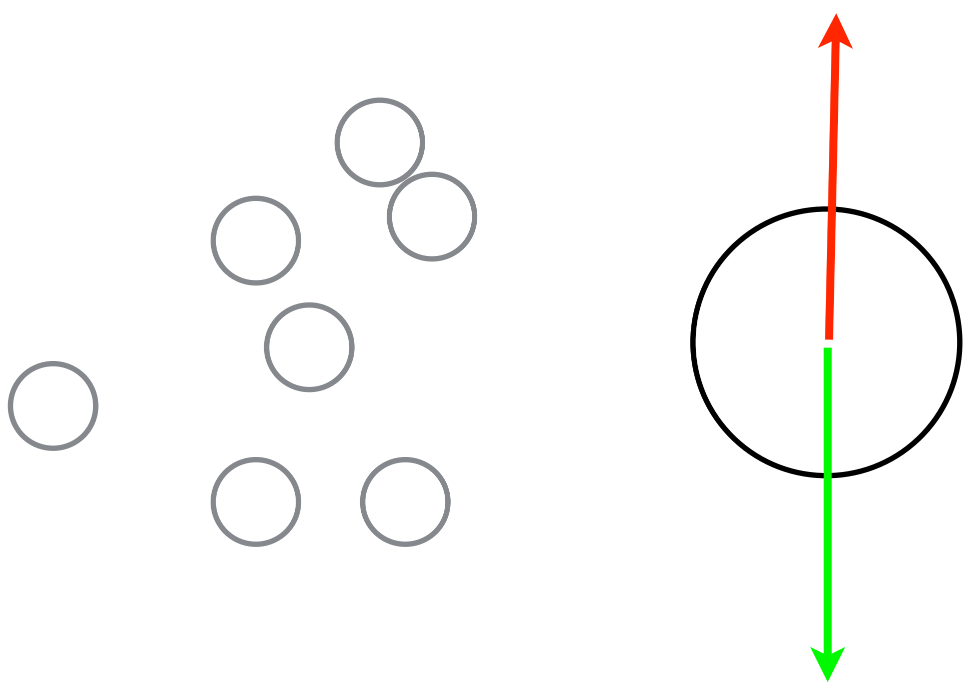

free fall equilibrium

$$\frac{4}{3}\pi(\Delta\rho)R^3 g = 6\pi\eta R V_s$$

terminal velocity

$$V_s = \frac{d^2}{18\eta}(\Delta\rho)g$$

characteristic flux

$$Q_s = \frac{d^3}{\eta}(\Delta\rho)g$$

Lagrangian   dilute

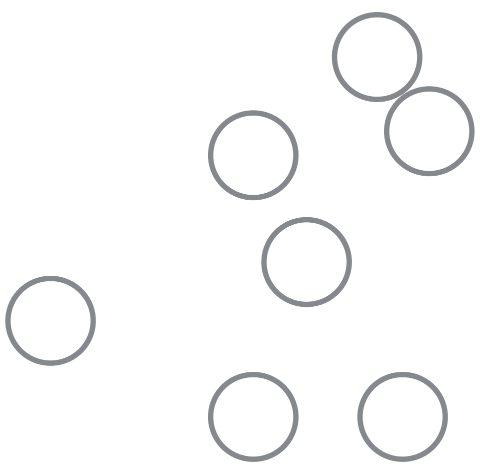

Basset historic term

$$\sigma_{xy} = -\sqrt{\frac{\eta\rho}{\pi}} \int_{-\infty}^{t} \frac{\mathrm{d}u(\tau)}{\mathrm{d}\tau} \frac{\mathrm{d}\tau}{\sqrt{(t-\tau)}};$$

added mass/ acceleration

Turbulent Dispersed
Multiphase Flow

S. Balachandar[1] and John K. Eaton[2]

Lagrangian dilute

feel each other

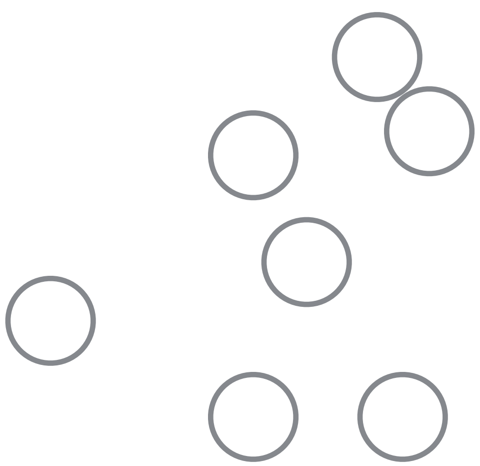

The continuum-mechanical modeling of sediments depends on its compaction, the particle volume fraction

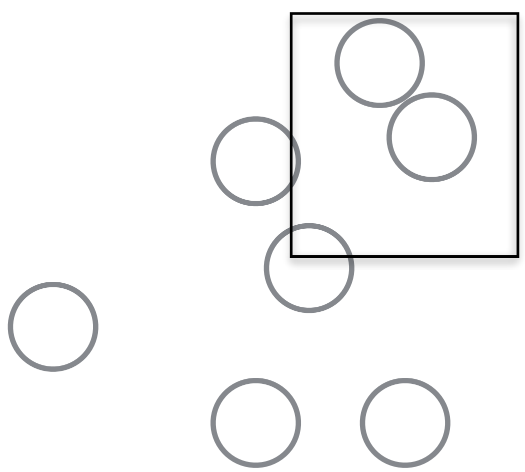

$$\phi = \frac{\text{volume of particules}}{\text{volume}}$$

if ϕ is smaller than the random loose packing with $\phi_m \approx 0.50$ concentrated suspension

if ϕ is larger than the random close packing with $\phi_M \approx 0.65$ the sediment behaves as a poro-elastic solid.

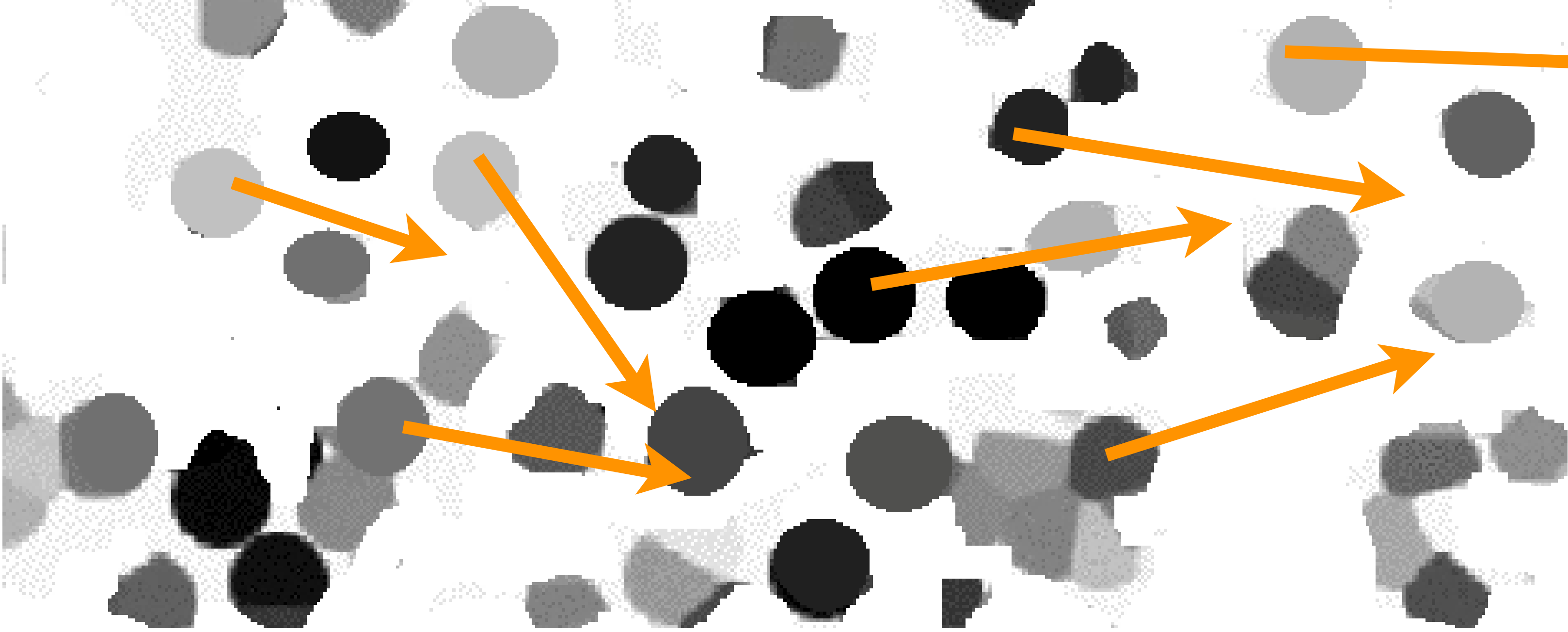

$\phi < \phi_m \approx 0.50$

from discrete to continuum

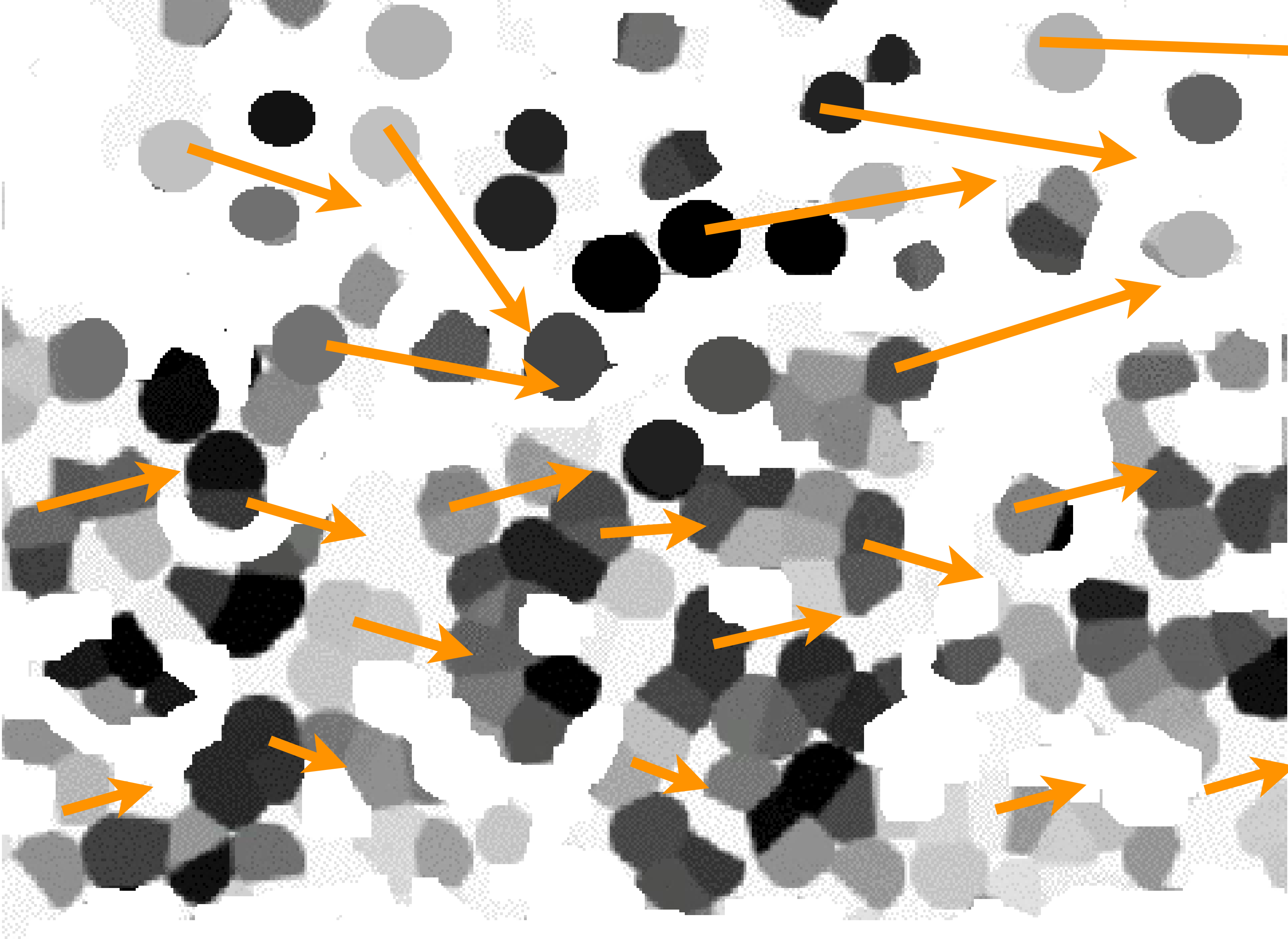

grains

suspension

$\phi < \phi_m \approx 0.50$

dense

$\phi_m \approx 0.50 < \phi < \phi_M \approx 0.65$

from discrete to continuum

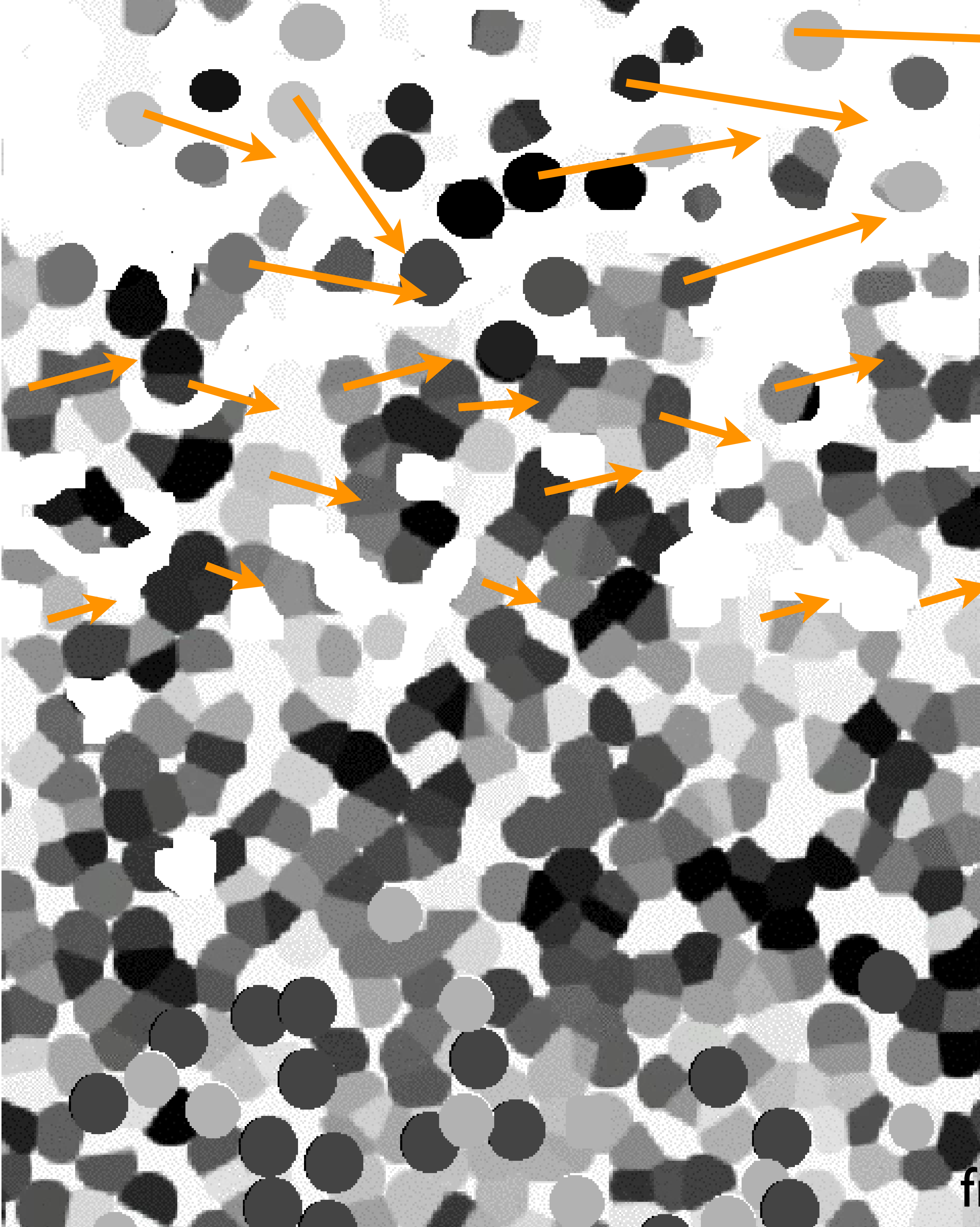

grains

suspension

$\phi<\phi_m \approx 0.50$

dense

$\phi_m \approx 0.50 < \phi < \phi_M \approx 0.65$

fixed

from discrete to continuum

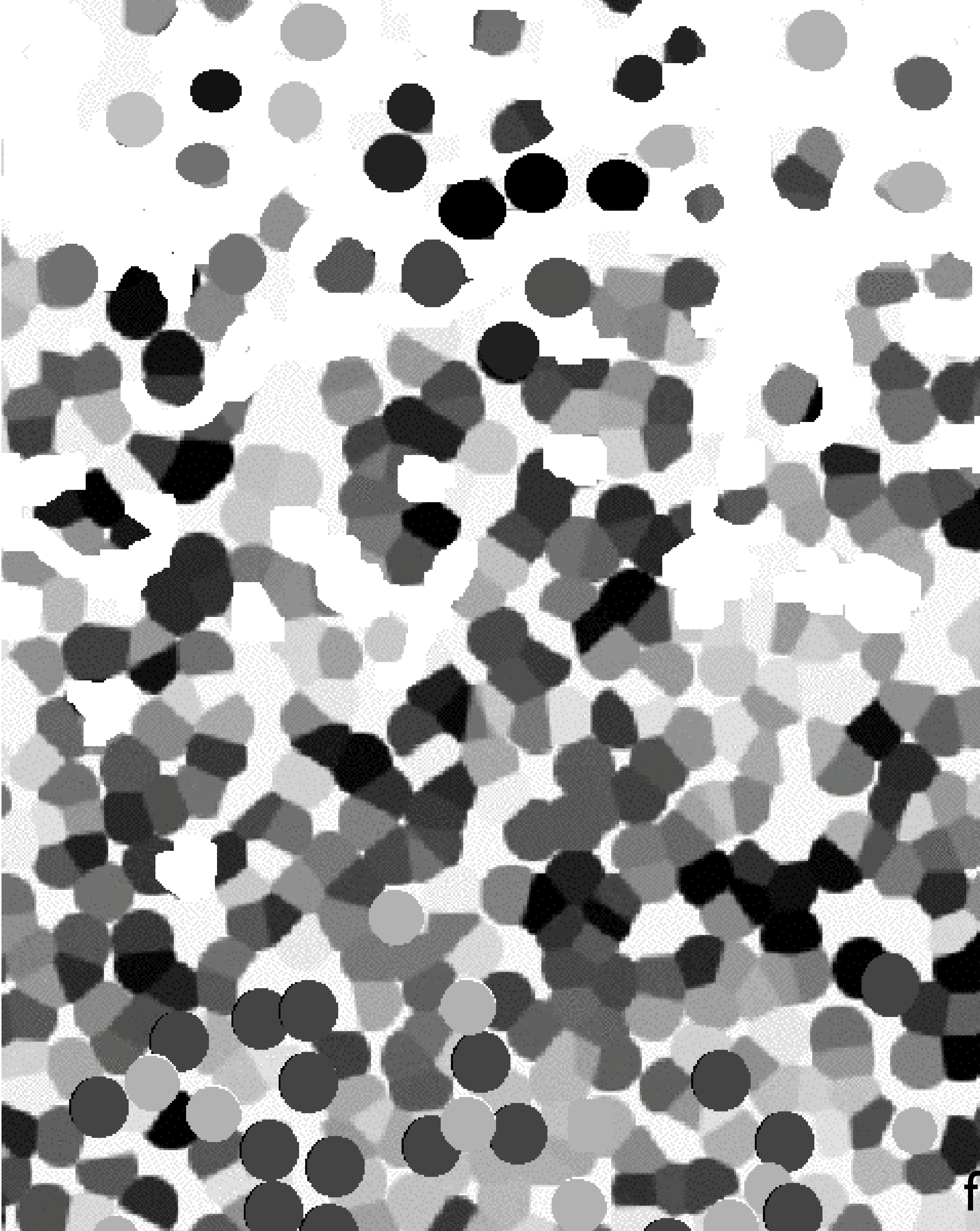

grains

suspension

$\phi < \phi_m \approx 0.50$

dense

$\phi_m \approx 0.50 < \phi < \phi_M \approx 0.65$

fixed

from discrete to continuum

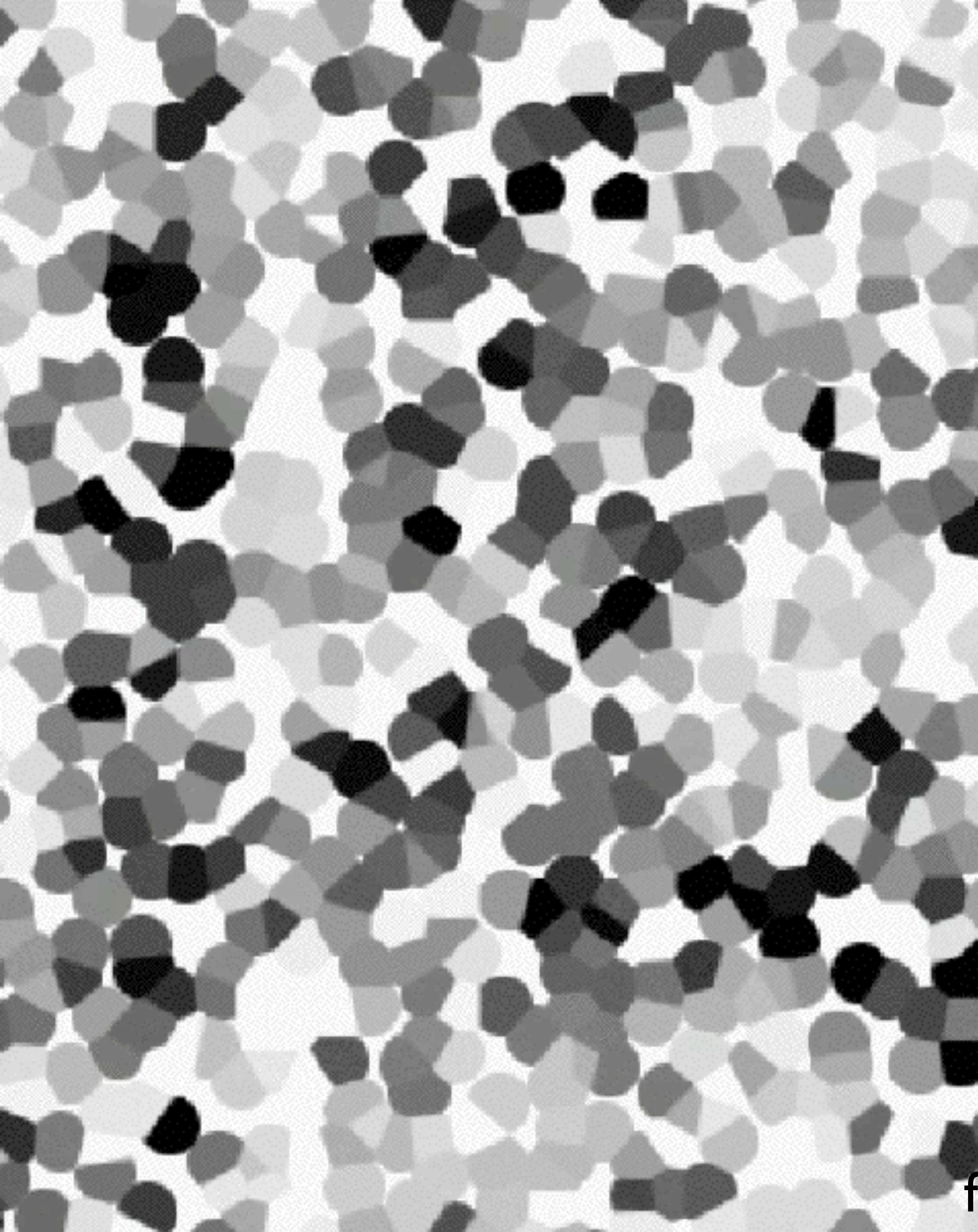

~~grains~~

continnum model

from discrete to continuum

Jean le Rond ∂'Alembert 1717-1783

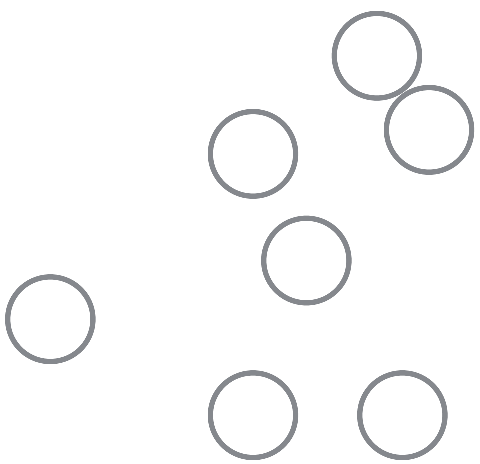

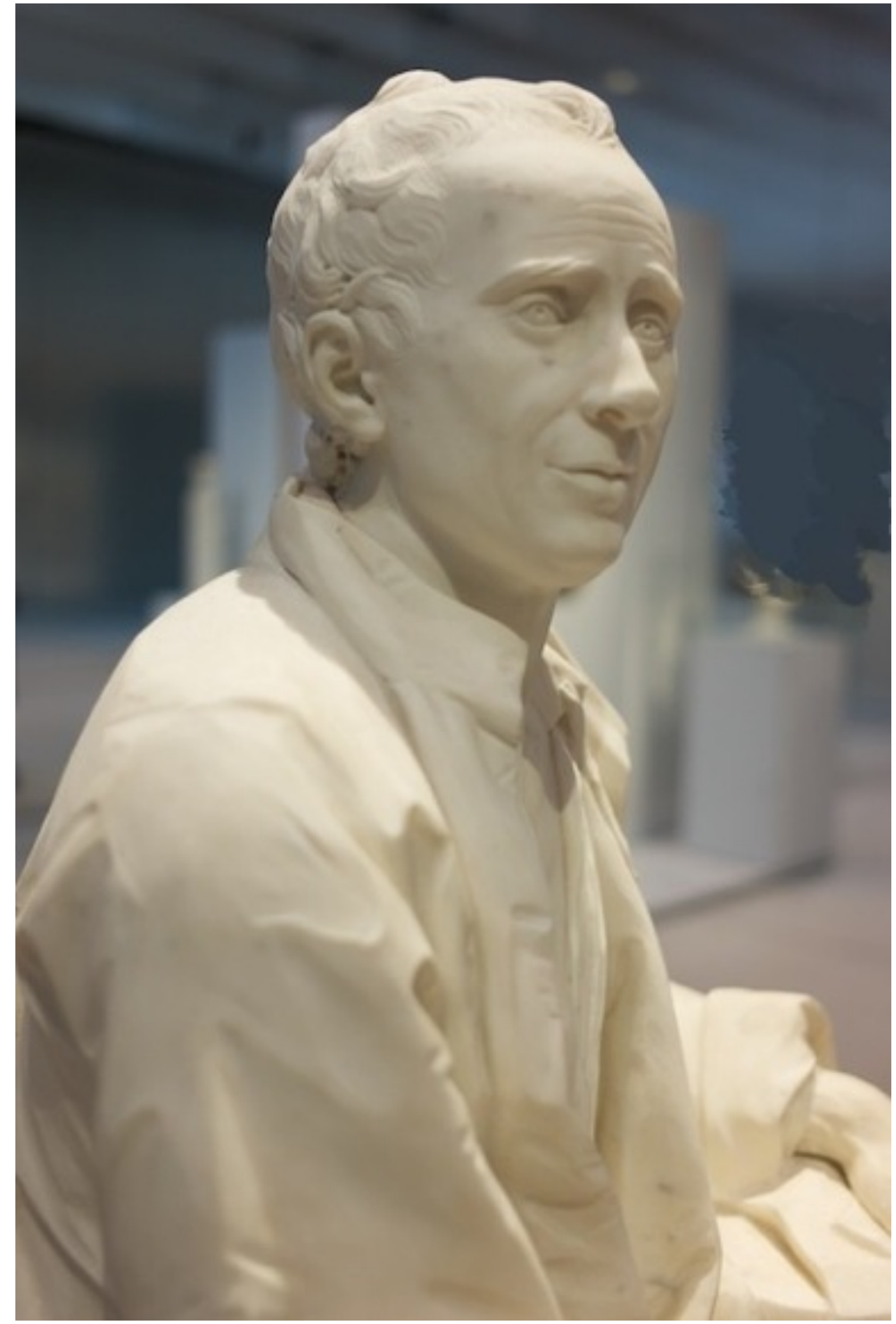

introduction of «continuum media»

Continuum approach

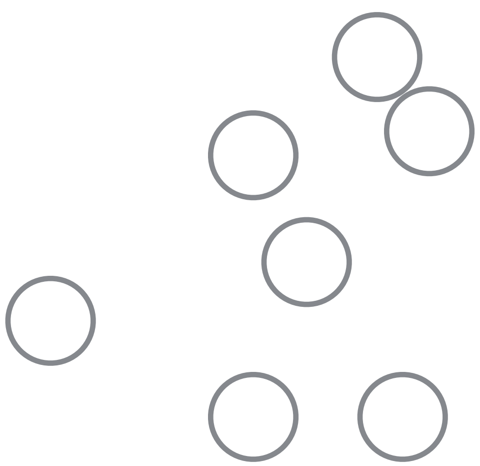

ensemble average

distribution function

volumic average

R. Jackson

D. Lhuillier

ergodicity…

Continuum approach

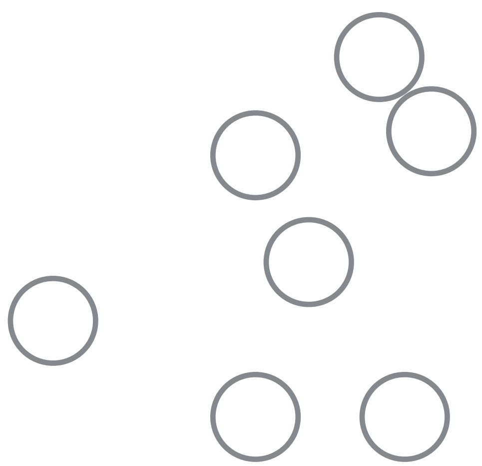

ensemble average

distribution function

volumic average

decompose : mean+ fluctuation

$$u_i =< u_i > +u_i'$$
$$< u_i u_j >=< (< u_i > +u_i')(< u_j > +u_j') >$$
$$< u_i u_j >=< u_i >< u_j > + < u_i' u_j' > +0 < u_i > +0 < u_j >$$

Continuum approach

$particle\ \ volume\ \ fraction\ \ \phi$

volume fraction of the carrier liquid 1-ϕ

flow is supposed incompressible

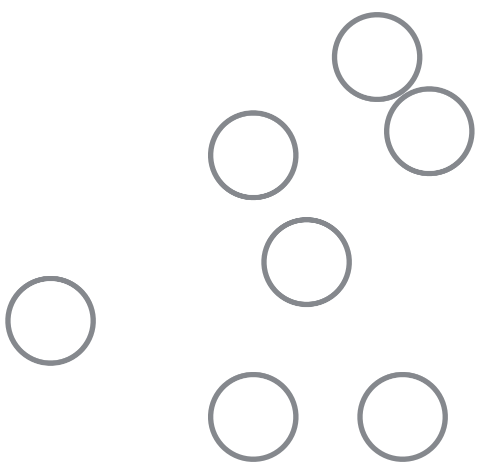

$$\frac{\partial \phi}{\partial t} + \nabla \cdot (\phi \mathbf{V}^p) = 0\ ,$$

$$\nabla \cdot \mathbf{V} = 0\ , \qquad \mathbf{V} = \phi \mathbf{V}^p + (1-\phi)\mathbf{V}^f$$

volume-averaged velocity of the mixture.

Continuum approach

$$particle\ \ volume\ \ fraction\ \ \phi$$

volume fraction of the carrier liquid 1-ϕ

flow is supposed incompressible

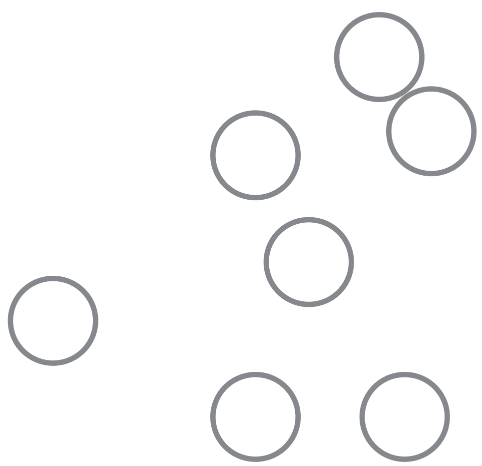

$$\frac{\partial \phi}{\partial t} + \nabla \cdot (\phi \mathbf{V}^p) = 0\ ,$$

$$\nabla \cdot \mathbf{V} = 0\ , \qquad \mathbf{V} = \phi \mathbf{V}^p + (1 - \phi)\mathbf{V}^f$$

volume-averaged velocity of the mixture.

mean value $$< u_i u_j > = < u_i > < u_j > + < u_i' u_j' >$$

total derivative $$\left\{ \begin{aligned} & \phi \rho_p \frac{d_p \mathbf{u}_p}{dt} + \nabla \cdot (\phi \rho_p < \mathbf{u}_p' \otimes \mathbf{u}_p' >) \\ & (1 - \phi)\rho_f \frac{d_f \mathbf{u}_f}{dt} + \nabla \cdot ((1 - \phi)\rho_f < \mathbf{u}_f' \otimes \mathbf{u}_f' >) \end{aligned} \right.$$

Continuum approach
particule phase

D. Lhuillier

constraints exerted by the particules

constraints exerted by the fluid

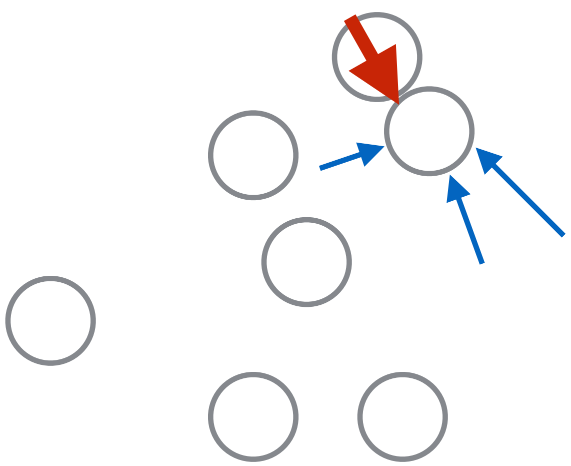

$$\boxed{\nabla\cdot\sigma^{pp}} + \boxed{\mathbf{F}^{pf} - \phi\nabla p_f} + \phi\rho_p\mathbf{g}$$

n mean nbr of part./vol.

$$\mathbf{F}^{pf} = n < \oint(\sigma^{f0} + p_f I)\cdot\mathbf{n}ds >$$

$$\boxed{\phi\rho_p\frac{d_p\mathbf{u}_p}{dt} + \nabla\cdot(\phi\rho_p < \mathbf{u}_p' \otimes \mathbf{u}_p' >) = \nabla\cdot\sigma^{pp} + \mathbf{F}^{pf} - \phi\nabla p_f + \phi\rho_p\mathbf{g}}$$

fluid phase

$$\boxed{\nabla\cdot\tau^f}\ \boxed{- \mathbf{F}^{pf} - (1-\phi)\nabla p_f} + (1-\phi)\rho_f\mathbf{g}$$

$$\boxed{(1-\phi)\rho_f\frac{d_f\mathbf{u}_f}{dt} + \nabla\cdot((1-\phi)\rho_f < \mathbf{u}_f' \otimes \mathbf{u}_f' >) = \nabla\cdot\tau^f - \mathbf{F}^{pf} - (1-\phi)\nabla p_f + (1-\phi)\rho_f\mathbf{g}}$$

Continuum approach

Jackson buoyant decomposition

$$\mathbf{F}^{pf} = \mathbf{F} + \mathbf{F}^{v} \quad , \quad \tau^{f} = \tau + \tau^{v} \, . \qquad \mathbf{F}^{v} = \phi \nabla \cdot \tau^{v} + (1-\phi)\mathbf{f}^{v}$$

$$\phi\rho_p \frac{d_p \mathbf{u}_p}{dt} = \phi\rho_f \frac{d_f \mathbf{u}_f}{dt} + \nabla \cdot \sigma^p + \boxed{\mathbf{f}^v} + \phi(\rho_p - \rho_f)\mathbf{g}$$

$$\rho_f \frac{d_f \mathbf{u}_f}{dt} = \nabla \cdot \tau^v - \boxed{\mathbf{f}^v} - \nabla p_f + \rho_f \mathbf{g} \, .$$

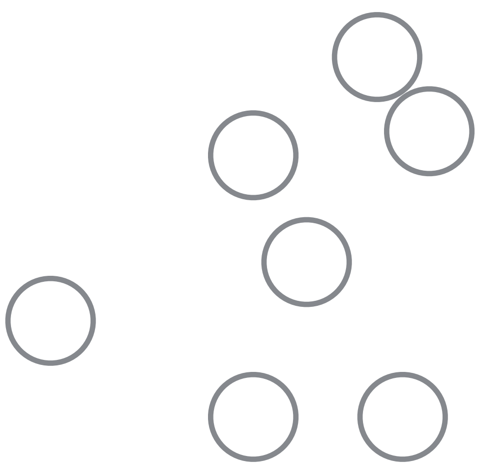

Average value of the resultant force exerted by the fluid on the particule

The form of one contribution to this local average force exerted by the fluid on a particle, namely the buoyancy, is usually regarded as fairly obvious, so **f** is next decomposed without further ado into a sum of the buoyancy force and all remaining contributions. Unfortunately, however, this decomposition is not completely unambiguous. In this connection the description of buoyancy by a sixteenth century shipwright is interesting:

The syde [of a ship] being rounde and full, it is the more boyenter a great deale. (W. Bourne. Treas. for Trav., 1578)

Jackson 00

Continuum approach

Jackson buoyant decomposition

$$\mathbf{F}^{pf} = \mathbf{F} + \mathbf{F}^{v} \quad , \quad \tau^{f} = \tau + \tau^{v} \ . \qquad \mathbf{F}^{v} = \phi \nabla \cdot \tau^{v} + (1-\phi)\mathbf{f}^{v}$$

$$\phi \rho_p \frac{d_p \mathbf{u}_p}{dt} = \phi \rho_f \frac{d_f \mathbf{u}_f}{dt} + \nabla \cdot \sigma^p + \boxed{\mathbf{f}^v} + \phi(\rho_p - \rho_f)\mathbf{g}$$

$$\rho_f \frac{d_f \mathbf{u}_f}{dt} = \nabla \cdot \tau^v - \boxed{\mathbf{f}^v} - \nabla p_f + \rho_f \mathbf{g} \ .$$

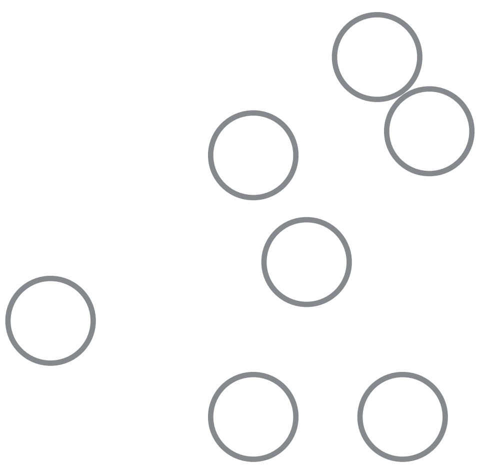

Average value of the resultant force exerted by the fluid on the particule

not so simple….

As an example of fallacious equations based on the partition (2.38) we consider the following pair, due to F[redacted]ro (1987):

Jackson 00

Continuum approach

$$\phi\rho_p \frac{d_p \mathbf{u}_p}{dt} = \phi\rho_f \frac{d_f \mathbf{u}_f}{dt} + \nabla\cdot\sigma^p + \mathbf{f}^v + \phi(\rho_p - \rho_f)\mathbf{g}$$

$$\rho_f \frac{d_f \mathbf{u}_f}{dt} = \nabla\cdot\tau^v - \mathbf{f}^v - \nabla p_f + \rho_f \mathbf{g}\ .$$

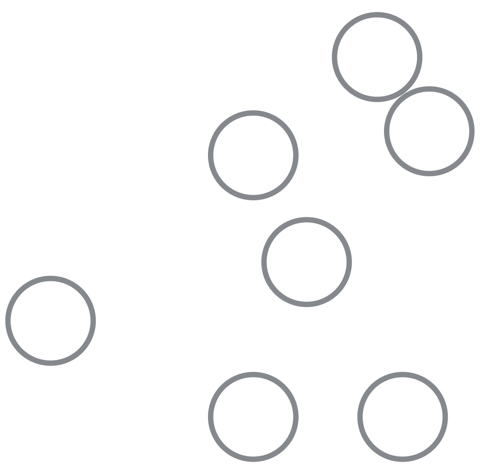

Continuum approach

$$\phi\rho_p \frac{d_p \mathbf{u}_p}{dt} = \phi\rho_f \frac{d_f \mathbf{u}_f}{dt} + \nabla \cdot \sigma^p + \mathbf{f}^v + \phi(\rho_p - \rho_f)\mathbf{g}$$

$$\rho_f \frac{d_f \mathbf{u}_f}{dt} = \nabla \cdot \tau^v - \mathbf{f}^v - \nabla p_f + \rho_f \mathbf{g} \ .$$

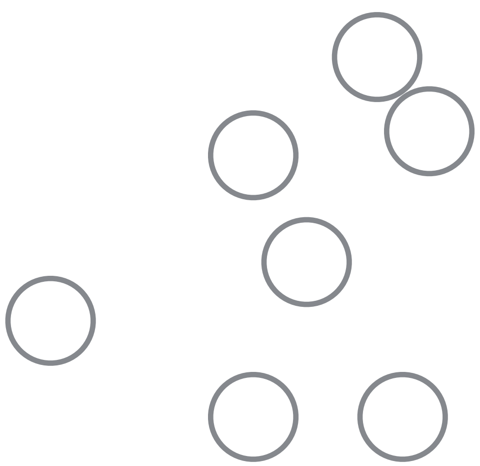

force

$$\mathbf{f}^v = -\frac{\phi\eta_f}{d^2} \ \lambda(\phi)(\mathbf{V^p} - \mathbf{V}) \ .$$

Darcy

Continuum approach

$$\phi\rho_p \frac{d_p \mathbf{u}_p}{dt} = \phi\rho_f \frac{d_f \mathbf{u}_f}{dt} + \nabla\cdot\sigma^p + \mathbf{f}^v + \phi(\rho_p - \rho_f)\mathbf{g}$$

$$\rho_f \frac{d_f \mathbf{u}_f}{dt} = \nabla\cdot\tau^v - \mathbf{f}^v - \nabla p_f + \rho_f \mathbf{g}\ .$$

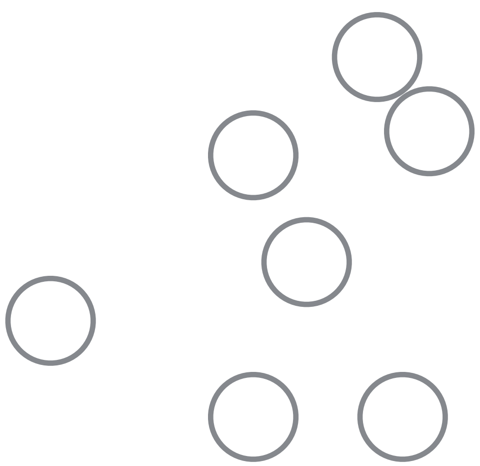

force

$$\mathbf{f}^v = -\frac{\phi\eta_f}{d^2}\ \lambda(\phi)(\mathbf{V^p} - \mathbf{V}) - \phi\nabla(\eta_f \nu(\phi)\dot{\gamma})$$

Darcy Resuspension

Darcy

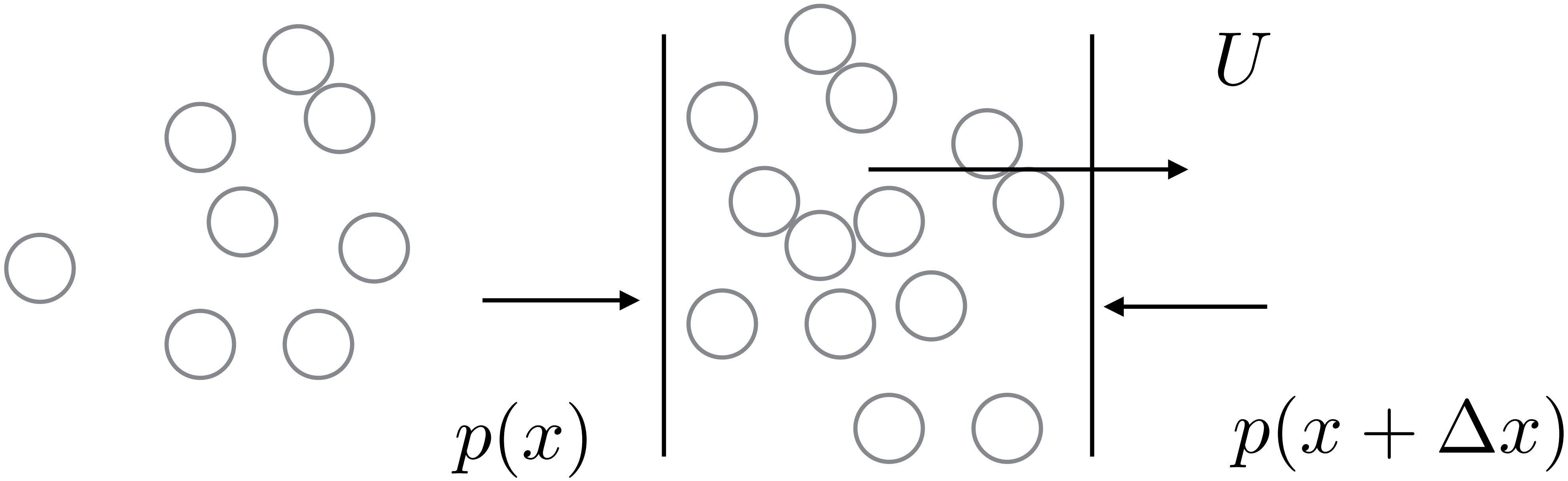

$$p(x+\Delta x) - p(x) \simeq -\Delta x \frac{\eta}{R^2} U$$

Resuspension Leighton Acrivos

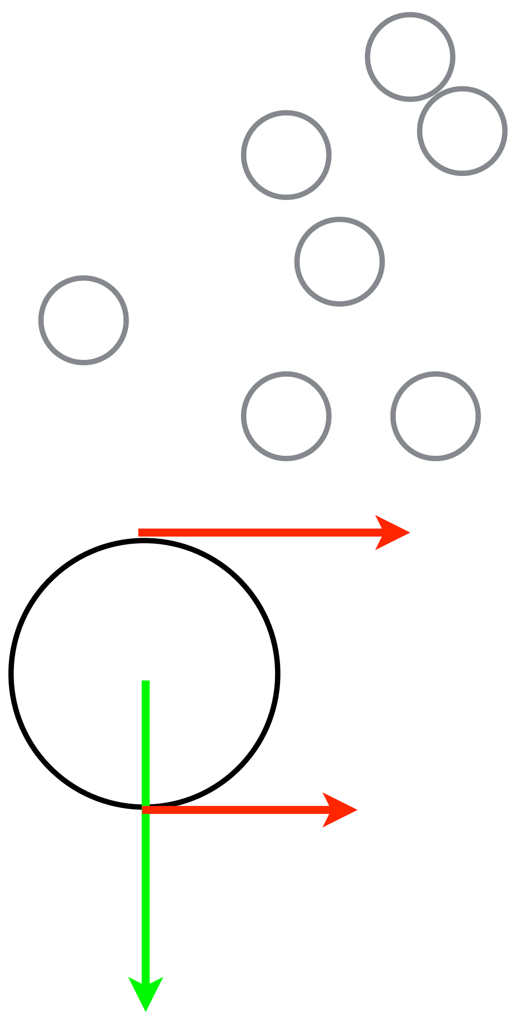

free fall equilibrium in shear

$$-\frac{4}{3}\pi(\Delta\rho)R^3 g = (\pi\eta R^2)(\dot{\gamma}(y+R)\phi(y+R) - \dot{\gamma}(y)\phi(y))$$

free fall flux due to shear

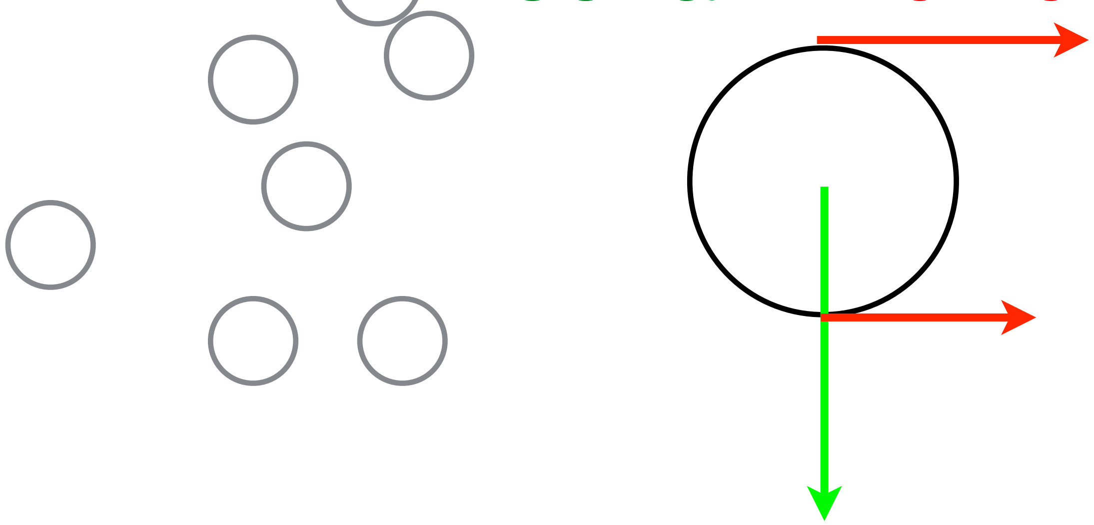

terminal velocity

$$V_s = \frac{d^2}{18\eta}(\Delta\rho)g$$

$$\frac{4}{3\eta}(\Delta\rho)R^g + (R^2)\dot{\gamma}(y)\frac{\partial}{\partial y}\phi = 0$$

Continuum approach

$$\phi\rho_p \frac{d_p \mathbf{u}_p}{dt} = \phi\rho_f \frac{d_f \mathbf{u}_f}{dt} + \nabla \cdot \sigma^p + \mathbf{f}^v + \phi(\rho_p - \rho_f)\mathbf{g}$$

$$\rho_f \frac{d_f \mathbf{u}_f}{dt} = \nabla \cdot \tau^v - \mathbf{f}^v - \nabla p_f + \rho_f \mathbf{g}\ .$$

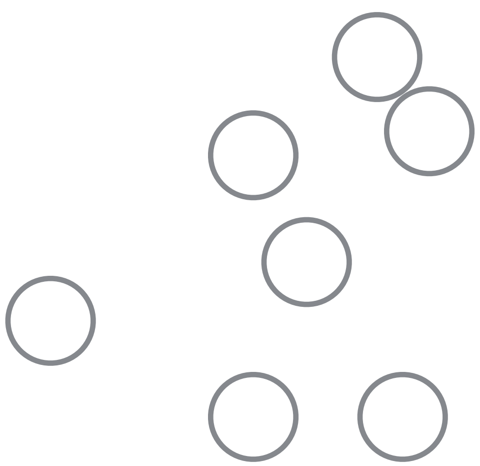

force

$$\mathbf{f}^v = -\frac{\phi\eta_f}{d^2}\ \lambda(\phi)(\mathbf{V^p} - \mathbf{V}) - \phi\nabla(\eta_f \nu(\phi)\dot{\gamma})$$

Darcy Resuspension

Continuum approach

$$\phi\rho_p \frac{d_p \mathbf{u}_p}{dt} = \phi\rho_f \frac{d_f \mathbf{u}_f}{dt} + \nabla \cdot \sigma^p + \mathbf{f}^v + \phi(\rho_p - \rho_f)\mathbf{g}$$

$$\rho_f \frac{d_f \mathbf{u}_f}{dt} = \nabla \cdot \tau^v - \mathbf{f}^v - \nabla p_f + \rho_f \mathbf{g}\ .$$

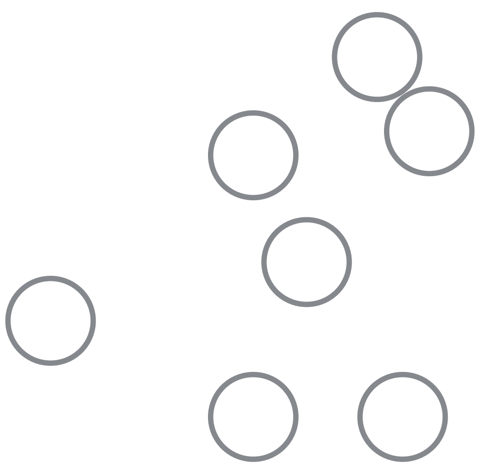

force

$$\mathbf{f}^v = -\frac{\phi\eta_f}{d^2}\ \lambda(\phi)(\mathbf{V^p} - \cancel{\mathbf{V}}) - \phi\nabla(\eta_f \nu(\phi)\dot{\gamma})$$

Darcy

particules sediment

Resuspension

$\eta_f \dot{\gamma} \partial_y (\nu(\phi))$

First simple case

J. Fluid Mech. (2002), vol. 452, pp. 303–323. © 2002 Cambridge University Press
DOI: 10.1017/S0022112001006747 Printed in the United Kingdom

Instability of a bed of particles sheared by a viscous flow

By FRANÇOIS CHARRU AND HÉLÈNE MOUILLERON-ARNOULD

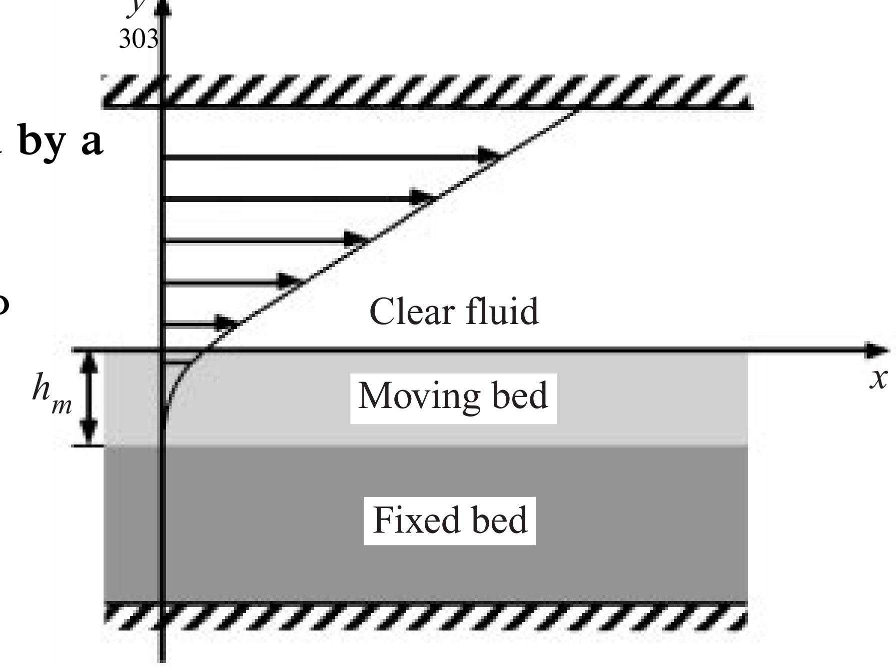

FIGURE 6. Sketch of the Couette resuspension flow.

$$\begin{cases} \partial_y(\mu \partial_y U) = 0, \\ f(\phi) V_S \phi + (\gamma d^2/4) D(\phi) \partial_y \phi = 0. \end{cases}$$

free fall flux due to shear

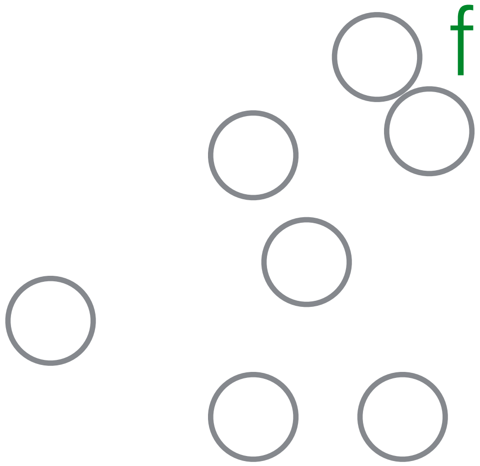

$$f(\phi) = \frac{1-\phi}{\mu_r(\phi)}, \quad \mu_r(\phi) = \left(1 + \frac{1.5\phi}{1-\phi/\phi_0}\right)^2, \quad D(\phi) = \tfrac{1}{3}\phi^2(1 + \tfrac{1}{2}\exp(8.8\phi)),$$

random loose packing

$$\phi_0 = 0.55$$

$$\frac{h_u}{d} = \tfrac{9}{2}\Theta \int_0^{\phi_0} \left(\frac{1}{\phi} - \frac{1}{\phi_0}\right) \frac{D}{f\mu_r} \, \mathrm{d}\phi \approx 1.86\Theta,$$

$$\frac{h_l}{d} = \tfrac{9}{2}\Theta \int_0^{\phi_0} \frac{1}{\phi_0} \frac{D}{f\mu_r} \, \mathrm{d}\phi \approx 11.8\Theta.$$

$$\boxed{\frac{Q}{V_S d} = \frac{1}{V_S d} \int_{-h_l}^{h_u} \phi U \, \mathrm{d}y = C\Theta^3,}$$

$$C = 4(\tfrac{9}{2})^3 \int_0^{\phi_0} \left\{ \frac{D}{f\mu_r} \int_{\phi}^{\phi_0} \frac{1}{\phi} \frac{D}{f\mu_r^2} \, \mathrm{d}\phi \right\} \mathrm{d}\phi \approx 7.5.$$

no threshold

AN EXPERIMENTAL STUDY OF VISCOUS RESUSPENSION IN A PRESSURE-DRIVEN PLANE CHANNEL FLOW

U. SCHAFLINGER, A. ACRIVOS† and H. STIBI

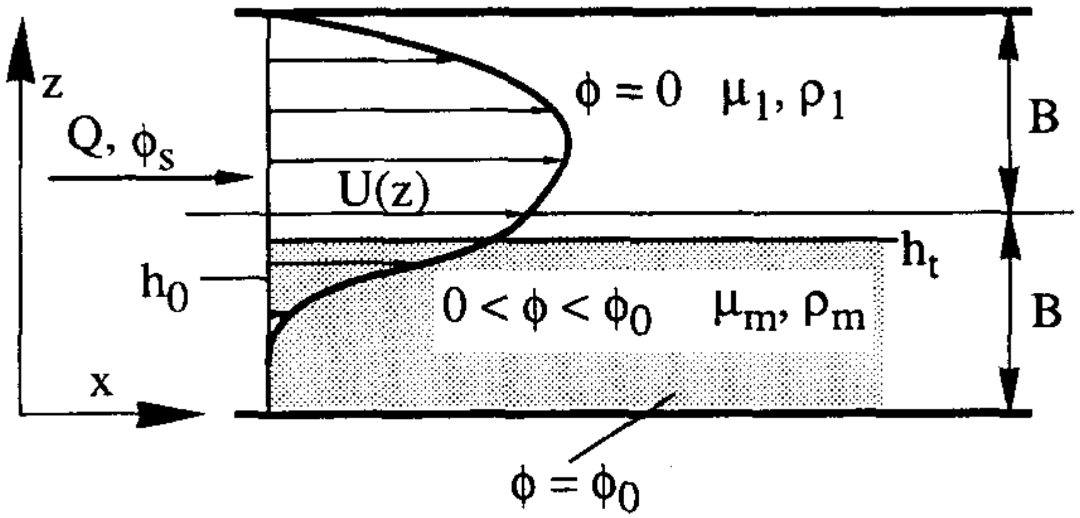

Figure 1. Schematic of a 2D Hagen–Poiseuille flow indicating the notation.

For uni-directional fully-developed laminar flows, the particle flux due to a gradient in concentration and a gradient in the shear stress τ is balanced by the particle flux due to gravity, hence

$$\frac{2\phi a^2 \mathbf{g}\epsilon}{9\nu_1} f(\phi) + \dot{\gamma}(z)a^2\hat{D}\frac{\mathrm{d}\phi}{\mathrm{d}z} + \dot{\gamma}(z)a^2\tilde{D}\frac{1}{\tau}\frac{\mathrm{d}\tau}{\mathrm{d}z} = 0, \quad [1]$$

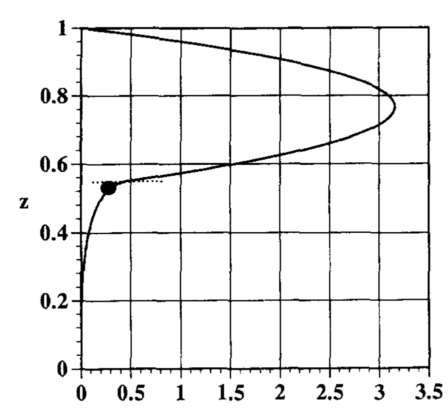

Figure 10. Measured interfacial velocity (●) and comparison with the theoretical velocity profile (solid line). The dotted line marks the position of the theoretically predicted interface. $\kappa = 0.004$, $\phi_s = 0.016$, $\rho_1 = 963$ kg/m^3, $\nu_1 = 2.86 \times 10^{-6}$ m^2/s (water–ethanol mixture); $a = 185$ μm, $\rho_2 = 1043$ kg/m$_3$ (polystyrene beads).

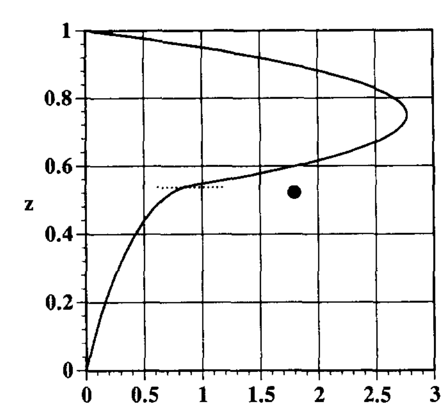

Figure 11. Measured interfacial velocity (●) and comparison with the theoretical velocity profile (solid line). The dotted line marks the position of the theoretically predicted interface. $\kappa = 0.01$, $\phi_s = 0.065$, $\rho_1 = 963$ kg/m^3, $\nu_1 = 2.86 \times 10^{-6}$ m^2/s (water–ethanol mixture); $a = 185$ μm, $\rho_2 = 1043$ kg/m$_3$ (polystyrene beads).

Reynolds of the particule

$$Re = \frac{d^2}{\nu}\frac{\partial u}{\partial y}$$

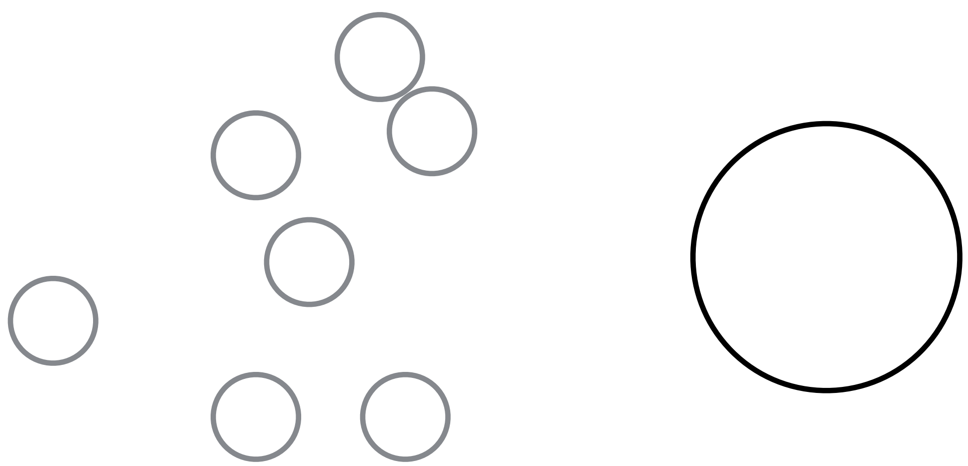

terminal velocity

$$V_s = \frac{d^2}{18\eta}(\Delta\rho)g$$

Reynolds associated= Galileo

$$Ga = \frac{(\Delta\rho)gd^3}{\eta^2}$$

Shields number

$$\frac{\tau}{(\rho_p - \rho)gd} = \frac{Re}{Ga}$$

Coulomb friction

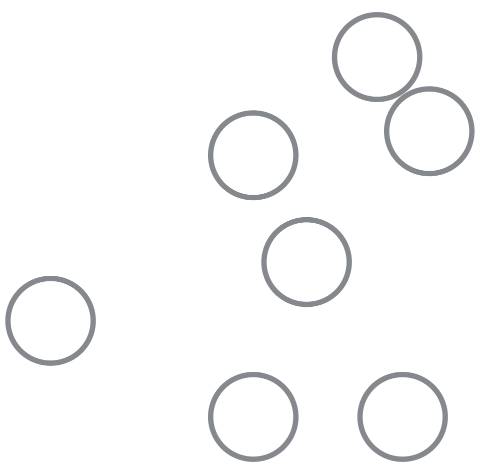

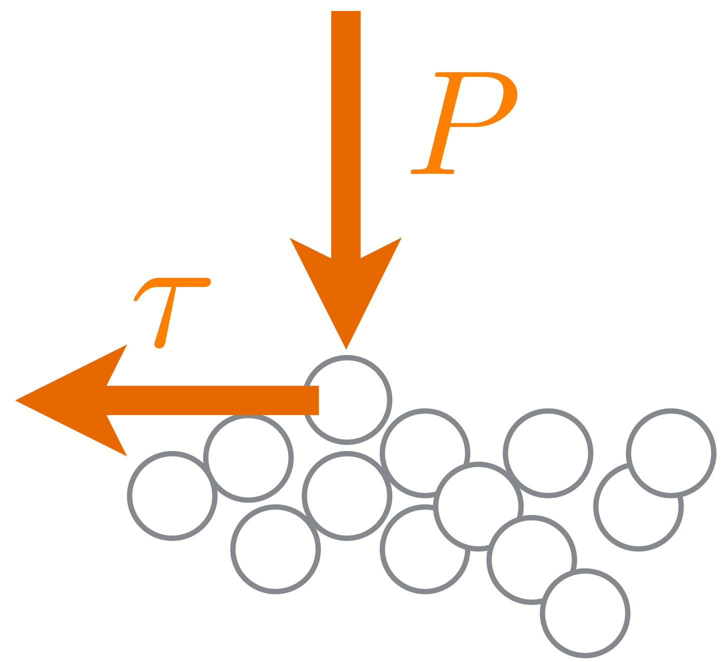

$$\tau = \mu P$$

$$\left.\begin{aligned} & u(y) \\ & \tau = \eta \frac{\partial u}{\partial y} \\ & \tau = \mu P \end{aligned}\right\} \quad \eta = \frac{\mu P}{\partial u / \partial y}$$

Ouiremi Aussillous Guazzelli

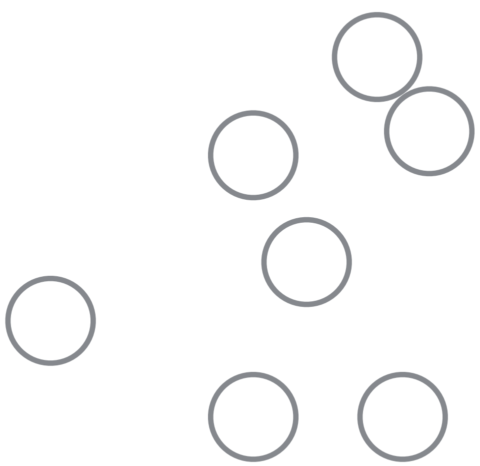

Sediment dynamics. Part 1. Bed-load transport 5

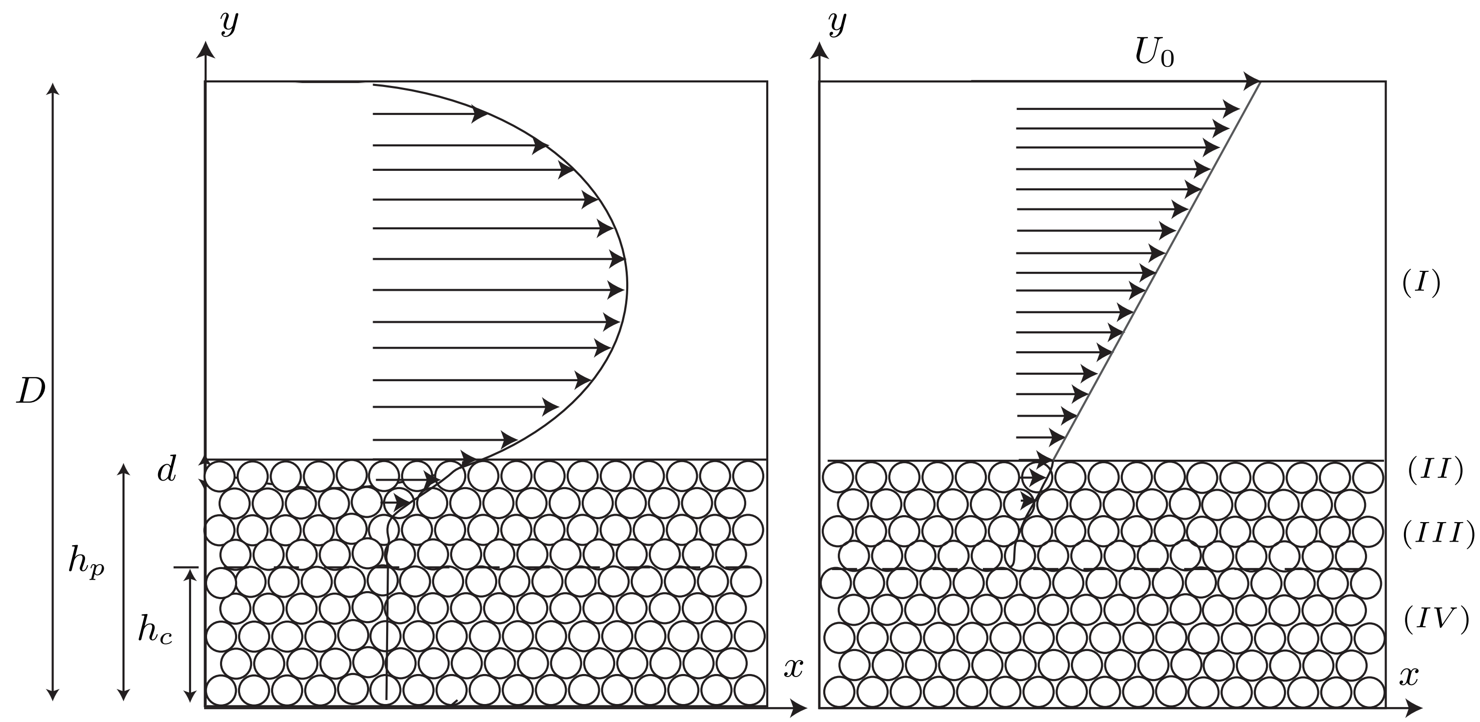

Figure 1. Sketch of a particle bed submitted to a Poiseuille (left) or a Couette (right) flow in a two dimensional channel.

Continuum approach
particule phase

constraints exerted by the particules

constraints exerted by the fluid

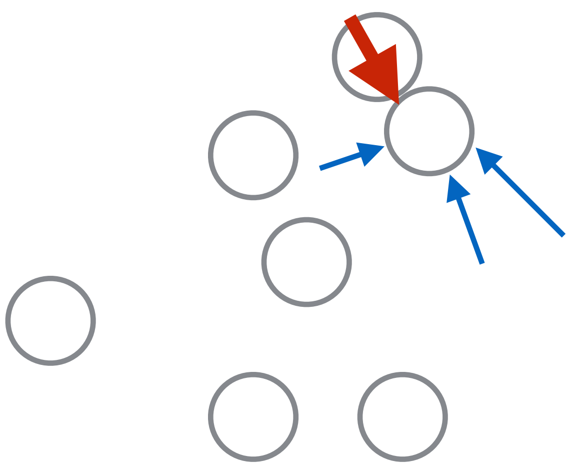

$$\boxed{\nabla \cdot \sigma^{pp}} + \boxed{\mathbf{F}^{pf} - \phi \nabla p_f} + \phi \rho_p \mathbf{g}$$

$$\mathbf{F}^{pf} = n < \oint (\sigma^{f0} + p_f I) \cdot \mathbf{n} ds >$$

$$\phi \rho_p \frac{d_p \mathbf{u}_p}{dt} + \nabla \cdot (\phi \rho_p < \mathbf{u}'_p \otimes \mathbf{u}'_p >) = \nabla \cdot \sigma^{pp} + \mathbf{F}^{pf} - \phi \nabla p_f + \phi \rho_p \mathbf{g}$$

fluid phase

$$\boxed{\nabla \cdot \tau^f} \boxed{- \mathbf{F}^{pf} - (1-\phi) \nabla p_f} + (1-\phi) \rho_f \mathbf{g}$$

$$(1-\phi) \rho_f \frac{d_f \mathbf{u}_f}{dt} + \nabla \cdot ((1-\phi) \rho_f < \mathbf{u}'_f \otimes \mathbf{u}'_f >) = \nabla \cdot \tau^f - \mathbf{F}^{pf} - (1-\phi) \nabla p_f + (1-\phi) \rho_f \mathbf{g}$$

Ouiremi Aussillous Guazzelli

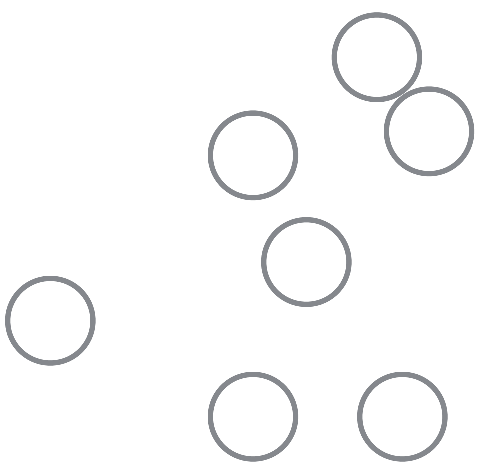

proposed a two phases problem (Jackson)

viscous law for the fluid

Darcy law for the interphase force

no resuspension

Coulomb friction for the dense phase

steady uniform flows

Ouiremi Aussillous Guazzelli

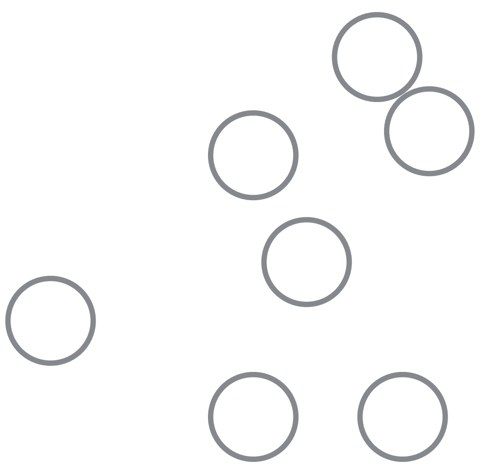

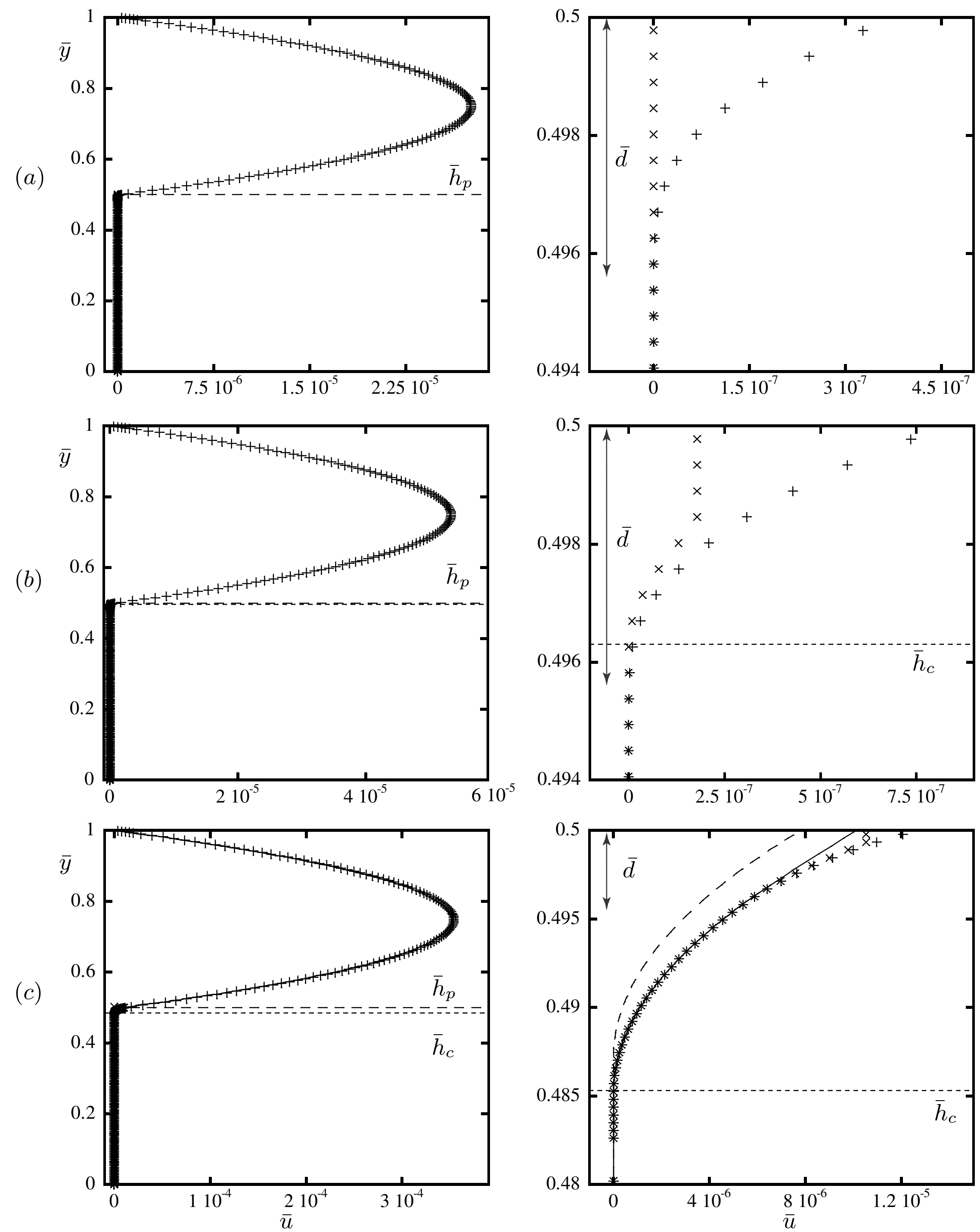

FIGURE 3. Numerical velocity profiles for the fluid (+) and the particles (×) in the case of particles of batch A in fluid 3 at $\phi_0 = 0.55$ and $\theta = 0.048$ (a), 0.094 (b), 0.62 (c) and analytical velocity profiles given in table 3 (solid line) and obtained by skipping region (II) (dashed line) (left). Blow-up of the profiles for the same conditions (right).

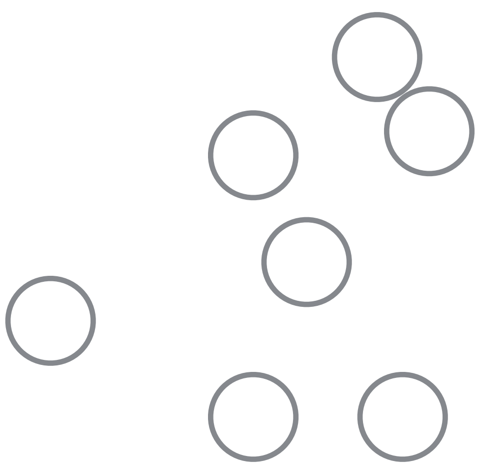

random loose packing, friction

$$\phi_0 = 0.55 \qquad \mu = 0.43$$

incipient motion

$$\theta^c = \frac{\partial \bar{p}^f}{\partial \bar{x}} + \mu \frac{\phi_0}{2} \approx \mu \frac{\phi_0}{2},$$

Critical Shear

$$\theta^c = 0.12$$

Transport law

$$q_p / \frac{\Delta \rho g d^3}{\eta_e} = \phi_0 \frac{\theta^c}{12} \left[\frac{\theta}{2\theta^c} \left(\frac{\theta^2}{\theta^{c2}} + 1 \right) - \frac{1}{5} \right],$$

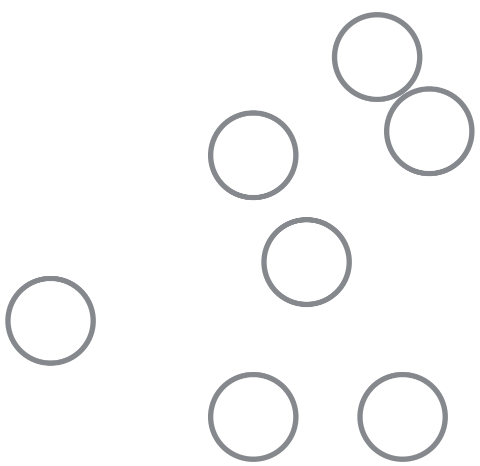

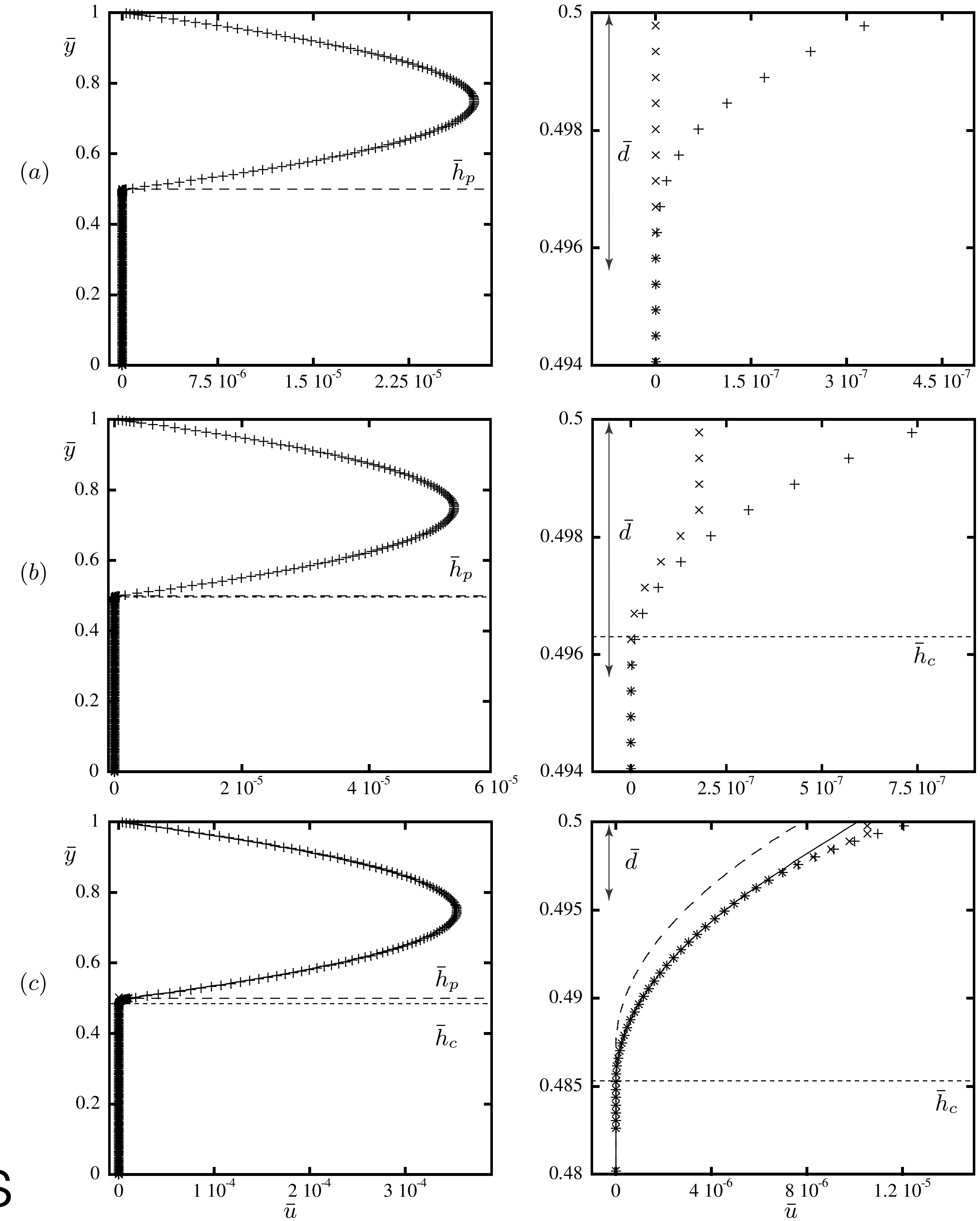

FIGURE 3. Numerical velocity profiles for the fluid (+) and the particles (×) in the case of particles of batch A in fluid 3 at $\phi_0 = 0.55$ and $\theta = 0.048$ (a), 0.094 (b), 0.62 (c) and analytical velocity profiles given in table 3 (solid line) and obtained by skipping region (II) (dashed line) (left). Blow-up of the profiles for the same conditions (right).

Transport law at small Shields

$$q_p / \frac{\Delta\rho g d^3}{\eta_e} = \phi_0 \left(\frac{\mu_s}{\mu_2}\right)^2 \frac{\theta^c}{24} \left(\frac{\theta}{\theta^c}\right)^3 .$$

Numerical resolution

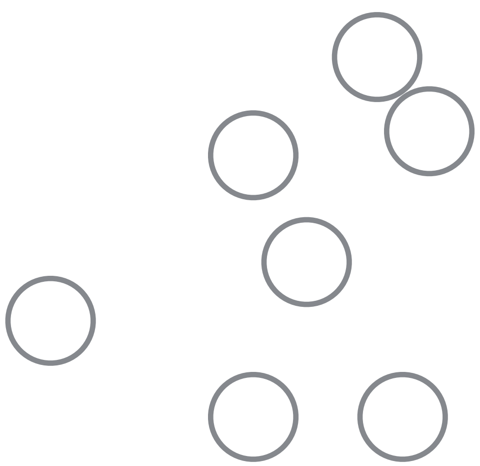

Ouriemi Aussillous Guazzelli

ODE

result: a critical shear
a law of sediment transport

J. Chauchat, M. Médale / Comput. Methods Appl. Mech. Engrg. 199 (2010) 439–449

Ouriemi Aussillous Guazzelli eq.
solved in finite elements, homogenous in x

J. Chauchat, M. Médale / Comput. Methods Appl. Mech. Engrg. 199 (2010) 439–449

conservation of mass, phase volume fraction

$$\frac{\partial \epsilon}{\partial t} + \nabla \cdot \left(\epsilon \vec{u^f} \right) = 0, \qquad \frac{\partial \phi}{\partial t} + \nabla \cdot \left(\phi \vec{u^p} \right) = 0, \qquad \phi + \epsilon = 1.$$

conservation of momentum

$$\rho_f \left[\frac{\partial \epsilon \vec{u^f}}{\partial t} + \nabla \cdot \left(\epsilon \vec{u^f} \otimes \vec{u^f} \right) \right] = \nabla \cdot (\overline{\overline{\sigma^f}}) - n\vec{f} + \epsilon \rho_f \vec{g},$$

$$\rho_p \left[\frac{\partial \phi \vec{u^p}}{\partial t} + \nabla \cdot \left(\phi \vec{u^p} \otimes \vec{u^p} \right) \right] = \nabla \cdot (\overline{\overline{\sigma^p}}) + n\vec{f} + \phi \rho_p \vec{g},$$

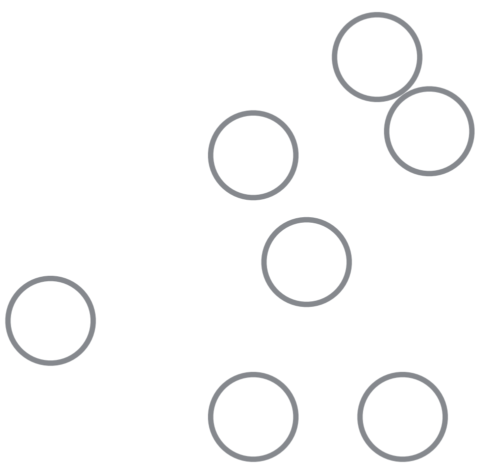

general buoyancy + all other contributions

$$n\vec{f} = \phi \nabla \cdot (\overline{\overline{\sigma^f}}) + n\vec{f^1}$$

Darcy Law, Carman-Kozeny coeficient

$$n\vec{f^1} = \eta \frac{\epsilon^2}{K} \left(\vec{u^f} - \vec{u^p} \right), \qquad K = \frac{\epsilon^3 d^2}{k_{CK} (1-\epsilon)^2}$$

Fluid stress tensor, effective viscosity

$$\overline{\overline{\sigma^f}} = -p^f \overline{\overline{I}} + \overline{\overline{\tau^f}} = -p^f \overline{\overline{I}} + \eta_e \left(\nabla \vec{u^m} + (\nabla \vec{u^m})^T \right), \qquad \eta_e = \eta(1 + 5\phi/2)$$

$$\vec{u^m} = \epsilon \vec{u^f} + \phi \vec{u^p}$$

Particule stress tensor, μ model

$$\overline{\overline{\sigma^p}} = -p^p \overline{\overline{I}} + \overline{\overline{\tau^p}} \qquad \overline{\overline{\tau^p}} = \eta_p(\|\overline{\overline{\dot{\gamma}^p}}\|, p^p) \overline{\overline{\dot{\gamma}^p}}, \qquad \eta_p(\|\overline{\overline{\dot{\gamma}^p}}\|, p^p) = \frac{\mu p^p}{\|\overline{\overline{\dot{\gamma}^p}}\|},$$

$$\overline{\overline{\dot{\gamma}^p}} = \nabla \vec{u^p} + (\nabla \vec{u^p})^T$$

J. Chauchat, M. Médale / Comput. Methods Appl. Mech. Engrg. 199 (2010) 439–449

$$\overline{\overline{\tau^p}} = \eta_p(\|\overline{\overline{\dot{\gamma}^p}}\|, p^p)\overline{\overline{\dot{\gamma}^p}},$$

with

$$\eta_p(\|\overline{\overline{\dot{\gamma}^p}}\|, p^p) = \frac{\mu p^p}{\|\overline{\overline{\dot{\gamma}^p}}\|},$$

$$\eta_e = \eta(1 + 5\phi/2)$$

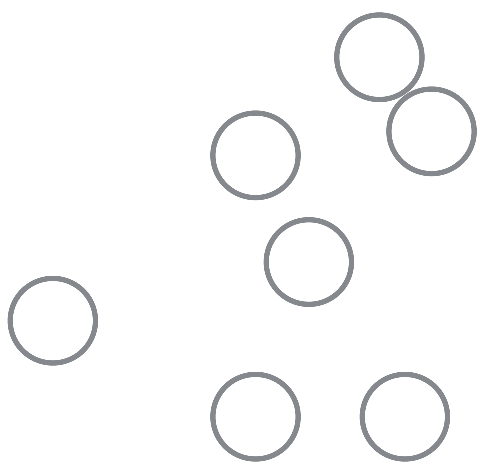

$$Ga = d^3 \rho_f \Delta\rho g/\eta^2$$

$$R_\rho = \rho_f/\rho_p$$

$$Bn = \tau_0 H/\eta U$$

$$\begin{cases} \nabla \cdot \left(\vec{u^m}\right) = 0 \\ \nabla \cdot \left(\vec{u^p}\right) = 0 \\ Ga\frac{H^3}{d^3}\frac{D\vec{u^m}}{Dt} = -\nabla p^f + \nabla \cdot \left(\frac{\eta_e}{\eta}\left(\nabla \vec{u^m} + \nabla \vec{u^m}^T\right)\right) - \frac{H^2}{K}\left(\vec{u^m} - \vec{u^p}\right) + \frac{\rho_f \vec{g}}{\Delta\rho\|\vec{g}\|} \\ Ga\frac{H^3}{d^3}R_\rho\phi\frac{D\vec{u^p}}{Dt} = -\nabla p^p + \nabla \cdot \left(\frac{\eta_p}{\eta}\left(\nabla \vec{u^p} + \nabla \vec{u^p}^T\right)\right) - \phi\nabla p^f \\ \qquad + \phi\nabla \cdot \left(\frac{\eta_e}{\eta}\left(\nabla \vec{u^m} + \nabla \vec{u^m}^T\right)\right) + \frac{(1-\phi)H^2}{K}\left(\vec{u^m} - \vec{u^p}\right) + \frac{\phi\vec{g}}{\|\vec{g}\|} \end{cases}$$

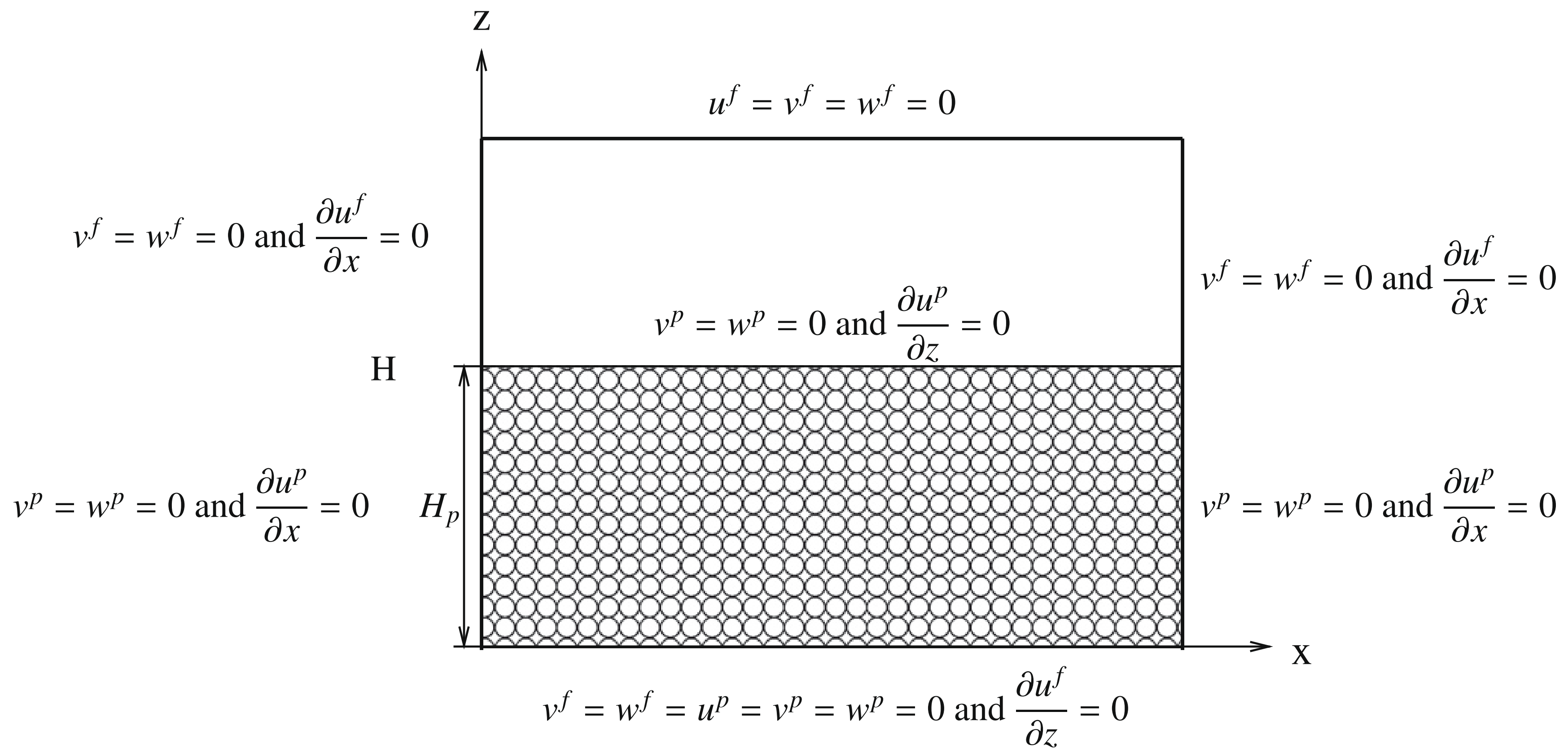

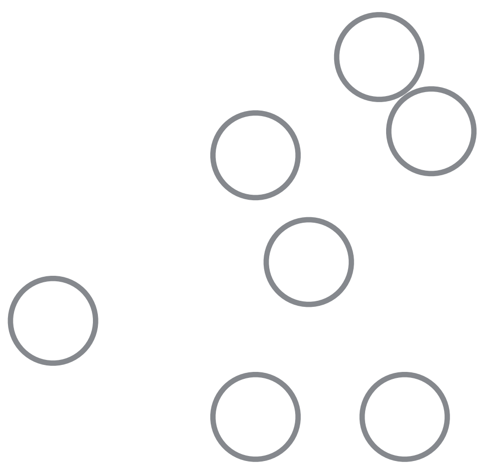

Fig. 7. Sketch of the flow of a Newtonian fluid over a granular bed.

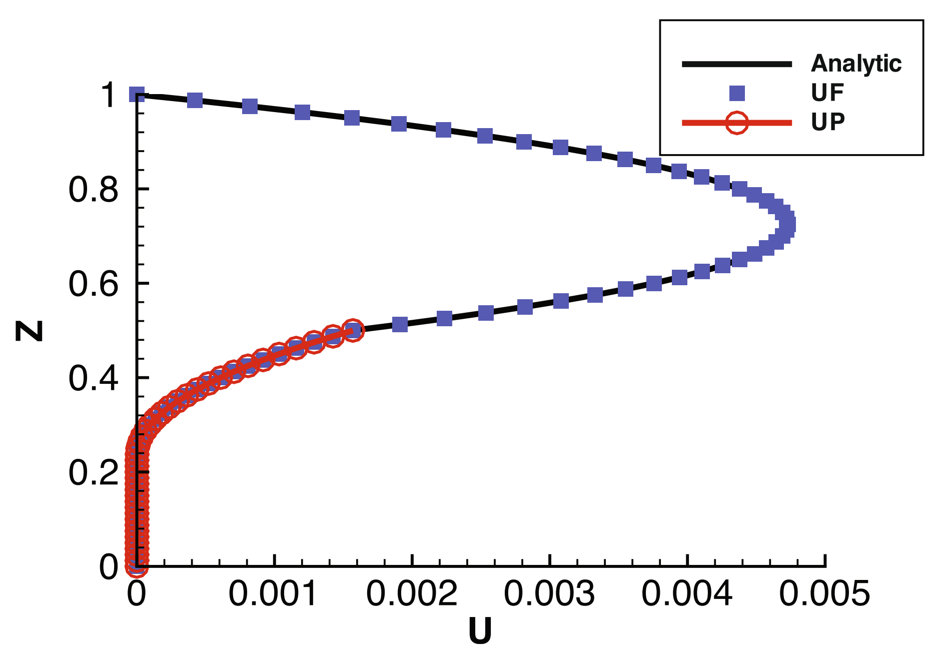

(a) Two-fluid model

Fig. 8. Comparison of the longitudinal velocity profiles for the flow of a Newtonian fluid over a granular bed between two infinite parallel planes obtained by numerical simulations (two-fluid model) with the analytical solution of Ouriemi et al. [26].

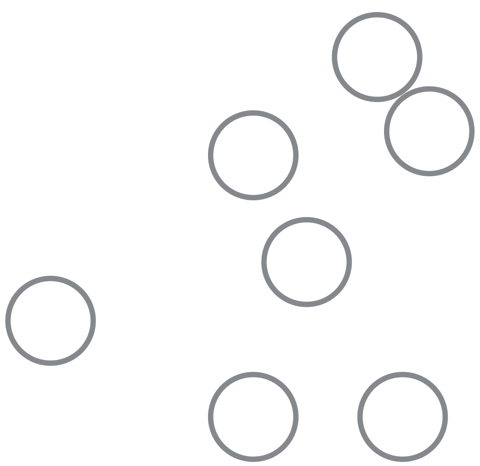

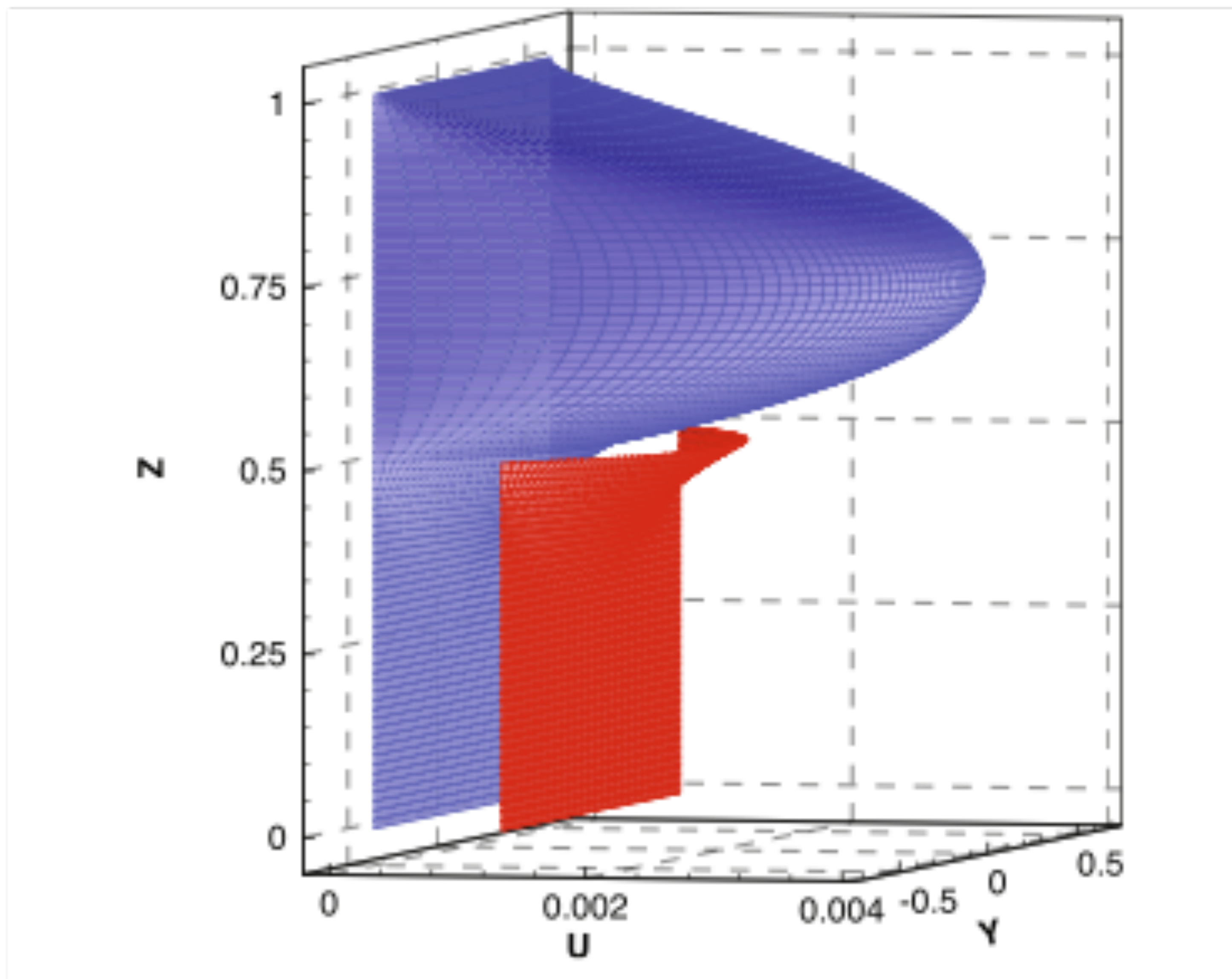

Fig. 12. Velocity profile obtained by numerical simulations with the two-fluid model for the square cross-section duct ($6 \times 20 \times 40$). The fluid phase velocity is in blue and the particulate phase velocity is in red. An offset of 10^{-3} has been added to the velocity of the particulate phase (up) to make it visible. (For interpretation of the references to color in this figure legend, the reader is referred to the web version of this article.)

Continuum approach
particule phase

constraints exerted by the particules

constraints exerted by the fluid

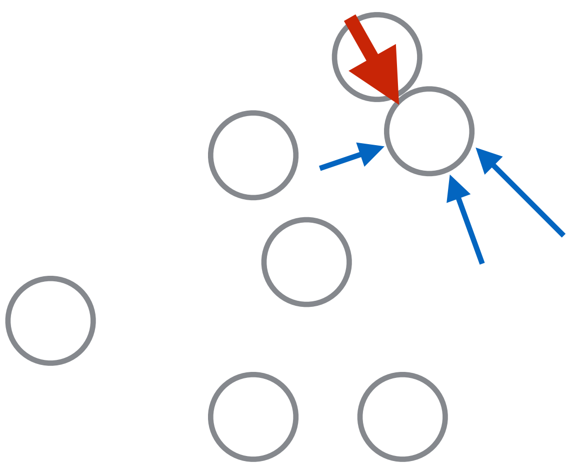

$$\boxed{\nabla \cdot \sigma^{pp}} + \boxed{\mathbf{F}^{pf} - \phi \nabla p_f} + \phi \rho_p \mathbf{g}$$

$$\mathbf{F}^{pf} = n < \oint (\sigma^{f0} + p_f I) \cdot \mathbf{n} ds >$$

$$\boxed{\phi \rho_p \frac{d_p \mathbf{u}_p}{dt} + \nabla \cdot (\phi \rho_p < \mathbf{u}'_p \otimes \mathbf{u}'_p >) = \nabla \cdot \sigma^{pp} + \mathbf{F}^{pf} - \phi \nabla p_f + \phi \rho_p \mathbf{g}}$$

fluid phase

$$\boxed{\nabla \cdot \tau^f} \boxed{- \mathbf{F}^{pf} - (1 - \phi) \nabla p_f} + (1 - \phi) \rho_f \mathbf{g}$$

$$\boxed{(1 - \phi) \rho_f \frac{d_f \mathbf{u}_f}{dt} + \nabla \cdot ((1 - \phi) \rho_f < \mathbf{u}'_f \otimes \mathbf{u}'_f >) = \nabla \cdot \tau^f - \mathbf{F}^{pf} - (1 - \phi) \nabla p_f + (1 - \phi) \rho_f \mathbf{g}}$$

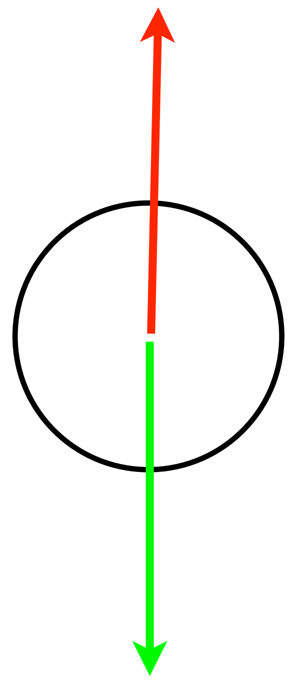

free fall equilibrium

$$\frac{4}{3}\pi(\Delta\rho)R^3 g = 6\pi\eta R V_s$$

terminal velocity

$$V_s = \frac{d^2}{18\eta}(\Delta\rho)g$$

flux

$$Q_s = \frac{d^3}{\eta}(\Delta\rho)g$$

free fall equilibrium

$$\frac{4}{3}\pi(\Delta\rho)R^3 g = \frac{\rho C_D V_s^2}{2}$$

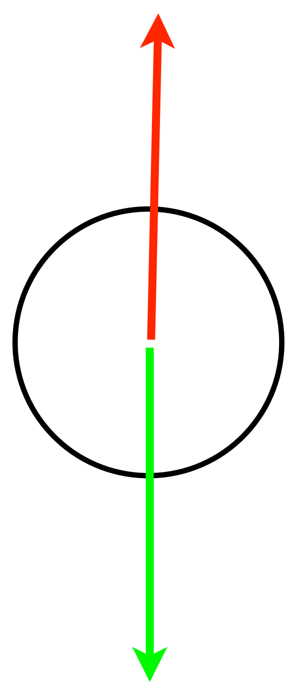

terminal velocity

$$V_s = \sqrt{\frac{(\Delta\rho)gd}{\rho C_D}}$$

flux

$$Q_s = \sqrt{\frac{(\Delta\rho)gd^3}{\rho}}$$

R. Bakhtyar et al./Advances in Water Resources 33 (2010) 277–290

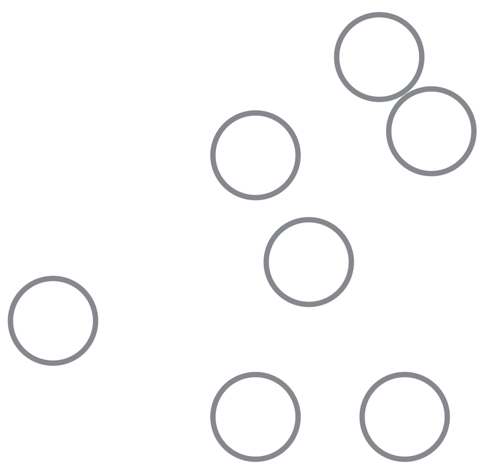

2.1. Governing equations

Fluid phase hydrodynamics [5]

$$\frac{\partial\left[(1-C)\rho_f\right]}{\partial t}+\nabla\cdot[(1-C)\rho_f\cdot\vec{U}]=0, \tag{1}$$

$$\frac{\partial[(1-C)\rho_f\vec{U}]}{\partial t}+\nabla\cdot[(1-C)\rho_f\vec{U}\,\vec{U}]$$
$$=(1-C)\rho_f\vec{g}-\nabla\cdot[(1-C)P]+\nabla\cdot\vec{\vec{T}}_f-\vec{f}_{in}, \tag{2}$$

Sediment phase hydrodynamics [5]

$$\frac{\partial(C\rho_s)}{\partial t}+\nabla\cdot(C\rho_s\vec{V})=0, \tag{3}$$

$$\frac{\partial(C\rho_s\vec{V})}{\partial t}+\nabla\cdot(C\rho_s\vec{V}\,\vec{V})=C\rho_s\vec{g}-\nabla\cdot(CP)+\nabla\cdot\vec{\vec{T}}_s+\vec{f}_{in}, \tag{4}$$

Interphase forces [12,37]

$$\vec{f}_{in}=\frac{3C\rho_f}{4d}C_D\left(\vec{U}-\vec{V}\right)\left|\vec{U}-\vec{V}\right|+\frac{3C\rho_f}{4d}C_L|\vec{U}-\vec{V}|\nabla\left(\vec{U}-\vec{V}\right)\cdot\vec{k}, \tag{5}$$

$$C_D=\left(\frac{24\nu}{d|\vec{U}-\vec{V}|}+2\right)(1-C)^{-9/2}\quad\text{and}\quad C_L=\frac{4}{3}, \tag{6}$$

$$\overline{U_i'U_j'}=-\nu_t(U_{i,j}+U_{j,i})+\frac{2}{3}\delta_{ij}k-\frac{2}{3}\nu_t\delta_{ij}U_{j,i},$$
$$\overline{C'U_i'}=\overline{C'V_i'}=-\nu_t\frac{\partial C}{\partial z},$$

$$\nu_t=C_d\frac{k^2}{\varepsilon},$$

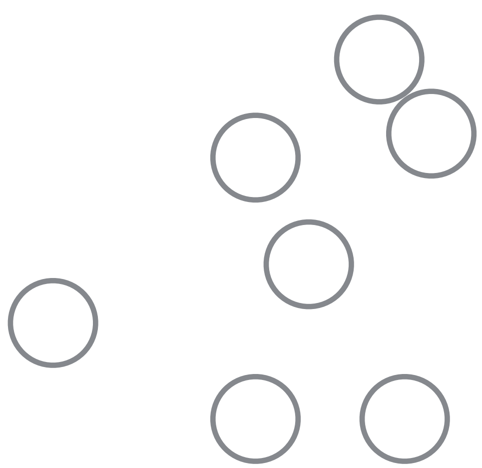

$$\frac{Dk}{Dt} = \nabla \cdot \left(v + \frac{v_t}{\sigma_k}\right)\nabla k + P_r + \frac{\rho_s - \rho_f}{\rho_f}\vec{g} v_t \nabla C \cdot \vec{k} - \varepsilon - v_t F_d \nabla C \cdot \vec{k},$$

$$\frac{D\varepsilon}{Dt} = \nabla \cdot \left(v + \frac{v_t}{\sigma_\varepsilon}\right)\nabla \varepsilon + \frac{\varepsilon}{k}\left(C_{1\varepsilon} P_r + C_{2\varepsilon}\vec{g} v_t \frac{\rho_s - \rho_f}{\rho_f}\nabla C \cdot \vec{k} - C_{3\varepsilon}\varepsilon - v_t F_d \nabla C \cdot \vec{k}\right),$$

$$F_d = \frac{C}{1 - C}\frac{3C_D}{4d}|\vec{U} - \vec{V}|^2,$$

$$C_{1\varepsilon} = 1.44, \quad C_{2\varepsilon} = 1.92, \quad C_{3\varepsilon} = 1.2, \qquad ($$

Closure of particle stresses [3,11]

$$T_{xz} = \frac{6v\rho_f}{5[(C_m/C)^{\frac{1}{3}} - 1]^2}\frac{\partial V_x}{\partial z}, \qquad ($$

$$T_{zz} = \frac{T_{xz}}{\tan\varphi}, \qquad ($$

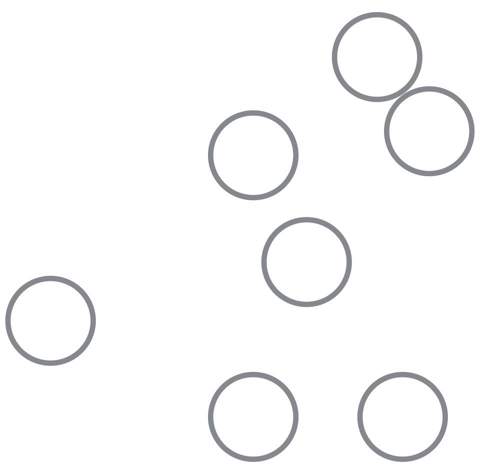

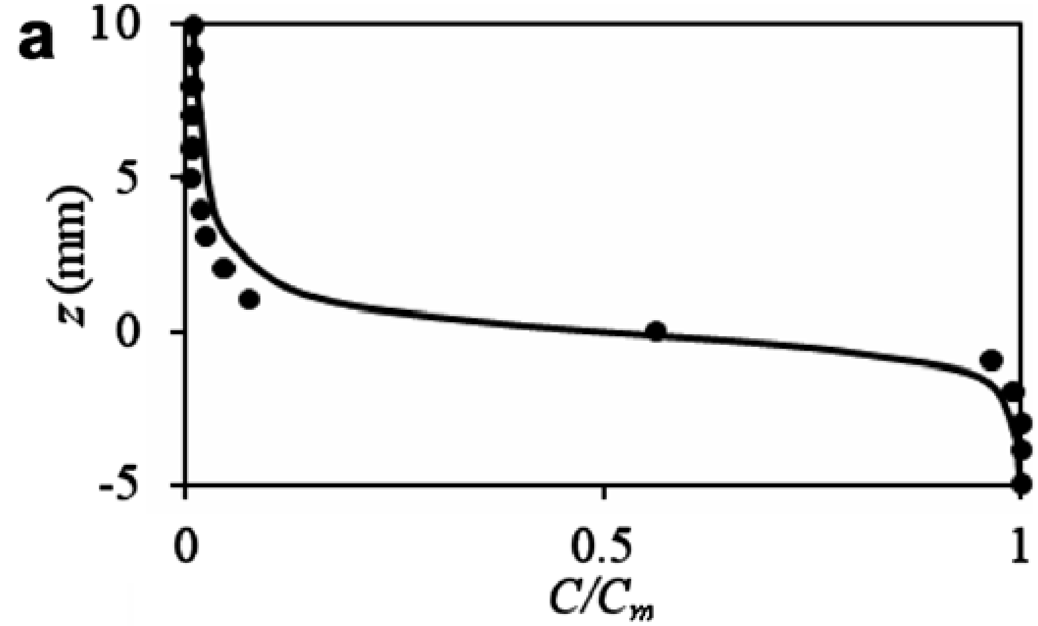
a
10
5
0
-5
z (mm)
0
0.5
1
C/C_m

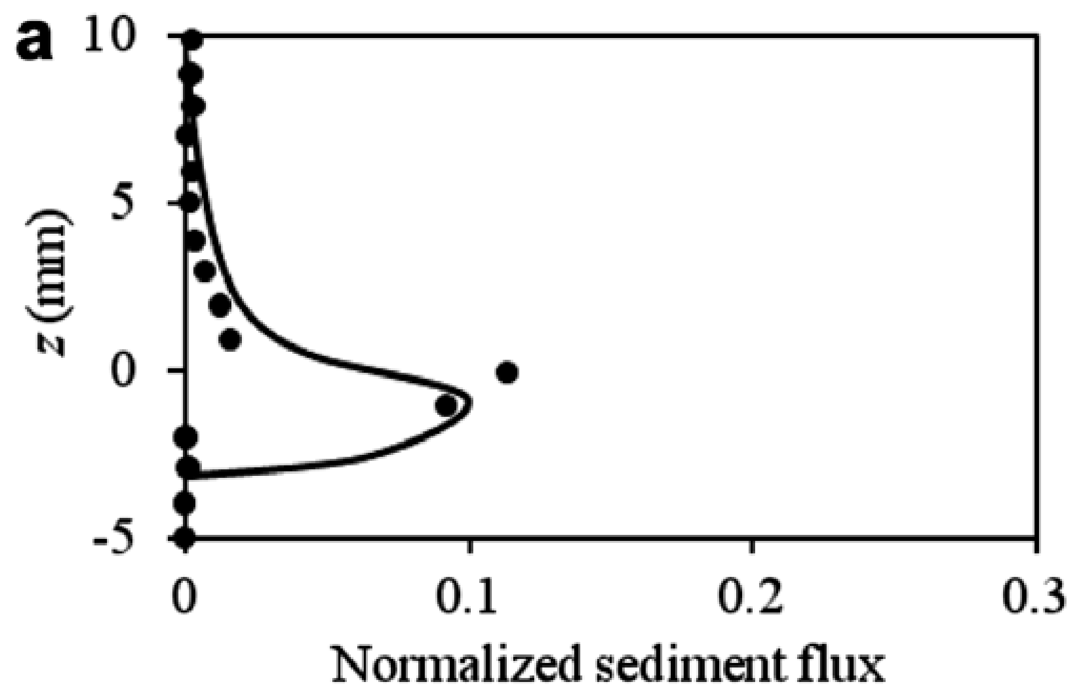
a
10
5
0
-5
z (mm)
0
0.1
0.2
0.3
Normalized sediment flux

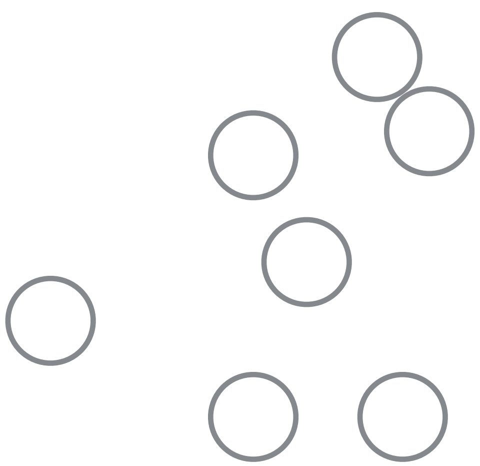

more simple models
but no shallow water

Over simplification: considering only the Stokes velocity

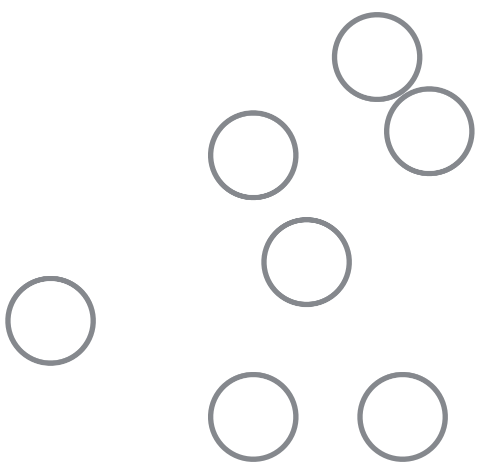

Over simplification:
considering only the fall velocity

Over simplification: considering only the Stokes velocity

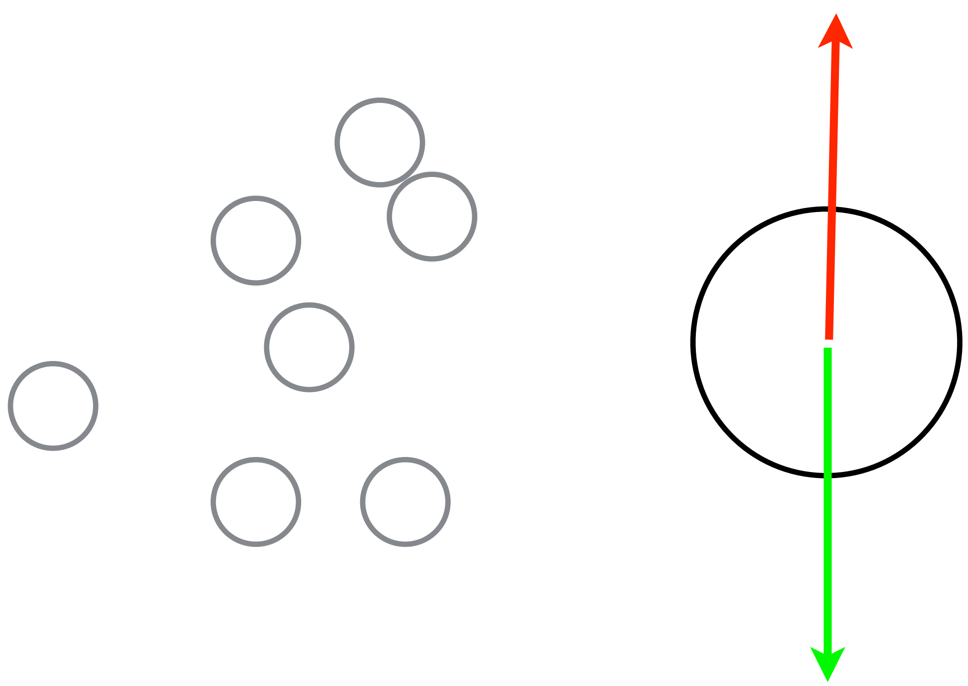

free fall equilibrium

$$\frac{4}{3}\pi(\Delta\rho)R^3 g = 6\pi\eta R V_s$$

terminal velocity

$$V_s = \frac{d^2}{18\eta}(\Delta\rho)g$$

characteristic flux

$$Q_s = \frac{d^3}{\eta}(\Delta\rho)g$$

Over simplification: considering only the Stokes velocity

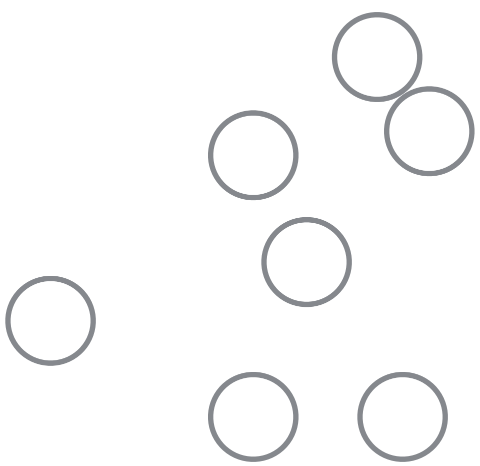

$$\cancel{\phi\rho_p \frac{d_p \mathbf{u}_p}{dt} = \phi\rho_f \frac{d_f \mathbf{u}_f}{dt}} + \nabla\cdot\sigma^p + \boxed{\mathbf{f}^v + \phi(\rho_p - \rho_f)\mathbf{g}}$$

$$\rho_f \frac{d_f \mathbf{u}_f}{dt} = \nabla\cdot\tau^v - \mathbf{f}^v - \nabla p_f + \rho_f \mathbf{g}\ .$$

Over simplification: considering only the Stokes velocity

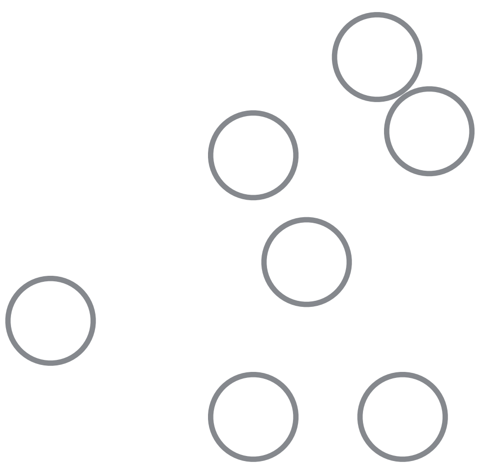

$$\cancel{\phi\rho_p \frac{d_p \mathbf{u}_p}{dt} = \phi\rho_f \frac{d_f \mathbf{u}_f}{dt}} + \nabla \cdot \sigma^p + \boxed{\mathbf{f}^v + \phi(\rho_p - \rho_f)\mathbf{g}}$$

$$\rho_f \frac{d_f \mathbf{u}_f}{dt} = \nabla \tau_v - \nabla p_f + \rho_f (1 + \phi \frac{\rho_p - \rho_f}{\rho_f})\mathbf{g}$$

Over simplification: considering only the Stokes velocity

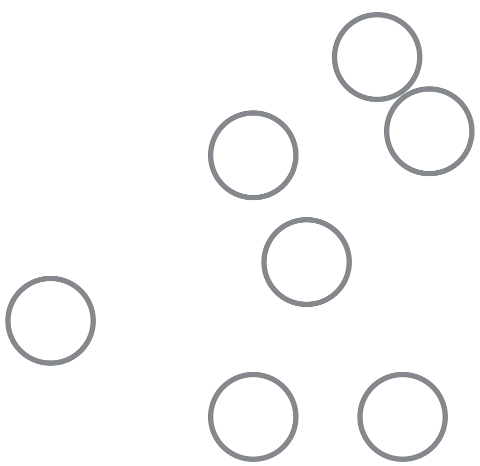

$$\cancel{\phi\rho_p \frac{d_p \mathbf{u}_p}{dt} = \phi\rho_f \frac{d_f \mathbf{u}_f}{dt}} + \nabla \cdot \sigma^p + \boxed{\mathbf{f}^v + \phi(\rho_p - \rho_f)\mathbf{g}}$$

$$\rho_f \frac{d_f \mathbf{u}_f}{dt} = \nabla \tau_v - \nabla p_f + \rho_f (1 + \phi \frac{\rho_p - \rho_f}{\rho_f})\mathbf{g}$$

dilute

excess of mass

$$\mathbf{f} = -\frac{\phi \eta_f}{d^2} \, \lambda(\phi)(\mathbf{V^p} - \mathbf{V})$$

Darcy

$$\overrightarrow{u_p} \simeq \overrightarrow{u}_f + \overrightarrow{V}_f + ...$$

one fluid

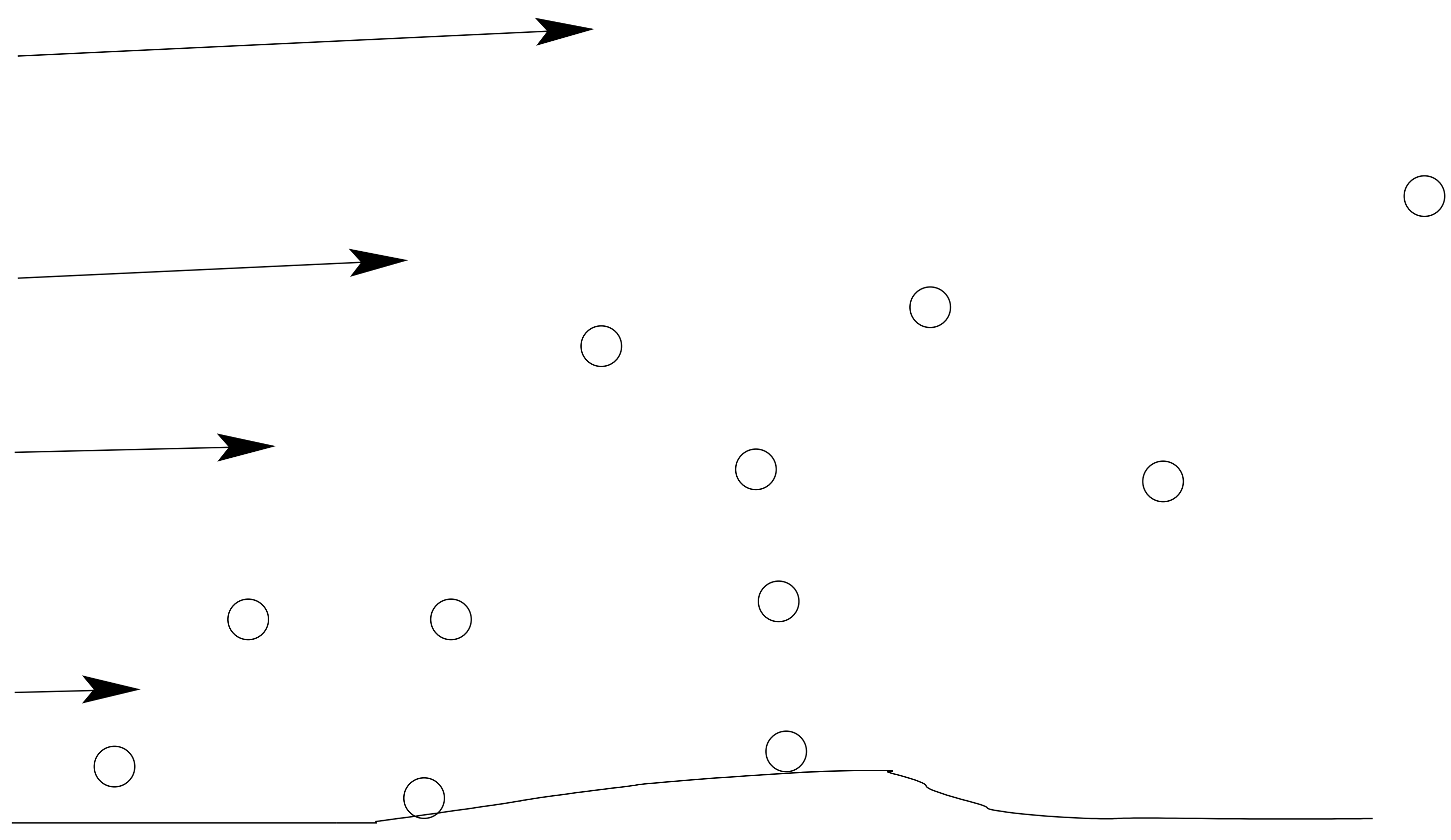

one fluid

Velocity of the sediments:

$u_p = u$

$v_p = v$

Convection

one fluid

Velocity of the sediments:

$u_p = u$
$v_p = v - V_f$
Sedimentation

Velocity of the sediments:

$u_p = u - D\frac{\partial c}{\partial x}$
$v_p = v - V_f - D\frac{\partial c}{\partial y}$
Diffusion

one fluid

Mass conservation of the sediments:

local form;

$$\frac{\partial cu}{\partial x} + \frac{\partial c(v - V_f)}{\partial y} = \frac{\partial c}{\partial x} D \frac{\partial c}{\partial x} + \frac{\partial}{\partial y} D \frac{\partial c}{\partial y}$$

one fluid

Mass conservation of the sediments:

local form;

$$\frac{\partial cu}{\partial x} + \frac{\partial c(v - V_f)}{\partial y} = \frac{\partial c}{\partial x} D \frac{\partial c}{\partial x} + \frac{\partial}{\partial y} D \frac{\partial c}{\partial y}$$

integral form: $\int_0^\infty cudy = q$, ...

$$\frac{\partial q}{\partial x} + c(x,0)(V_f) = -D\frac{\partial c}{\partial y}(x,0) \qquad \frac{\partial f}{\partial t} = c(x,0)(V_f) + D\frac{\partial c}{\partial y}(x,0)$$

one fluid

Mass conservation of the sediments:

local form;

$$\frac{\partial cu}{\partial x} + \frac{\partial c(v - V_f)}{\partial y} = \frac{\partial c}{\partial x} D \frac{\partial c}{\partial x} + \frac{\partial}{\partial y} D \frac{\partial c}{\partial y}$$

integral form: $\int_0^\infty cudy = q$, ...

$$\frac{\partial q}{\partial x} + c(x,0)(V_f) = -D\frac{\partial c}{\partial y}(x,0) \qquad \frac{\partial f}{\partial t} = c(x,0)(V_f) + D\frac{\partial c}{\partial y}(x,0)$$

if $\frac{\partial \tilde{u}}{\partial \tilde{y}}|_0 > \tau_s$ then $-\frac{\partial \tilde{c}}{\partial \tilde{y}}|_0 = \beta(\frac{\partial \tilde{u}}{\partial \tilde{y}}|_0)^a(\frac{\partial \tilde{u}}{\partial \tilde{y}}|_0 - \tau_s)^b,$ else $-\frac{\partial \tilde{c}}{\partial \tilde{y}}|_0 = 0.$

$$\frac{\partial f}{\partial t} = -\frac{\partial q}{\partial x}.$$

Brivois 2005/ Lagrée 2000, 2003

one fluid

Mass conservation of the sediments:

local form;

$$\frac{\partial cu}{\partial x} + \frac{\partial c(v - V_f)}{\partial y} = \frac{\partial c}{\partial x} D \frac{\partial c}{\partial x} + \frac{\partial}{\partial y} D \frac{\partial c}{\partial y}$$

integral form: $\int_0^\infty cudy = q$, ...

$$\frac{\partial q}{\partial x} + c(x,0)(V_f) = -D\frac{\partial c}{\partial y}(x,0) \qquad \frac{\partial f}{\partial t} = c(x,0)(V_f) + D\frac{\partial c}{\partial y}(x,0)$$

deposition

$$\frac{\partial q}{\partial x} = Erosion \text{ - } deposition \qquad \frac{\partial f}{\partial t} = -Erosion + deposition$$

$$Erosion = E(\tau - \tau_s)_+$$

one fluid

Mass conservation of the sediments:

local form;

$$\frac{\partial cu}{\partial x} + \frac{\partial c(v - V_f)}{\partial y} = \frac{\partial c}{\partial x} D \frac{\partial c}{\partial x} + \frac{\partial}{\partial y} D \frac{\partial c}{\partial y}$$

integral form: $\int_0^\infty cudy = q$, ...

$$\frac{\partial q}{\partial x} + qV_f/H = \beta(\frac{\partial \tilde{u}}{\partial \tilde{y}}|_0)^a(\frac{\partial \tilde{u}}{\partial \tilde{y}}|_0 - \tau_s)^b) \qquad \frac{\partial f}{\partial t} = -\frac{\partial q}{\partial x}.$$

$$l_{sat}\frac{\partial q}{\partial x} + q = q_{sat}$$

$$q_{sat} = E(\tau - \tau_s)_+$$

one fluid

$$l_s \frac{\partial q}{\partial x} + q = q_s \qquad \frac{\partial f}{\partial t} = -\frac{\partial q}{\partial x}$$

$$q_s = E(\tau - \tau_s)_+$$

$$\rho(\boldsymbol{x}) = \rho_f [1 + \gamma c(\boldsymbol{x})], \text{ where } \gamma = (\rho_p - \rho_f)/\rho_f$$

one fluid

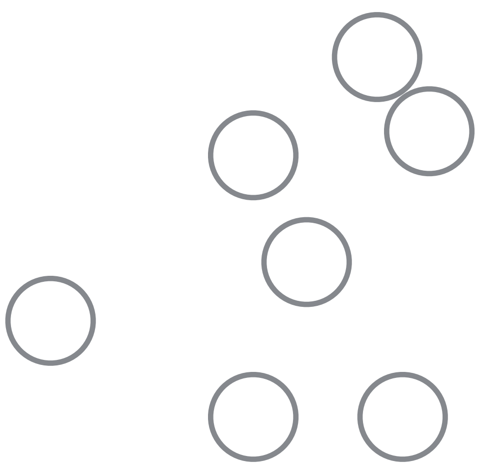

$$\frac{\partial u}{\partial x} + \frac{\partial w}{\partial z} = 0,$$

$$\frac{\partial u}{\partial t} + u\frac{\partial u}{\partial x} + w\frac{\partial u}{\partial z} = -\frac{1}{\rho_f}\frac{\partial p}{\partial x} + \nu\left(\frac{\partial^2 u}{\partial x^2} + \frac{\partial^2 u}{\partial z^2}\right),$$

$$\frac{\partial w}{\partial t} + u\frac{\partial w}{\partial x} + w\frac{\partial w}{\partial z} = -\frac{1}{\rho_f}\frac{\partial p}{\partial z} + \nu\left(\frac{\partial^2 w}{\partial x^2} + \frac{\partial^2 w}{\partial z^2}\right) - \frac{\rho}{\rho_f}g,$$

$$\frac{\partial c}{\partial t} + u\frac{\partial c}{\partial x} + (w - w_s)\frac{\partial c}{\partial z} = D\left(\frac{\partial^2 c}{\partial x^2} + \frac{\partial^2 c}{\partial z^2}\right).$$

$$\frac{\partial \eta}{\partial t} = w_s\, c(z = \eta) - \beta\frac{\tau_n}{n_z}. \qquad D\left.\frac{\partial c}{\partial n}\right|_{z=\eta} = -\beta\tau_n.$$

Deep-water sediment wave formation: linear stability analysis of coupled flow/bed interaction
Lesshafft Hall Meiburg Kneller JFM11

Mixing and dissipation in particle-driven gravity currents
Neckel Härtel Kleiser Meiburg JFM 05

one fluid

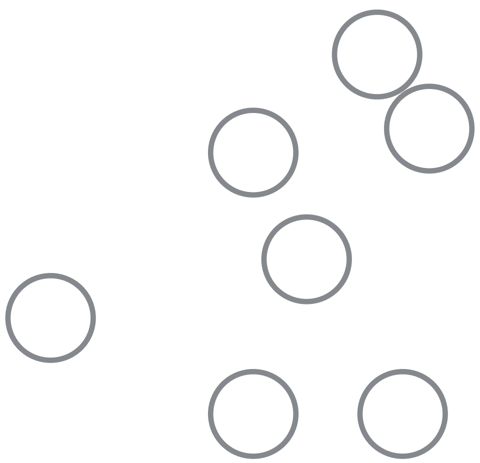

Neckel Härtel Kleiser Meiburg JFM 05

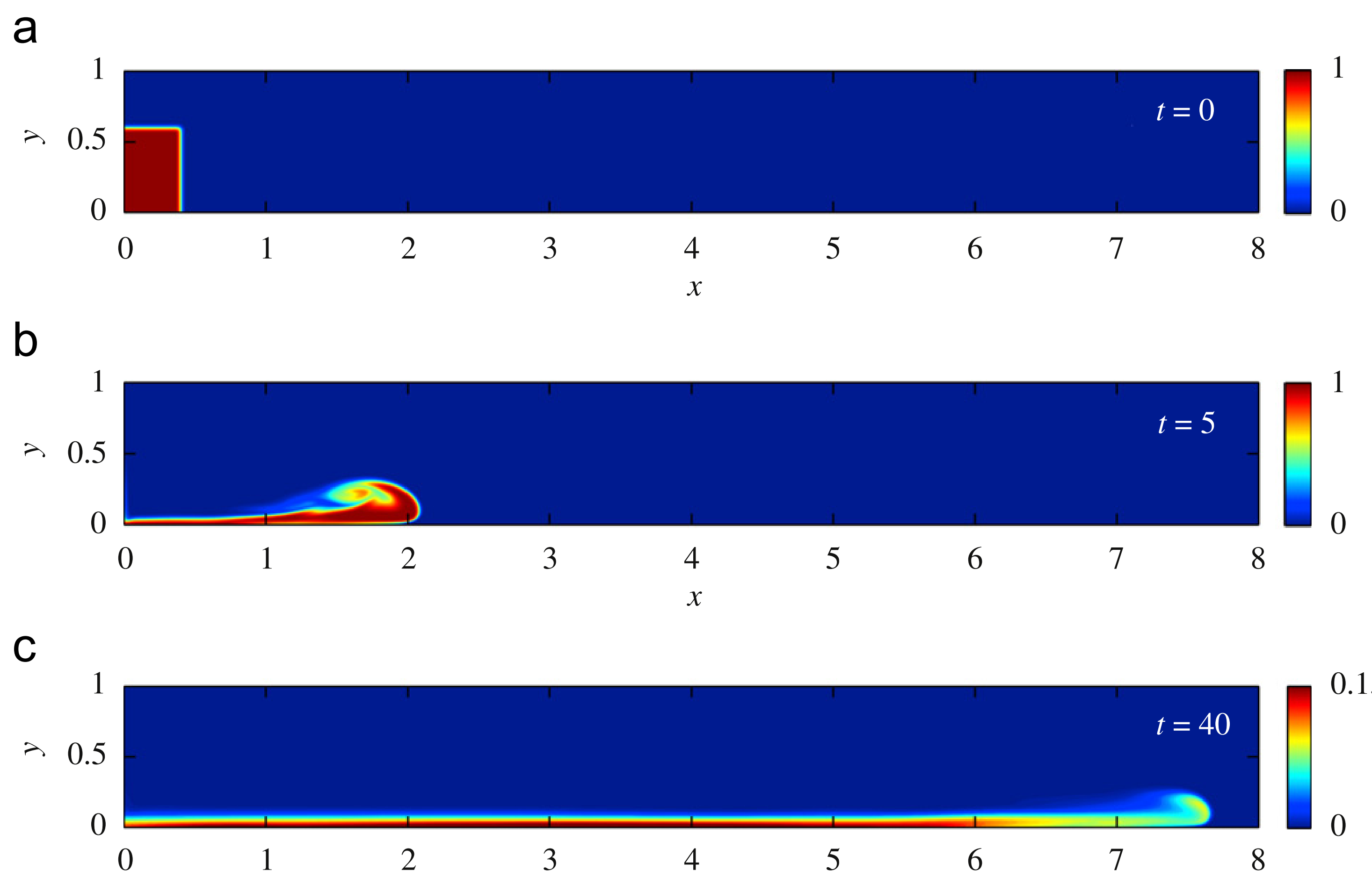

Gerris

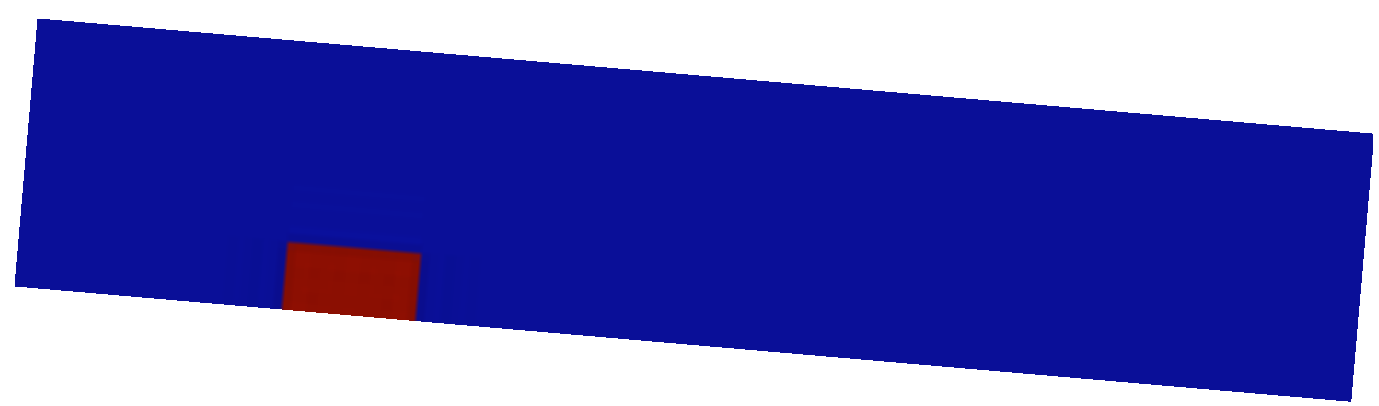

one fluid

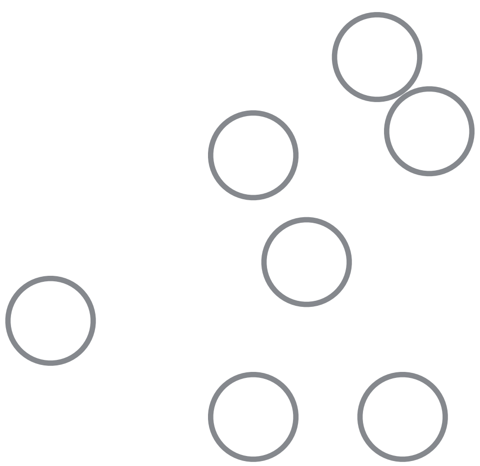

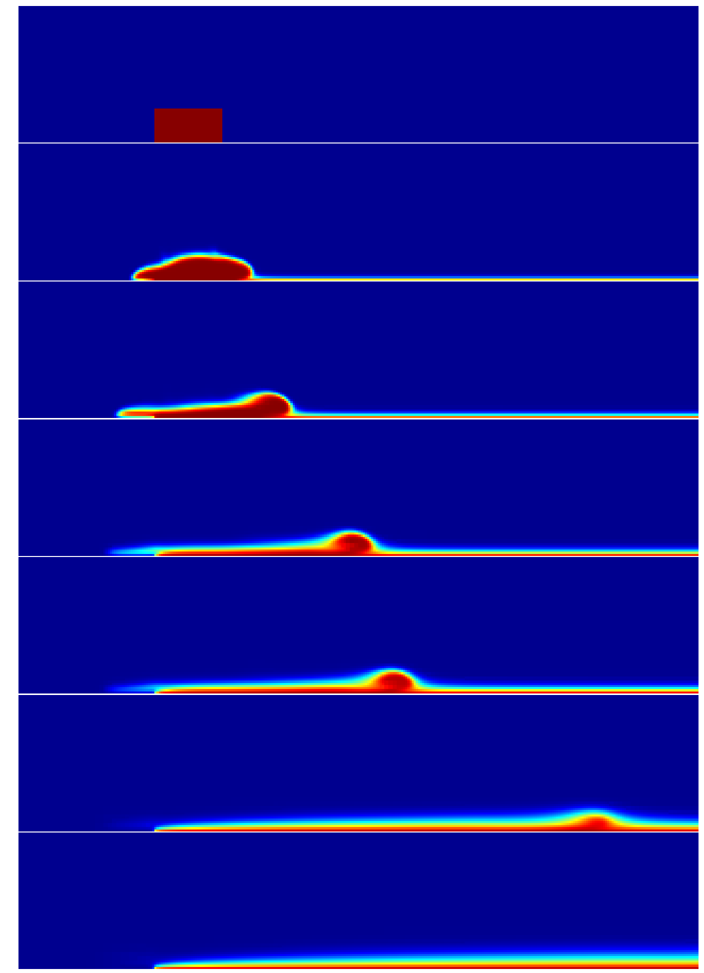

FIGURE 3 – Ecoulements gravitaire sur une pente de 15^o, $t = 0, 1, 2, 3, 4$, 5 et 10. $V_f \neq 0$

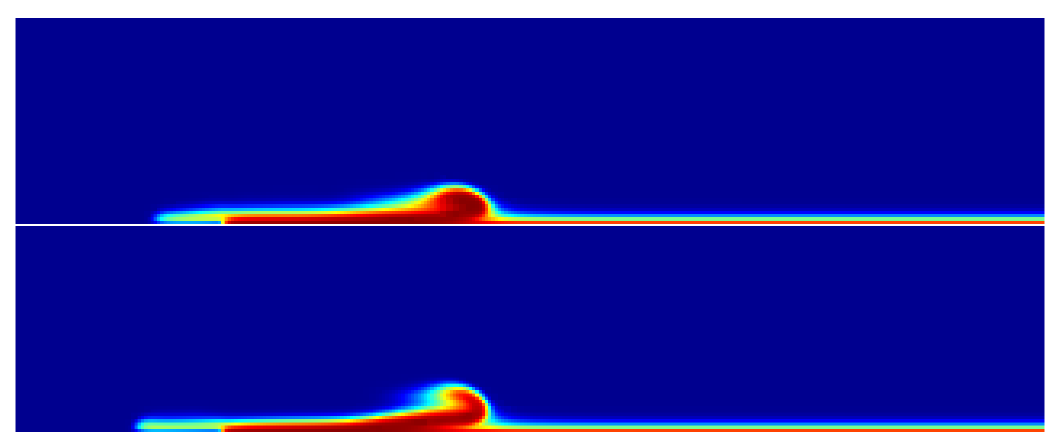

FIGURE 5 – Ecoulements gravitaire sur une pente de 15^o comparaison au temps $t = 3$. $V_f \neq 0$ en haut et $V_f = 0$ en bas, on constate que la vitesse de sédimentation V_f fait retomber le panache. pour $V_f \neq 0$ le front de l'avalanche est plus ramassé.

Flow over a bump, ideal fluid / boundary layer interaction

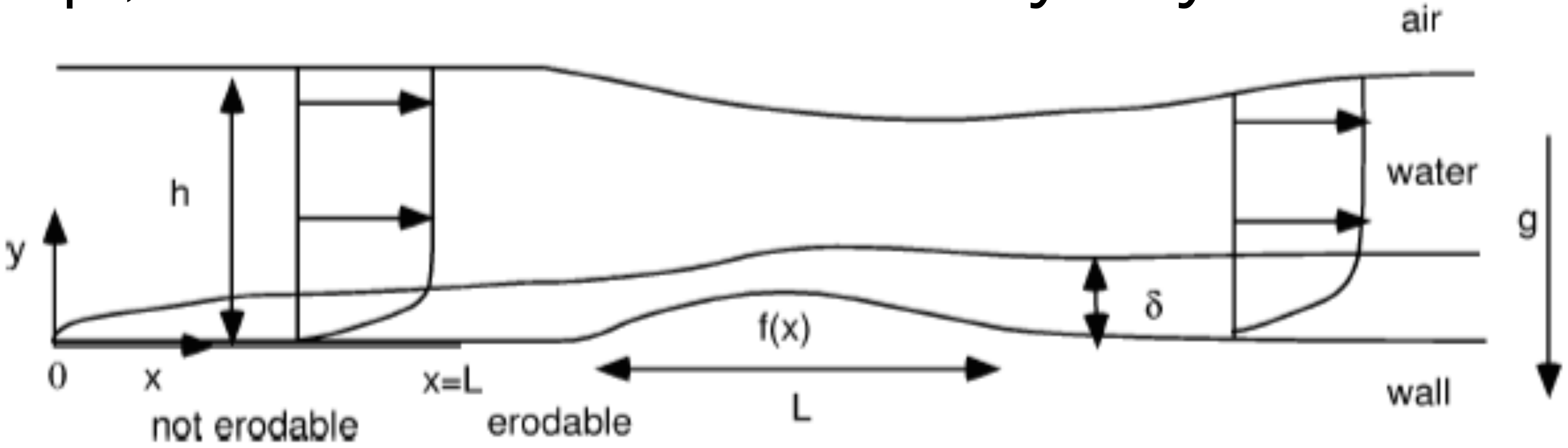

Figure 1. Sketch of the flow, before $\bar{x}=1$ the bottom is not erodable.

ideal fluid $\bar{u}_e(\bar{x}) = 1 + \varepsilon \dfrac{\delta_1 + \hat{f}}{1 - F_r^2}$

boundary layer

$$\frac{\partial}{\partial \bar{x}}\tilde{u} + \frac{\partial}{\partial \tilde{y}}\tilde{v} = 0 \quad \text{et} \quad \tilde{u}\frac{\partial}{\partial \bar{x}}\tilde{u} + \tilde{v}\frac{\partial}{\partial \tilde{y}}\tilde{u} = \bar{u}_e(\bar{x})\frac{\mathrm{d}}{\mathrm{d}\bar{x}}\bar{u}_e(\bar{x}) + \frac{\partial^2}{\partial \tilde{y}^2}\tilde{u}$$

$$\tilde{u}(\bar{x}, \tilde{y}=0) = 0, \tilde{v}(\bar{x}, \tilde{y}=0) = 0 \quad \text{et} \quad \lim_{\tilde{y}\to\infty} \tilde{u}(\bar{x}, \tilde{y}) = \bar{u}_e(\bar{x})$$

transport $\tilde{u}\dfrac{\partial}{\partial \bar{x}}\tilde{c} + (\tilde{v} - \tilde{V}_f)\dfrac{\partial}{\partial \tilde{y}}\tilde{c} = \mathrm{S}_c^{-1}\dfrac{\partial^2}{\partial \tilde{y}^2}\tilde{c}$

erosion $\tilde{c}(\bar{x} < 1, \tilde{y}) = 0, \quad \tilde{c}(\bar{x}, \tilde{y} \to \infty) = 0, \quad -\left.\dfrac{\partial \tilde{c}}{\partial \tilde{y}}\right|_0 = \beta\left(\mathrm{H}\left(\left.\dfrac{\partial \tilde{u}}{\partial \tilde{y}}\right|_0 - \tau_s\right)\right)\left(\left.\dfrac{\partial \tilde{u}}{\partial \tilde{y}}\right|_0 - \tau_s\right)^\gamma$

Lagrée 00 update $\dfrac{\partial \hat{f}}{\partial \check{t}} = \mathrm{S}_c^{-1}\left.\dfrac{\partial \tilde{c}}{\partial \tilde{y}}\right|_0 + \tilde{V}_f \tilde{c}|_0$

Flow over a bump, ideal fluid / boundary layer interaction

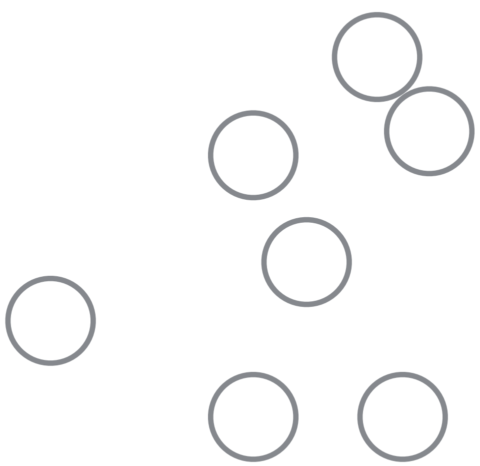

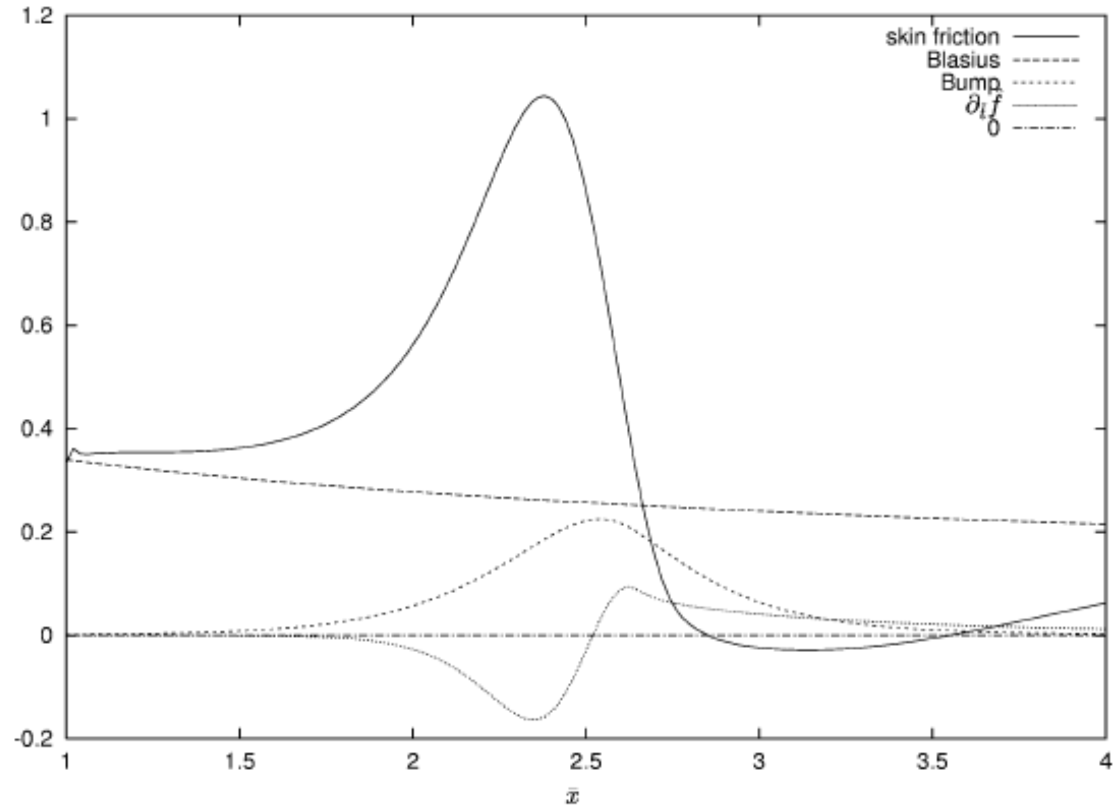

Figure 2. At initial time, the initial bump $\hat{f}(\bar{x}, \check{t}=0)$ and the associated computed skin friction at the wall $\partial_{\tilde{y}}\tilde{u}$ and total flux of sediments: $\partial_{\check{t}}\hat{f}$.

Figure 2. *Au temps initial, tracé de la distribution de frottement, de la forme initiale de la bosse $\hat{f}(\bar{x}, \check{t}=0)$ et de la variation de la forme de la bosse $\partial_{\check{t}}\hat{f}$.*

Lagrée 00

Flow over a bump, ideal fluid / boundary layer interaction

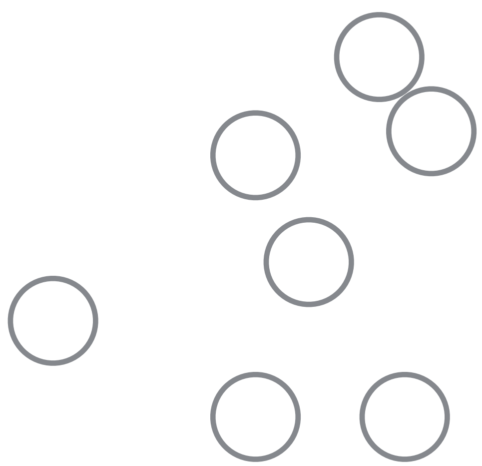

Figure 3. The dune shape $(\hat{f}(\bar{x}, \check{t}))$ as a function of time $\check{t} = 0, 1, 2, 3, \ldots, 16, \infty$.

Figure 3. *Évolution de la forme de la bosse en fonction du temps* $\check{t} = 0, 1, 2, 3, \ldots, 16, \infty$.

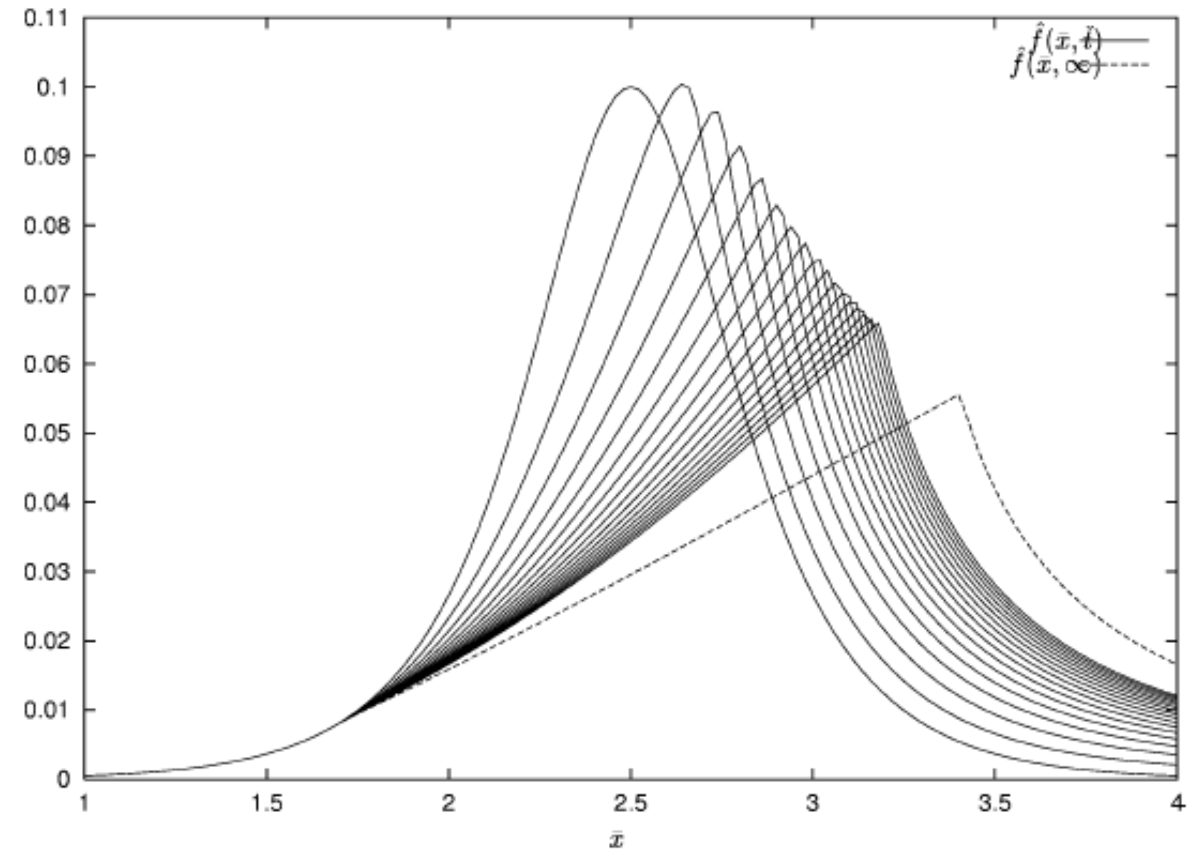

Figure 4. Final dune shapes for different starting values of α.

Figure 4. *Formes finales de dunes pour différentes valeurs de* α.

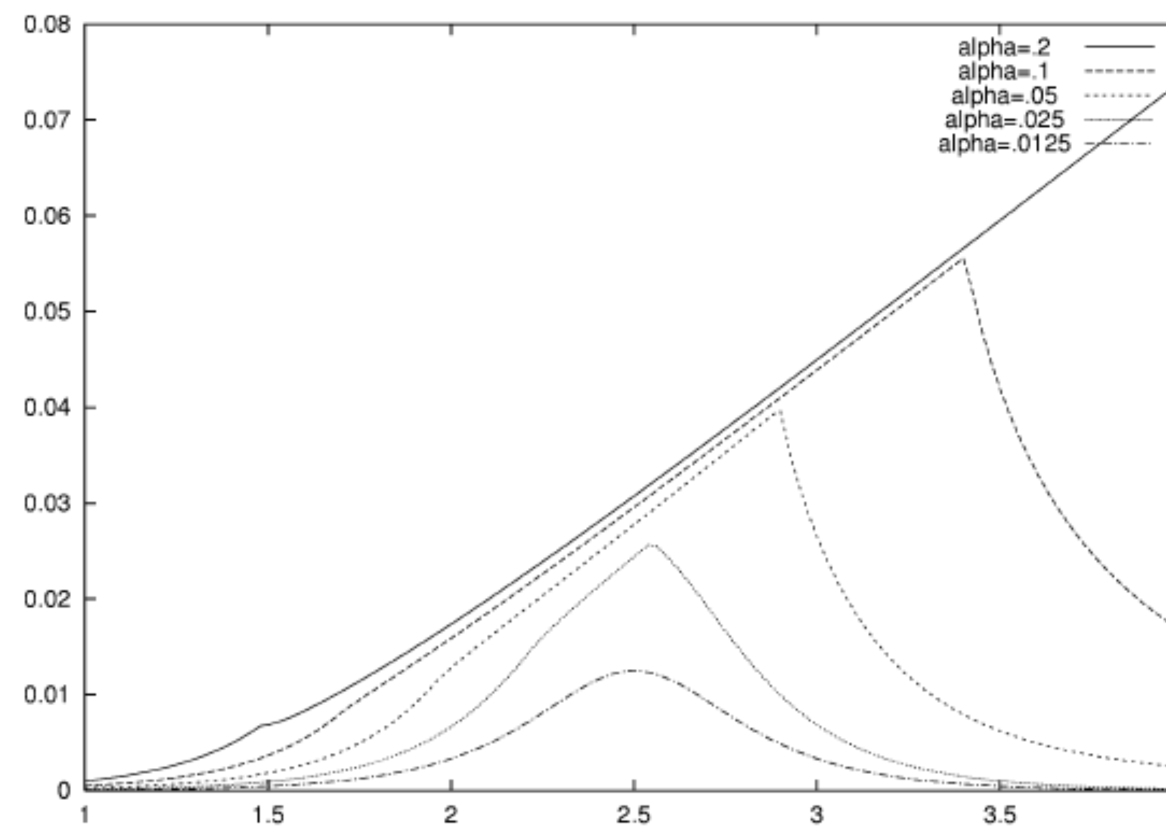

Lagrée 00

Sculpting of an erodible body by flowing water

L. Ristroph, M. Moore, S. Childress, M. Shelley et J. Zhang PNAS 12

Self-similar evolution of a body eroding in a fluid flow
Moore, Ristroph, Childress, Zhang, Shelley PoF 13

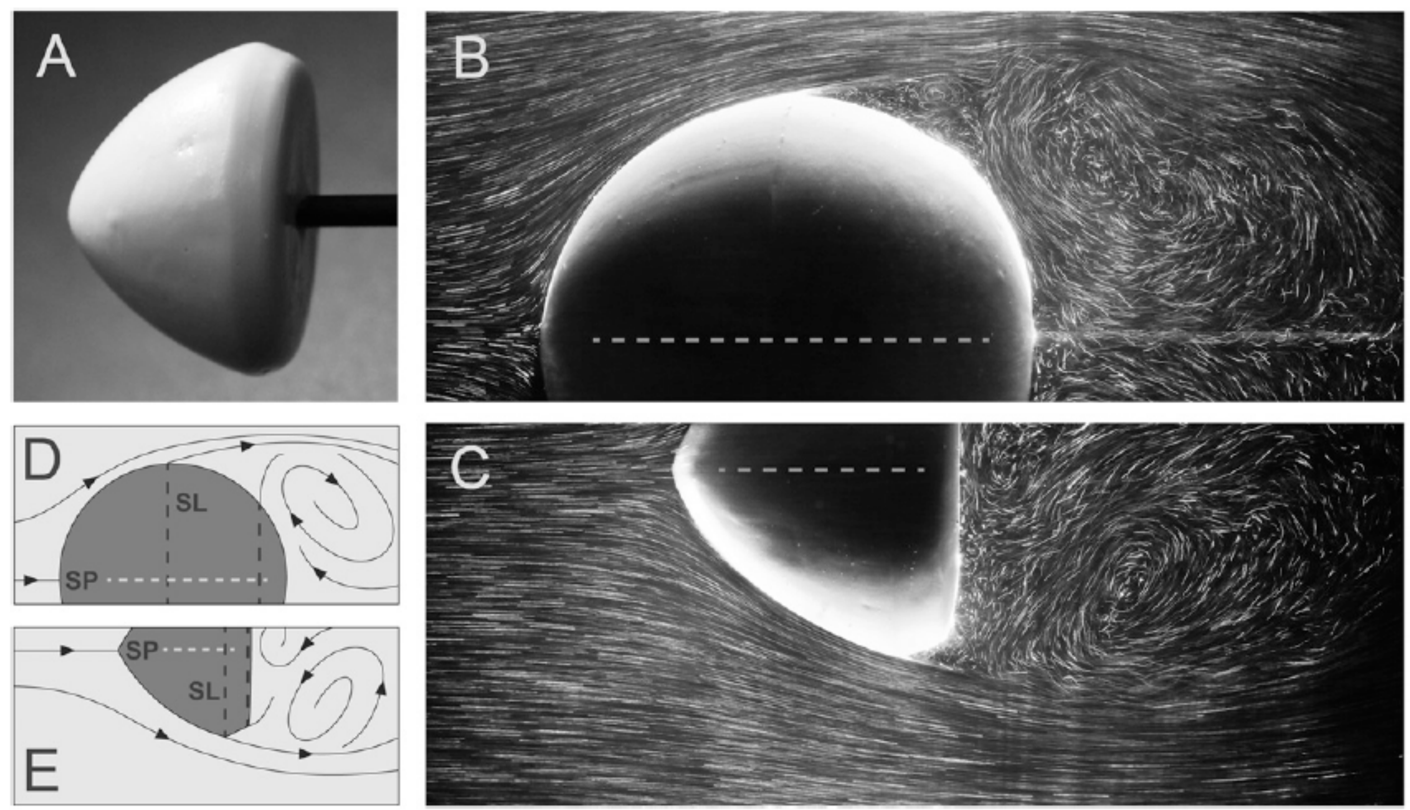

Fig. 1. Erosive sculpting of a clay sphere by flowing water. The flow speed is 46 cm/s and initial diameter 4.9 cm. (*A*) Removed after 70 min of erosio a water tunnel, the body has a conelike nose, angular ridges, and flattened back. (*B* and *C*) Photographs of 10-ms exposure reveal streaklines at 10 and 70 r The flow (left to right) conforms to the body before separating and forming a complex wake downstream. (*D* and *E*) Schematics show that the sharp feat at the nose and ridges are associated with the flow stagnation point (SP) and separation lines (SL), respectively.

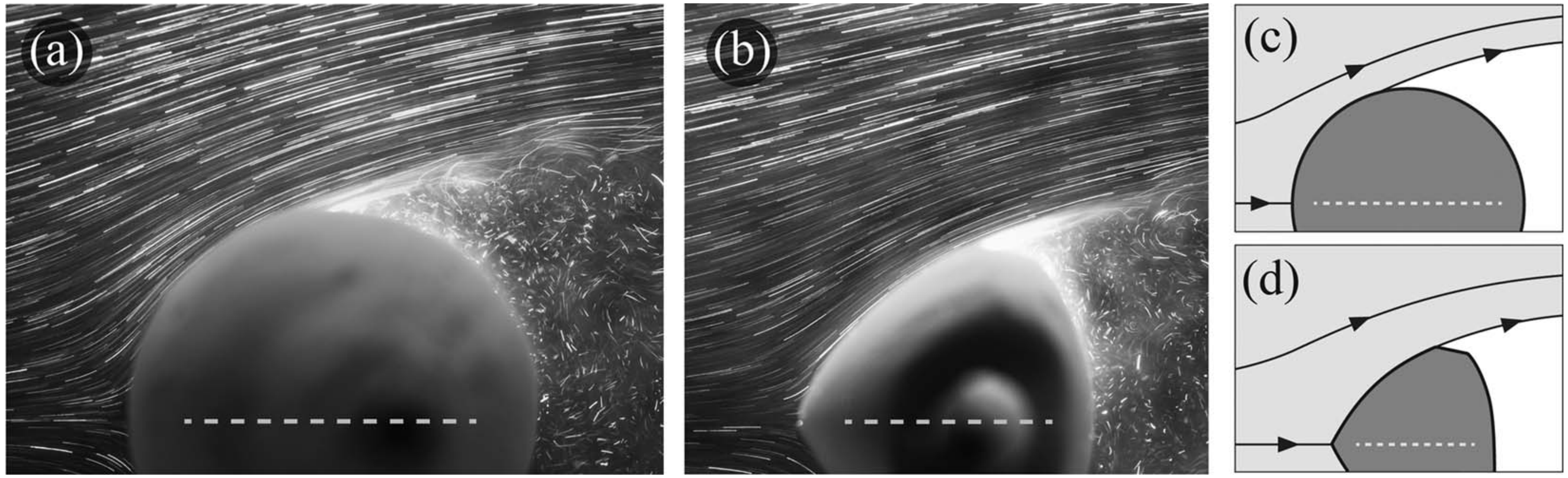

FIG. 2. Visualizing the flow around a cylindrical body at different times in the erosion process. Streaklines are captured by 10 ms exposure time photographs of tracer particles illuminated by a laser sheet, and the initial diameter of the body is 3.6 cm. (a) Early in the process, t = 5 min, the incoming flow stagnates at the nose and conforms to the body until separating just upstream of the widest portion. The wake behind the body consists of a relatively slow and unsteady flow. (b) At t = 55 min, the body has formed a quasi-triangular shape, yet the flow structure is qualitatively similar. The flow stagnates at the nose and separates near the body's widest portion, in this case near the back corners of the triangular shape. (c) and (d) Flow schematics.

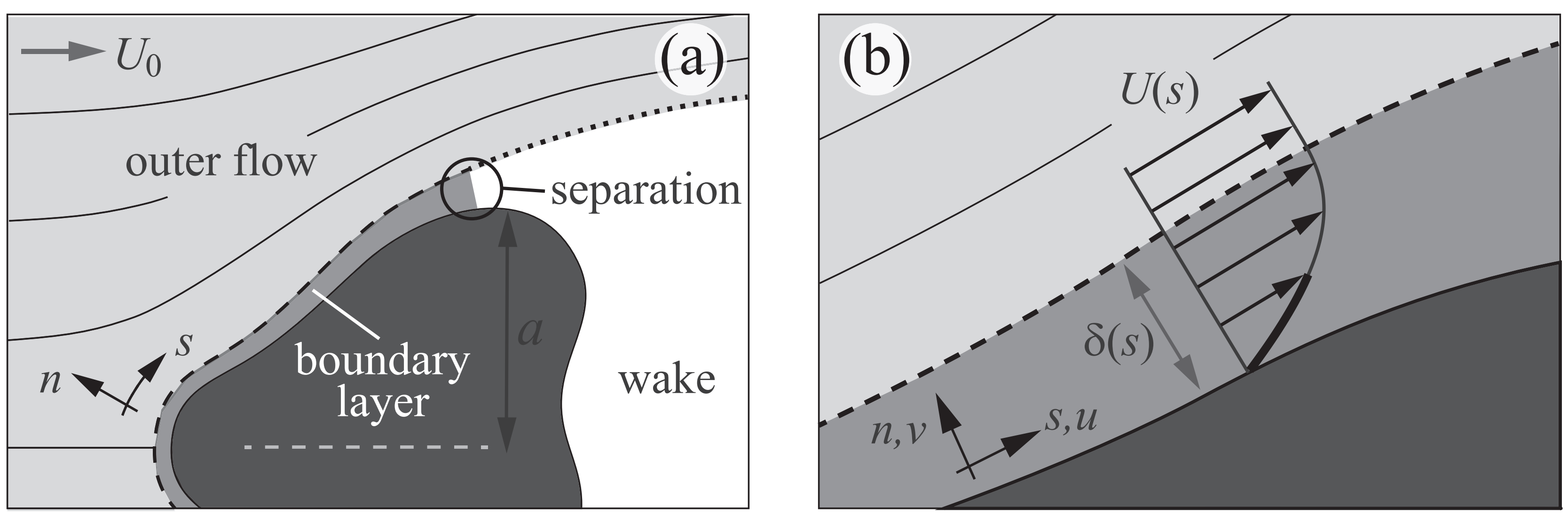

FIG. 3. High-Re flow past a bluff body in two dimensions. (a) The fluid flow is comprised of an outer and boundary layer flow, with the dashed curve indicating the thickness of the boundary layer. At the separation point, the boundary layer detaches and a wake is formed. The dotted curve represents the separating streamline. (b) Zoom into the boundary layer. The velocity profile inside the boundary layer approaches the outer tangential velocity $U(s)$ at a characteristic distance $\delta(s)$. Fluid shear stress is proportional to the slope of the velocity profile at the surface (darkened).

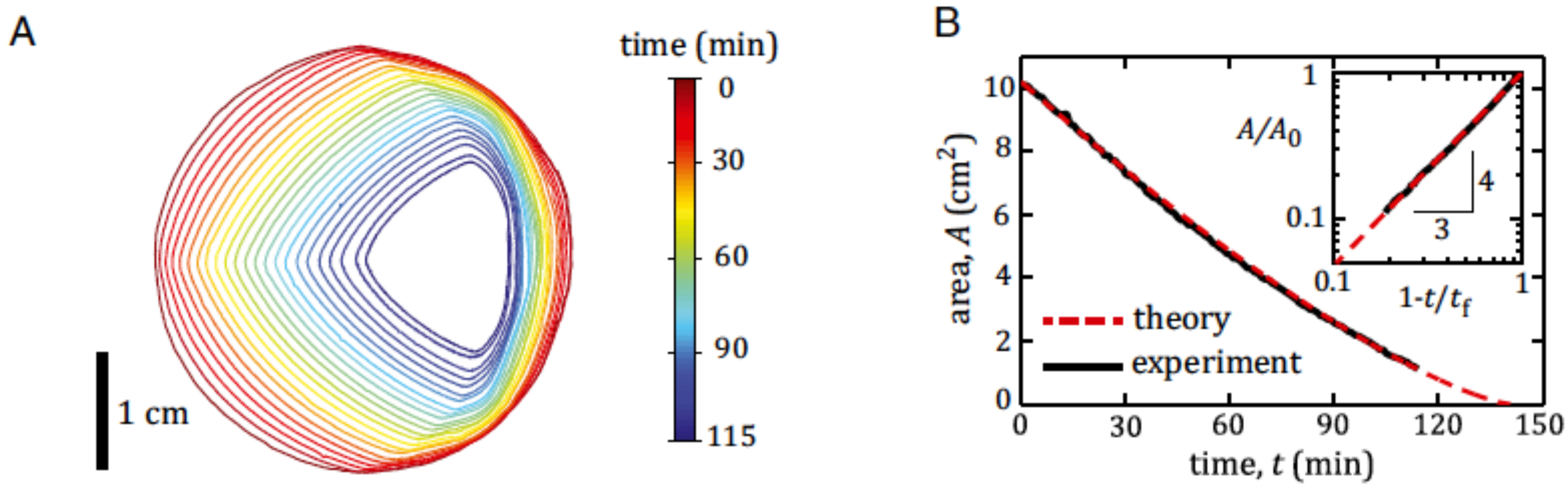

change of Area ~ shear x length

shear ~ $\rho U^2 \frac{1}{\sqrt{UL/\nu}}$

$$\dot{A} \sim -\frac{L}{\sqrt{L}} = -\sqrt{L} \sim -A^{\frac{1}{4}} \qquad A = A_0 \left(1 - \frac{t}{t_f}\right)^{\frac{4}{3}}$$

selfsimilarity

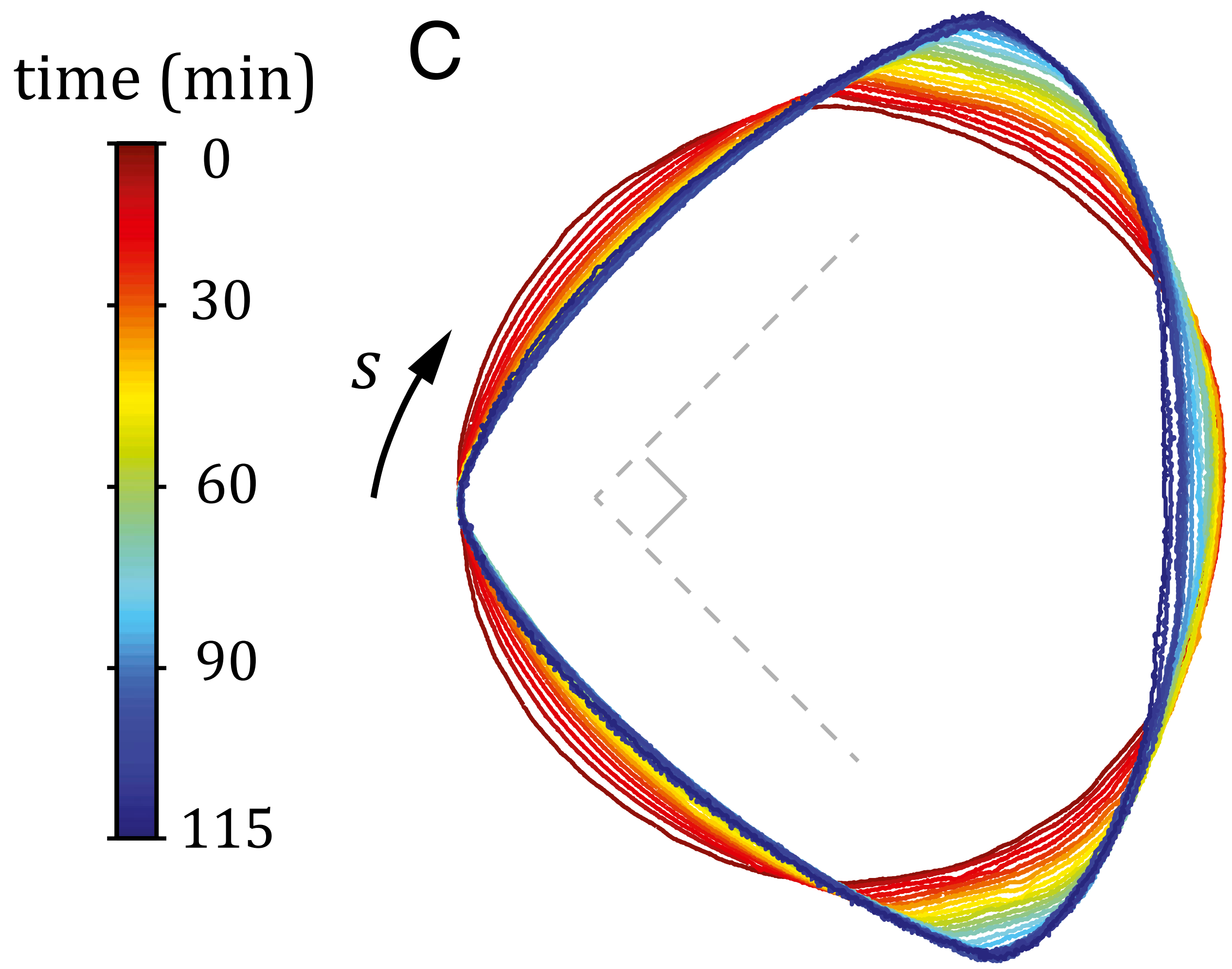

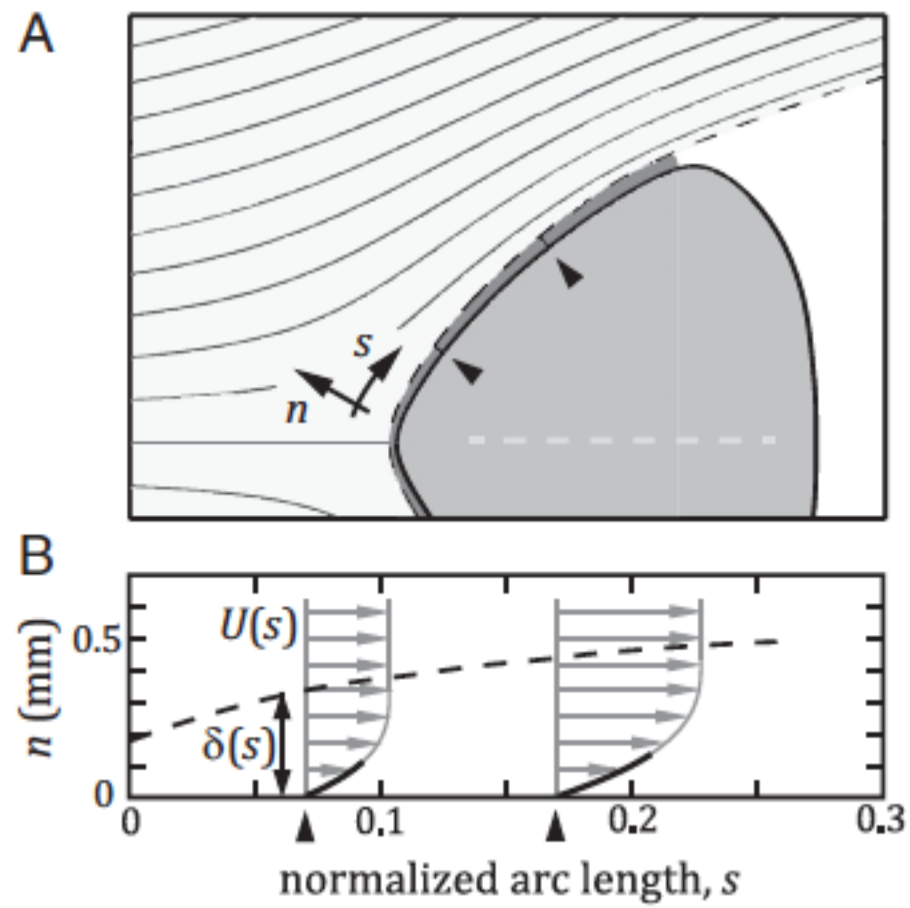

ideal fluid

$$\nabla^2\phi = 0, \qquad \nabla\phi\cdot\hat{\boldsymbol{n}} = 0 \qquad \text{on } \partial B$$

$$|\nabla\phi| = 1 \quad \text{on the free streamlines.}$$

Boundary layer

$$u\frac{\partial u}{\partial s} + v\frac{\partial u}{\partial n} - \nu\frac{\partial^2 u}{\partial n^2} = UU',$$

$$\frac{\partial u}{\partial s} + \frac{\partial v}{\partial n} = 0.$$

erosion

$$V_n = -C\,|\tau|\,,$$

cf Brivois Bonelli Borghi 07 (en turbulent)

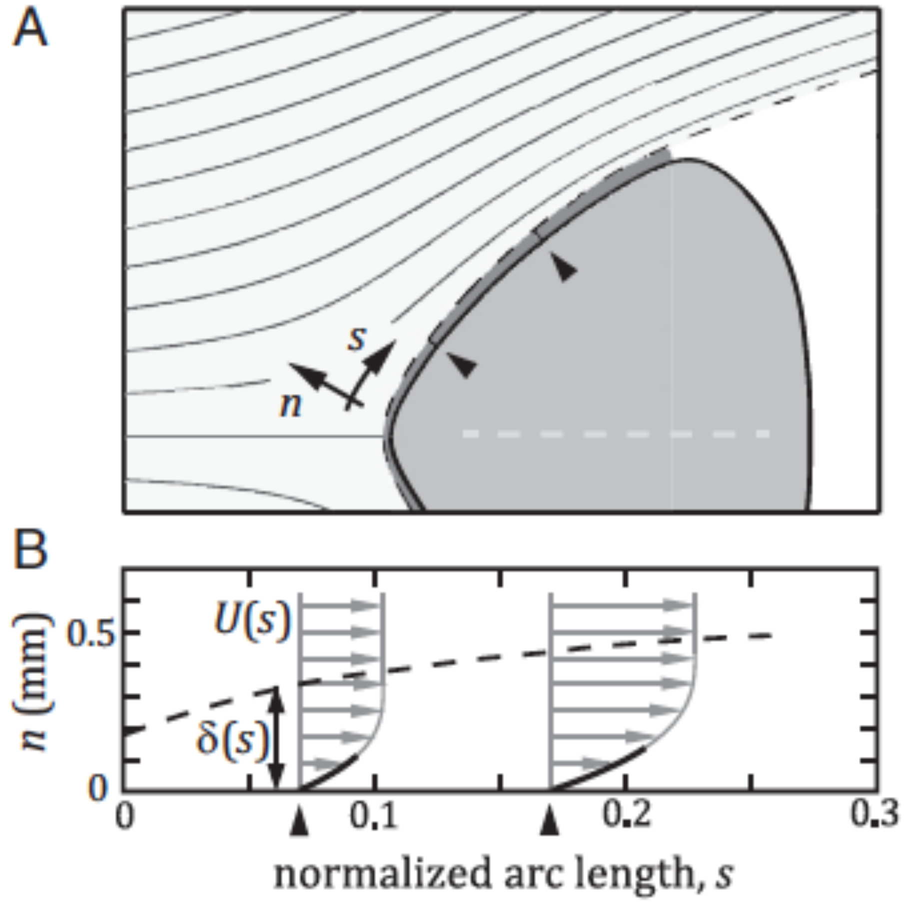

ideal fluid

$$m = \alpha/(\pi - \alpha),$$

$$U(s) = c_0 s^m.$$

Boundary layer

$$f''' + \frac{1}{2}(m+1) f f'' - m f'^2 + m = 0.$$

erosion

$$V_n = -C\,|\tau|\,,$$

$$\tau(s) = c_1\, s^{(3m-1)/2}.$$

constant erosion $m = 1/3$

$$\alpha = \pi/4$$

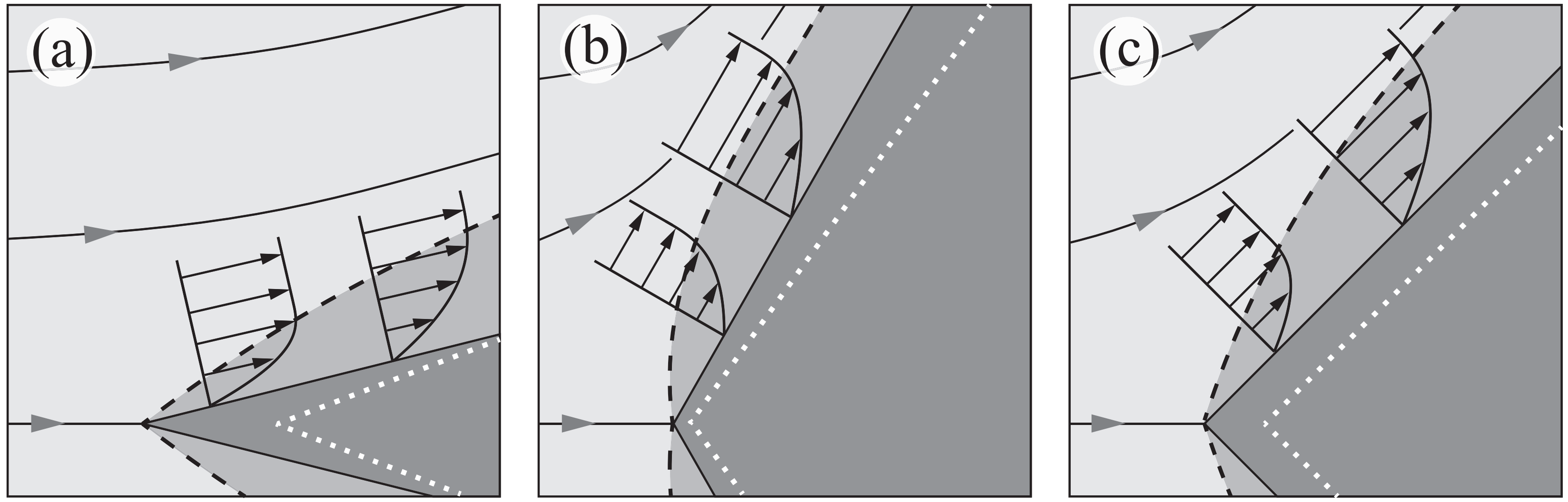

FIG. 5. Falkner-Skan similarity solutions for flow past wedges. (a) Illustration of the outer and boundary-layer flow past a wedge with acute opening angle. The shear stress is highest near the nose as indicated by the surface slopes of the velocity profiles. This causes the wedge to broaden as it erodes, which we indicate by the white dotted wedge. (b) For an obtuse opening angle, the shear stress increases downstream, and the wedge tends to become more narrow at later times. (c) A right-angled wedge produces uniform shear stress, which allows the shape to be maintained during erosion.

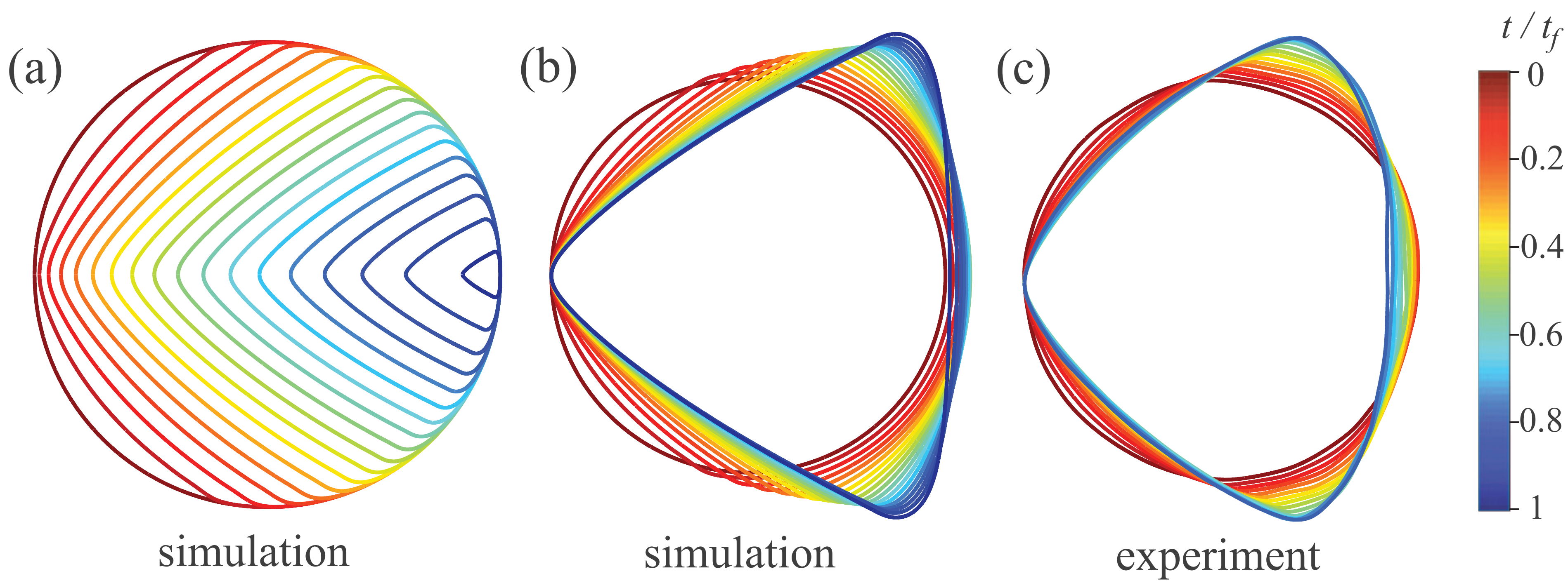

FIG. 6. Erosion of an initially circular body. (a) Interfaces from the simulation at evenly spaced time intervals of $0.06\,t_f$, with time indicated by the scale bar at right (color). As it shrinks, the body forms a quasi-triangular shape with a wedge-like front that points into the flow. (b) Shifting the interfaces to have the same leading point and rescaling to have equal area more clearly reveals the shape change. (c) The same rescaling procedure applied to the experimental interfaces shows similar evolution and terminal shape.

Messages

write 2 fluids equations (the best)

write 1 fluid equations

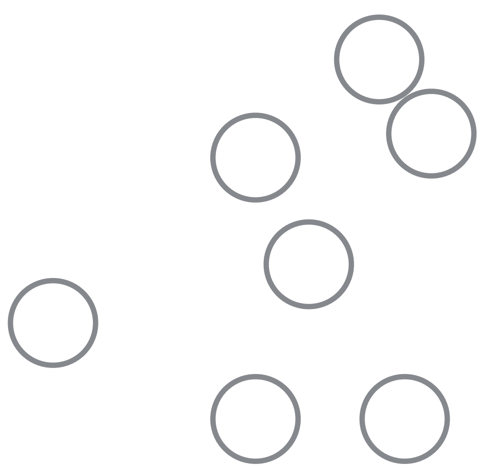

Importance of shear stress
boundary layer controls the erosion